Title
Three-dimensional organization of interphase chromosomes in different polytene tissues of Drosophila melanogaster

Author
Hochstrasser, Mark,

Publication Date
1987

Peer reviewed|Thesis/dissertation

THREE-DIMENSIONAL ORGANIZATION OF INTERPHASE CHROMOSOMES IN DIFFERENT POLYTENE TISSUES OF DROSOPHILA MELANOGASTER

by

Mark Hochstrasser

DISSERTATION

Submitted in partial satisfaction of the requirements for the degree of

DOCTOR OF PHILOSOPHY

in

Biochemistry

in the

GRADUATE DIVISION

of the

UNIVERSITY OF CALIFORNIA

San Francisco

Date University Librarian

Degree Conferred: January 4, 1987

ACKNOWLEDGEMENTS

I wish first of all to express my gratitude to my advisor, John Sedat. His sense of humor and willingness to run his "cooperative" in a spirit of open inquiry made my stay in his lab a most memorable and enjoyable one. His support and advice at certain crucial times in my first years here are also deeply appreciated.

It is difficult to thank sufficiently the people with whom I've worked and from whom I've learned a great deal. I will have to do so in much abbreviated form: Harry Saumweber for showing me the ropes of Drosophila cytology, David Mathog for writing IMP and supplying insight and a healthy dose of skepticism into our many discussions, Yosef Gruenbaum for his helpfulness and good nature in matters both inside and outside the lab, Andrew Belmont for being a great skiing companion and a learned voice on topics ranging from chromatin structure to hemorrhoids, Michael Paddy for his sympathetic ear and for almost picking us up at the airport, Mary Rykowski for trying to impart to me a sense of style, and Linda Mattson and Sue Parmilee for keeping the lab running in the face of ever-threatening chaos. To them and to all the other members of the lab I extend my thanks for making this a fun place to work.

The advice and assistance of many outside the lab is also gratefully acknowledged. I would like in particular to thank David Agard for patiently reading manuscripts and for holding the reins in on suspended disbelief, Robert Stroud for introducing me to the electron microscope and, as chairman of my orals committee, making my exam, well, almost fun, Pat Clausen and Sandra Miner for helping me to stitch together manuscripts and the present tome, Mei Lie Wong for help in using EM

facilities, and Bruce Krajewski for his warm friendship and for reminding me that there is another Culture besides Science.

I owe my deepest debt of gratitude to my wife Robin, who waited two years in New Jersey to marry me. Her love and support have made me happy and secure. She has brought home the fact that there is much more to life than what is found inside a laboratory.

Chapter 1 of this thesis consists of material reprinted from the Journal of Microscopy, Vol. 137, Part 3, 1985, pp. 241-252 by permission of the Royal Microscopical Society and from Nature, Vol. 308, No. 5958, pp. 414-421 by permission of Macmillan Journals Limited, Copyright (c) 1984. Chapter 2 is reproduced from The Journal of Cell Biology, 1986, Vol. 102, pp. 112-123 by copyright permission of The Rockefeller University Press. Chapters 3 and 4 have been submitted for publication to The Journal of Cell Biology while Chapter 5 has been submitted to Chromosoma. This research was funded by NIH grant GM25101 to John Sedat. Support was also received from an NSF predoctoral fellowship and NIH training grant 5T32GM07810.

Three-dimensional Organization of Interphase Chromosomes in Different Polytene Tissues of Drosophila Melanogaster

Mark Hochstrasser

ABSTRACT

While chromosome behavior during mitosis has been extensively studied, chromosome topology during interphase has not. The giant nuclei in polytene tissues of Drosophila melanogaster allow analysis of interphase chromosome folding by direct optical methods. The architecture of these nuclei is the subject of this thesis.

Chromosome paths were determined from optical sections of nuclei in intact tissues using a computer-based modeling system. Identification of chromosome bands allowed objective comparisons between nuclei. First, 24 salivary gland nuclei were analyzed. Surprisingly, chromosome coiling shows a right-handed chirality, independent of homologous pairing. The chromocenter(s) is always attached to the nuclear envelope, with telomeres usually arrayed at the opposite nuclear pole. High frequency interactions between chromosomes and the envelope occur almost exclusively at "intercalary heterochromatin" loci. Chromosomes lie in nonintertwined spatial domains, with each autosome's arms in close proximity. Centromere aggregation is not required for these properties.

Thereafter, a comparison of three other wild-type tissues, prothoracic gland, hindgut, and middle midgut, was performed (representing the first characterization of these less polytenized

chromosomes). The following conclusions could be drawn: Almost identical loci in prothoracic and salivary glands interact specifically with the envelope despite very different patterns of transcription. Conversely, chromocenters have a unique structure, intranuclear location, and tendency to associate in each tissue. Nucleolar chromatin also has a tissue-specific structure. The nucleolar organizer, but no other locus, is closely linked to the nucleolus. Right-handed coiling is a fundamental property of all polytene chromosomes. Polarized chromosome orientations, nonintertwined domains, and close-packing of autosome arms appear to remain from the last telophase, implying a remarkable positional stability in the absence of disruptive external forces. Specific interactions between heterologous loci were not found. Finally, morphometric measurements suggest that polytenization involves a reiteration of a regular folding regime within bands that may reflect the structure of diploid chromatin as well; they also give insights into band substructure and nuclear growth. Methods are also described for studying non-salivary gland tissues in squashes and for doing three-dimensional immunofluorescence analysis. These data provide a framework for models of nuclear architecture and the functional organization of the genome.

TABLE OF CONTENTS

LIST OF ILLUSTRATIONS

LIST OF TABLES

Introduction

This thesis is concerned with the three-dimensional organization of DNA, or more specifically, of chromosomes, within the interphase nucleus. Typically, about 10^5 μm of DNA must pack into a diploid nucleus only ~5 μm in diameter (Rasch et al., 1971). In a polytene interphase nucleus, chromosomes undergo repeated rounds of DNA replication with neither division nor separation of replicated chromatids. As a result, a ~35 μm wide salivary gland nucleus may contain over 85 m of DNA. The compaction of DNA is accomplished through a hierarchy of foldings within each chromosome and the folding of the chromosomes themselves inside the nucleus. This packing is under two fundamental constraints: it must permit the controlled transcription and precise replication of the genome, and it must allow the orderly process of division into duplicate daughter nuclei.

The first level of DNA packing involves the wrapping of the double helix into the 10 nm nucleosomal fiber (reviewed by Kornberg, 1977). Nucleosomes consist of an octamer of 4 different core histones and a single molecule of histone H1. The core particle constrains ~145 base pairs of DNA while H1 is associated with the linker DNA between core particles. With approximately two left-handed windings per nucleosome, the ratio of fully extended B-DNA to the 10 nm fiber is about 6-7. Beyond this level, the manner in which chromatin is organized is poorly understood. Both in isolated chromatin and in intact nuclei a 25-30 nm fiber is most frequenly found (Williams et al., 1986 and references therein), although a 50 nm fiber has also been reported (Sedat and Manuelidis, 1978). How the 10 nm fiber folds into the 30 nm wide structure remains controversial. Solenoid, superbead, and crossed-linker models have all been proposed, but the existing data are

not sufficient to decide between them (reviewed in Felsenfeld, 1986). A 30 nm fiber provides a further ~6-fold contraction of the original DNA length.

Clearly, additional folding of the 30 (or 50) nm fiber is necessary for it to fit into an interphase nucleus or a metaphase chromosome. A major point of contention is whether this folding occurs via a discrete higher order level(s) of packing or whether the 30 nm fiber represents a "unit fiber" which folds into a continuum of different sized structures (Sedat and Manuelidis, 1978 and references therein). Many technical difficulties are faced in studies of higher order structure because of the complexity of chromatin organization within the nucleus, the extreme sensitivity of chromatin to ionic strength, pH, and a host of other variables, and the fact that structures in this size range fall below the resolution limit of the light microscope yet are inconveniently large for conventional electron microscopy.

While these bulk properties are certainly important, chromatin is not a homogeneous substance, and it is the heterogeneities that have stimulated the most intense interest. The reason for this is that local variations in structural organization are likely to be linked with the differential control of gene transcription (or DNA replication). Eukaryotic cells can control the expression of a gene over a range of more than 8-9 orders of magnitude, almost a million-fold greater range than is observed in prokaryotic cells (Ivarie et al., 1983; Weintraub, 1985). The assessibility of particular DNA sequences to regulatory factors and to the transcriptional machinery will almost certainly depend on the manner in which these sequences are packaged into chromatin. Treatment of nuclei with various nucleases has shown that

different regions of the genome are differentially sensitive to digestion (reviewed in Weintraub, 1985). Hypersensitivity is often found in mutationally defined cis-acting regulatory regions of particular genes (e.g., McGinnis et al., 1983). Changes in sensitivity are generally detected when a gene is activated or inactivated.

Two highly specialized types of chromosomes have provided the paradigms for the differential organization of active and inactive chromatin in interphase cells: lampbrush and polytene chromosomes. The lampbrush chromosomes of amphibian oocytes consist of axial chromosome fibers punctuated with dense structures called chromomeres from which extend large DNA loops (Bostoch and Sumner, 1978). These lateral loops are covered with actively-transcribing RNA polymerases. Polytene chromosomes, found primarily in certain Dipteran tissues, are giant banded structures made up of hundreds or thousands of parallel chromatids that result from multiple rounds of DNA replication with neither nuclear division nor chromosome segregation (Beermann, 1962). When a banded region is heavily transcribed, it often decondenses into a puff, the pattern of chromosome puffs being specific to both tissue type and developmental time (reviewed in Ashburner and Berendes, 1978). Lampbrush and polytene chromosomes thus supply a vivid picture, visible in the light microscope, of genes in action.

The banding in polytene chromosomes has a highly characteristic pattern, allowing detailed cytogenetic maps to be constructed (Painter, 1933; Bridges, 1935; Beermann, 1962). The specificity of the banding pattern indicates that chromatin is organized into regular higher order domains ranging from a few to several hundred kilobases in length (Beermann, 1962). One goal of this thesis has been to determine if this

regularity extends beyond the level of the chromomere or band to long stretches of the chromosome. The idea of a defined intranuclear chromosome topology has been around for over 100 years, but the difficulty of analyzing the complex three-dimensional folding of interphase chromosomes has prevented a definitive experimental test. In the following paragraphs, I will review the development of this idea over the past century, and place it in the modern context that has led to its renewed appeal.

That chromosomes even exist as discrete entities between the mitotic phases of the cell cycle was originally quite difficult to demonstrate since the chromosomes unfold and generally disappear from view. In the 1880's, Boveri was able to show that the conspicuous lobes in the nuclei of Ascaris megalocephala blastomeres embryos are occupied by telomeres both in telophase and in the ensuing prophase, indicating that in the intervening period, chromosomes were maintained in relatively fixed locations and did not lose their individuality (see Wilson, 1925). At about the same time, Rabl observed that chromosomes reappearing in early prophase were still in the polarized orientations seen at telophase, with centromeres grouped on one side of the nucleus and telomeres on the other (Rabl, 1885).

It was in this connection that the question of how chromosomes are organized in the interphase nucleus first arose. The evidence suggesting the morphological individuality of chromosomes throughout the cell cycle was a significant factor in the development of the chromosme theory of inheritance (Sutton, 1903, Wilson, 1925). According to this theory, the hereditary particles or genes are borne by chromosomes, and the behavior of chromosomes during meiosis and fertilization can be used

to explain many aspects of gene transmission, such as independent assortment and segregation. One particular aspect of meiosis, the pairing of homologous maternal and paternal chromosomes, first stimulated the idea that chromosomes may hve a defined spatial arrangement within the interphase nucleus. A specific interphase arrangement, e.g., the association of homologs, could explain the otherwise mysterious process whereby meiotic chromosomes are able to locate and pair with their counterparts.

The relative positions of chromosomes in both premeiotic and somatic cells has been extensively studied by measuring the distances between pairs of chromosomes in squashes of metaphase plates. In many plant and animal species, statistically nonrandom distributions of homologs and non-homologs have been reported (reviewed in Avivi and Feldman, 1980). Not all studies are in agreement on this point, however, the data on mammalian cells being especially controversial (e.g., Zorn et al., 1979; Coll et al., 1980). More recently, Bennett (1983) made reconstructions from serially sectioned mitotic plant cells to circumvent the problem of artifacts resulting from squashing. From the relative positions of the centromeres, he concluded that chromosomes had a preferred arrangement, on average, that could be predicted from a model based on relative chromosome arm lengths. The model remains in dispute, however, in light of both criticisms of the statistical procedures used (Callow, 1985) and the failure to confirm the model in other organisms (Coates and Smith, 1984). Moreover, it is by no means clear that results from cells in metaphase can be extrapolated to the interphase condition.

Analyses of mitotic figures have, however, contributed to the concept that the propinquity of certain metaphase chromosomes reflects the formation of subdomains within the interphase nucleus in which functionally related loci are brought together. Probably the clearest example of this is the specific association of the acrocentric human chromosomes: the nucleolar organizers are borne exclusively on these chromosomes (see Bostock and Sumner, 1978). Heslop-Harrison and Bennett (1985) have analyzed mitotic chromosome positions in plant hybrids and noticed that the parental genomes were separated, with the set that contributes most strongly to the phenotype of the plant being located in the periphery of the other. They suggested that active genes may be segregated to a peripheral nuclear compartment as a means of regualting their expression.

Only a small amount of work has actually been done on interphase nuclei. Evidence for an active peripheral zone comes from a study of DNAase hypersensitive sites in isolated nuclei (Hutchison and Weintraub, 1985). Such sites, thought to mark active genes, appear to be concentrated near the nuclear surface. Belmont et al. (1986) reported that in triplo-X human fibroblasts, the two Barr bodies are preferentially positioned in the nuclear periphery; however, no evidence was found for a correlation between the positons of the two chromosomes. Finally, by irradiating small areas of the nucleus with a laser and then visualizing the damaged chromosome regions, chromosomes were shown to be stably positioned within the nucleus in the polarized orientations first noted by Rabl (Cremer et al., 1982).

Intergenic interactions have also been implicated from genetic studies of so-called position effects. In Drosophila melanogaster, the

transposition of a gene into a new chromosomal site, either by chromosome rearrangement or by P-element mediated transformation, frequently alters the degree of expression (Spradling and Rubin, 1983). When a euchromatic region is translocated to a positon next to a heterochromatic breakpoint, many of the translocated genes are inactivated in a variegated fashion from cell to cell (Baker, 1968; Spofford, 1976). Such "position effect variegation" seems to occur by a spreading in cis of a heterochromatic chromatin structure into the affected genes. Interestingly, the addition of a Y chromosome or certain portions of a Y chromosome ameliorates the inactivation effect. Variegation also differs in both degree and pattern between tissues bearing the same rearrangement.

For at least a small number of genes, the phenotype associated with a pair of alleles appears to depend on whether or not the alleles are homologously paired (Lewis, 1954; Jack and Judd, 1979; Gelbart, 1982; Kornher and Brutlag, 1986). This phenomenon, termed the "transvection effect", implies that the relative locations of some genes may affect the regulation of their expression. Another trans-effect has been documented in males bearing translocations between the X chromosome and an autosome: all such flies are sterile (Lindsley and Tokayasu, 1980). The sterility cannot result from the breakpoint per se because the same effect is seen with a wide range of X and autosomal breakpoints and is always dominant.

Squashes of polytene nuclei have also been examined for specific interactions between heterologous loci. Physical associations between specific loci, incluidng the 5S ribosomal RNA gene cluster, and the nucleolus have been reported in Drosophila (Steffensen, 1977; Ananiev et

al., 1981). In addition, a specific subset of bands has been shown to interact with one another via ectopic fibers. The particular pair of bands involved in each union are not always the same, but it is not known with what frequency squashing breaks the fibers (Kaufman and Iddles, 1963; Zhimulev et al., 1982). Telomeres are also often linked to each other (Berendes, 1963). This is reminiscent of a similar phenomenon in certain plant species which show specific end-to-end associations of chromosomes (Ashley, 1979).

How might direct intergenic interactions or the specific intranuclear positioning of genes affect gene transcription? Activatable loci may be placed in unique intranuclear "microenvironments" that either concentrate transcription factors or organize the transcriptional machinery (e.g., as supposed for the nuclear matrix; Jackson, 1986). One proposed mechanism for enhancers, which are regulatory DNA sequences that control the expression in cis of genes hundreds to thousands of base pairs away, is that they function by segregating a genetic unit to an active nuclear compartment (Khoury and Gruss, 1983). Transcriptional products or precursors may be channeled either between loci or between a locus and a particular sector of cytoplasm. This latter idea has been expressed by several authors with regard to positioning genes in the nuclear periphery (Kaufman and Gay, 1958; Blobel, 1985; Hutchison and Weintraub, 1985). The idea is especially attractive in light of the recent discovery that some mRNA's are localized in specific cytoplasmic domains (Singer ref). The transport of transciption (or replication) factors to particular loci may also be facilitated by placing these loci either against a two-dimensional surface, such as the nuclear membrane or the nucleolus,

or in an effectively one-dimensional structure, e.g., a closely linked cluster of sequences. The reduced dimensionality increases the efficiency, relative to simple three-dimensional diffusion, with which DNA binding proteins can search for their target sites (Berg and von Hippel, 1985). Finally, physical interaction between loci may affect cooperative chromatin transitions at either locus (Alberts et al., 1977).

Clearly, direct experimental data on the actual layout of the genome within the interphase nucleus is scant. Without a structural framework in which to consider the ideas outlined above, it has been virtually impossible to test them. Two previous attempts have been made to construct three-dimensional chromosome models from intact polytene nuclei. Skaer and Whytock (1975) made wire models from a small number of salivary gland nuclei in three Dipteran species. They concluded that chromosome folding was not trivially similar between nuclei. Agard and Sedat (1983) used fluorescence optical sectioning microscopy to construct a model of a Drosophila polytene nucleus. Citing preliminary data from another nucleus, they suggested that strong similarities in chromosome topology exist between nuclei. Missing from these studies was a means of aligning the three-dimensional structure with the genetic sequence; thus, the correctness of the models could not be checked nor could a quantitative comparison between nuclei be made.

In the present work, the approach used by Agard and Sedat (1983) has been modified and extended to allow a careful, objective study of three-dimensional polytene nuclear structure. Rather than construct physical models of nuclei, which are difficult to analyze quantitatively, models were made with the aid a computer graphics system

that allows models to be displayed on a color monitor and to be quantitatively compared. The computer-based data collection and modeling system is described in Chapter 1. The first phase of this project involved in analysis of 24 salivary gland nuclei. Preliminary results from 6 of them are included in Chapter 1. In the second chapter, a thorough, quantitative study of these 24 models, including statistical comparisons between nuclei, is described. A considerable number of consistent chromosome packing motifs were identified. Centric heterochromatin is invariantly positioned at the nuclear surface, while telomeres are generally arrayed at the opposite pole of the nucleus, resulting in a polarized (Rabl) orientation. Also associated with the nuclear surface is a specific subset of loci, almost all of which contain intercalary heterochromatin (Zhimulev et al., 1982). Chromosomes are always in distinct topological domains, with the arms of each autosome in close proximity but without other strongly favored relative arm positions. Most surprisingly, chromosome coiling is strongly chiral, with a predominance of right-handed gyres, and this chirality does not require homolog pairing. No evidence of specific three-dimensional configurations was found, although cell type heterogeneity could not be completely ruled out.

Two major factors allowed such a large amount of data to be analyzed and quantitated. First, conditions were found that preserve sufficient optical clarity to permit unfixed, unembedded glands to be optically sectioned. Second, by carefully tracking through the image stack along the model, it proved possible to identify the specific banding pattern in intact cells. In this way, the cytogenetic sequence could be fitted onto the model so that a direct comparison of precisely

the same chromosome regions in many nuclei became feasible. Thus, intact nuclei under virtually in vivo conditions could be rigorously studied.

The description of well-defined organizational motifs in salivary gland nuclei led to the second phase of the project, the comparison of chromosome spatial organization in different polytene tissues. By studying nuclei in various cell types, the generality and possible functional significance of these motifs could be assessed. Moreover, the tissues studied cover a considerable range in polyteny, and thus, the relationship between chromosome organization and nuclear size and growth could be determined. Chapter 3 gives a detailed description of nuclear architecture in 4 polytene tissues: the salivary gland, prothoracic gland, middle midgut, and hindgut. In Chapter 4, I use data from these tissues to explore the possible role of three-dimensional genome architecture in modulating tissue-specific gene expression.

These comparative studies have proved to be extremely informative. Chromosome-nuclear envelope interaction show a very similar specificity in both prothoracic and salivary glands. On the other hand, centric heterochromatin is positioned in the nuclear interior in the former tissue, in contrast to its invariant envelope association in the latter. The nucleolar organizer, at the base of the X chromosome, is tightly associated with the nucleolus, but no other chromosome locus is. No evidence was found for specific interactions between heterologous loci in any tissue either by statistical analysis of chromosome folding or by direct examination of chromosome models.

These experiments, which represent the first direct test of a potential role of three-dimensional gene positioning in gene regulation,

have shown the following. While specific chromosome regions are affixed to the nuclear envelope with high frequency, the similarity of these frequent contact sites in two tissues with very different patterns of gene activity indicates that peripheral localization is not a necessary condition for tissue-specific gene regulation. Loci in centric heterochromatin may be an exception to this rule. The absence of specific interactions between any euchromatic locus, even the 5S RNA gene cluster, and the nucleolus demonstrates that these are also not required for proper cell function. Finally, the fact that no pair (or small number) of loci that are not closely linked along the DNA axis specifically colocalizes within the nucleus of any cell type is inconsistent with models of nuclear function that stipulate such intergenic interactions. These conclusions, while of a rather negative character, are complemented by several useful insights into genome organization. If chromosomes fold up essentially as random linear polymers and remain in relatively fixed positions throughout interphase (see below), genetic transactions that involve the close juxtapositon of DNA molecules will be profoundly constrained. Such transactions include recombination, certain kinds of DNA repair, and perhaps even some cases of transcriptional regulation. I will consider several possibilities for the latter in Chapter 4.

Other, often suprising conclusions could be drawn from these comparative studies. A right-handed chirality is a basic property of polytene chromosome coiling. Indirect evidence suggests it may arise in the interphase nucleus before or in the earliest stages of polytenization; as such, it raises interesting questions about chromosome substructure and DNA topology. I will also present data

indicating that general packing motifs such as the Rabl orientation, nonintertwined chromosome domains, and nearest-neighbor packing of autosome arms are vestiges of the last embryonic mitosis, implying an extraordinary degree of positional stability within the interphase nucleus. Centric heterochromatin has a unique structure in each tissue; this has implications for tissue-specific differences in positon effect variegation and other aspects of heterochromatin function. Condensed nucleolar chromatin also has a tissue-specific organization, a result with intriguing genetic parallels (Endow, 1983; DeSalle and Templeton, 1986). Finally, morphometric measurements reveal an unexpected correspondence between polytene band structure and diploid chromatin; they also provide boundary conditions for models of band substructure and uncover tissue-dependent properties of relative nuclear and chromosome growth.

Chapter 5 provides a description of the polytene chromosomes from the three non-salivary gland tissues based on work with squashes. A model study of heat shock puffing in these tissues is included which reports an unusual kind of regulation of activity at the two hsp70 loci in the midgut. This represents the first detailed description of the chromosomes in these tissues and the first comparative study including autoradiographic analysis. It should therefore be of considerable utility to cytogeneticists studying polytene chromosome structure and function. The appendix describes methods for preparing salivary glands for three-dimensional immunofluorescence studies of nuclear antigens by optical sectioning microscopy.

Chapter 1

Light Microscope Based Analysis of Three-dimensional Structure: An Initial Study of *Drosophila* Salivary Gland Nuclei.

ABSTRACT

Many biological structures are large enough that they may be viewed by light microscope methods, yet they are sufficiently complicated that interpretation of what is seen is quite difficult. The salivary gland nuclei from Dipterans are an example of this. Previous attempts at determining the path of the giant chromosomes in these nuclei have depended on the laborious construction of models by hand. Here, a computer-based system for recording and analysing light microscope images, combined with classical cytogenetic analysis, has revealed the spatial organization of Drosophila salivary gland chromosomes. Each polytene chromosome arm folds up in a characteristic way, contacts the nuclear surface at specific sites and is topologically isolated from all other arms.

INTRODUCTION

There is little direct observational evidence for a large-scale regular architecture in interphase nuclei (briefly reviewed in Agard & Sedat, 1983). Extensive indirect evidence for a determined structure comes from studies of transvection (Lewis, 1954; Jack and Judd, 1979; Gelbart, 1982), position-effect variegation (Baker, 1968; Spofford, 1976), chromosome rearrangements (Werry, et al., 1977; Holliday, 1964; Cohen and Shaw, 1964), and ectopic pairing (Kauffman and Iddles, 1963).

We have chosen to work with the polytene chromosomes of the Drosophila salivary gland for several reasons: (1) they are large, having gone through about 10 rounds of replication without nuclear division, throughout which the homologous chromatids have remained in almost perfect lateral alignment, thus rendering the interphase

chromosomes visible under the light microscope; (2) there are only five major arms (X, 2L, 2R, 3L and 3R); and (3) they have a highly determinate pattern of condensed chromatin regions, known as bands, which have been catalogued in detail (Bridges, 1935) and which serve as a unique physical reference for correlation of structure to an extensive body of genetic data.

While the polytene chromosomes from Dipteran flies have been intensively studied for 50 years (Bridges, 1935; Painter, 1933), the investigations have been primarily with squashes. Squashing preserves the gross morphology of the individual chromosomes and spreads them for easy viewing, but the native structure of the entire nucleus is destroyed. Physically sectioning samples, whether for electron or light microscope observation, causes less drastic, but still significant changes in the overall nuclear morphology.

Previous attempts to delineate the organization of the nuclear contents in polytene nuclei have demonstrated certain problems with both the biological material and the use of simple physical models (Agard & Sedat, 1983; Skaer & Whytock, 1975, 1976). The Drosophila salivary gland is not the optimal structure optically for such a study, particularly with the use of fixatives (Skaer & Whytock, 1975, 1976). Physical models of nuclei, showing the paths of the polytene chromosomes, have been constructed (Agard & Sedat, 1983; Skaer & Whytock, 1975), but in no published case has the model been checked against the cytology to identify all of the chromosome arms. Little progress was made beyond the construction of simple wire models. One such study concluded that even though the telomeres and centromeres interact with the nuclear surface, the chromosome paths were not similar

between two nuclei (Skaer & Whytock, 1975). The evidence cited earlier, however, indicated that there should be some conserved order in these nuclei.

In order to approach this problem, we felt that a new methodology was needed. Earlier model building studies clearly indicated that there is considerable variation between nuclei. As a consequence, determining the significant components of nuclear architecture requires sifting those structural features which are conserved from the random fluctuations in chromosome position. The chromosomes are large enough that an optical microscope can be used to view the chromosomes within the nuclei in intact salivary glands (Skaer & Whytock, 1975; Agard & Sedat, 1983). Serial optical sections produced by focusing through a sample provide a source of data for the determination of the chromosome paths. By utilizing two newly developed tools, a computer-controlled data collection system and a computer-aided modelling system (IMP), it is now possible to rapidly determine the paths of the chromosomes in individual nuclei and to make meaningful structural comparisons between nuclei.

We provide here a general description of the computer-based data collection system and chromosome modeling and analysis techniques that have been developed. We also report the analysis of a set of nuclei in the unfixed salivary glands of a Drosophila melanogaster larva. The appearance of striking organizational motifs, based on quantitative comparisons of the paths of the chromosomes, implies the existence of an underlying order present beneath the considerable flexibility in the overall structure.

MATERIALS AND METHODS

Samples

Salivary glands from late third-instar D. melanogaster larvae (Oregon-R, inbred for 38 generations) were carefully dissected into a buffer optimized for preservation of chromosome structure (Buffer A; Sedat and Manuelidis, 1978; Hewish and Burgoyne, 1973). Buffer A consists of 60 mM KCl, 15 mM NaCl, 0.5 mM spermidine, 0.15 mM spermine, 15 mM PIPES, pH 7.5. The glands were stained with 100 µg/ml of the DNA specific dye 4', 6-diamidino-2-phenylindole (DAPI, Sigma) for 1 h. They were then washed, mounted between bridged cover slips, and sealed with paraffin oil.

Microscope

Data sets were collected using an inverted Zeiss Axiomat microscope slightly modified from an earlier study (Agard & Sedat, 1983). The tilt stage described in that study was not used; instead a slide holding stage was employed. The samples were viewed using epifluorescence optics which included a Zeiss 100X/1.3NA planapo achromat objective with 425 nm barrier filter, 420 nm dichroic mirror; excitation was by the 405-408 nm Hg line. The external focus drive motor is controlled by a Commodore PET microcomputer which is linked, in turn, to a VAX 11/780 minicomputer.

The image processing software runs as a single user program on a timeshare VAX 11/780 minicomputer. The VAX has three System Industries 300 Mbyte disks and a Kennedy magnetic tape drive for storage. The image processor is a DeAnza/Gould IP6400 with three image frames,

graphics overlay, digital video processor and a video rate analogue to digital converter. The image processor is connected by coaxial cable to the cameras mounted on the Axiomat microscope. The two cameras, a SIT and a Chalnicon, are both from the DAGE-MTI 66 series. A Barco CD51HR color monitor is the primary viewing device, while an RCA TC1209 is used to monitor data collection, and an RCA TC1212 directly monitors the camera. A Dunn Instruments 632 Color Camera System is used for taking photographs of the image processor output. A Floating Point Systems model 100B array processor became available during the course of this work (Fig. 1).

Software

It was recognized at the outset of this work that the structural determinants present in polytene nuclei would not be immediately apparent. The basic tenet of our approach is that structural problems should be analysed at sequential levels of abstraction. The lowest of these levels is manipulating the data, the next level is modelling the data, and the one above that is analysing the model. In general then, each succeeding level is based upon, and uses as input data, the results of the lower levels. In order to facilitate the analysis of structure and the development of further methods of analysis, it is essential to be able to move between equivalent 'points' at these various levels of abstraction.

Data collection.

Each frame (picture) is a 512x512 array of picture elements (pixels). The intensity of each pixel is stored as an unsigned byte,

and has the range 0-255. Typical data sets consist of twenty-four frames or a total of 6 Mbytes per data set. Each frame is generated by averaging the digital representation of the video signal from the camera 256 times. This operation occurs within the image processor and greatly improves the signal to noise ratio. Averaging occurs at video rates, with the conversion from the video signal performed by the image processor's digital to analogue converter. An averaged frame is available after 8 s. Faster data collection can be accomplished by averaging over fewer frames. Single unaveraged frames can be collected at 1 s intervals: 1/30 s to digitize the frame and 1 s to move the frame from the image processor to disk storage. The time required to collect a data set using maximum averaging is about 4 min. The data sets were not computationally processed to remove out of focus information as the images were sufficiently clear as collected to allow model building.

Modeling

The tool used in processing the data set is IMP (Interactive Modeling Program) (written by David Mathog). IMP allows an operator to start from a data set, construct a model from it, and to analyse certain features of that model. The time required to build a model depends both upon the operator's experience and on the complexity of the object. In practice, the minimum time for laying out the paths of the chromosomes within a nucleus is about a day. Models constructed by IMP are composed of points which are interconnected to represent paths, which may be branched. Once a model is partially built, it may be viewed as a stereo pair using a (software) vector representation (Fig. 4). This stick model can be rotated in nearly real time, so that it may be viewed from

different angles. Completing a model is facilitated by this feature as it allows the user to view the entire model at once, rather than just a restricted section of it.

Analysis

A major benefit of computer modelling over physical model building is that the model is in a form amenable to further processing. Visual analysis of complicated three-dimensional objects can be both time-consuming and misleading. A model may look radically different depending on the angle from which it is viewed. As simple a quantity as curvature can be readily misjudged. For many quantities of interest it is possible to define simple algorithms which do not suffer from the ambiguity often present in visual analyses. Quantities such as curvature, distance to the nuclear surface, and distance between points are all rotationally invariant; they may be calculated and displayed in a format which is unambiguous. Figure 2 indicates the overall scheme for the data collection and transformations, and also points out some of the advantages of these novel techniques.

RESULTS

The central question addressed in this study was whether the configurations of the chromosomes within an interphase nucleus are in some way determined. If so, one expects that in a single tissue at a given time in development, there will be similarities between these configurations in all the nuclei. Similarities can be gauged by analysing various quantitative properties of the three-dimensional

chromosome paths as a function of cytological position and comparing them between nuclei.

Plots are presented as a function of cytological position, rather than linear position along the chromosome, because of certain inherent complications in the use of the latter. The length of the same arm from different nuclei is not necessarily the same, for several reasons. The proximal endpoints of the arms are not well defined because the chromosomes are difficult to follow in the large, intensely fluorescing region where all the centromeres fuse (the chromocenter). Differences in the compression within the arms themselves and small modelling errors also lead to variation. To circumvent this problem a set of fiducial marks along the arms is needed which can be used to align the chromosomes from different nuclei. These are provided in the polytene banding patterns for which detailed cytological maps exist (Bridges, 1935; Lefevre, 1976). With the quality of data now available, band positions can be directly determined in the intact gland (Fig. 3). Also, to facilitate comparisons of quantities plotted as a function of cytological position, these marks (bands) were fitted onto a standard grid with intervening points placed by linear interpolation (Figs. 5-6). An important additional benefit of overlaying the cytology on the chromosome paths is that it serves as a check on the correctness of the models.

Visual inspection of nuclear models

Several significant results can be gleaned from the models even without knowledge of the detailed cytology. The most obvious is that the chromocenter always abuts the nuclear envelope (Fig. 3b). This is

in agreement with what is seen in Drosophila early embryos (Ellison and Howard, 1981) and also in other organisms (Fox, 1966; Skaer and Whytock, 1975). Whether or not this structure can slide along the nuclear surface cannot be determined from these data. There do seem to be limits on the extent to which it may roam this interior surface; in all the nuclei investigated, it is always in the hemisphere of the nucleus that is away from the lumen of the gland. Interestingly, centromeres are polarized towards the outside of the embryo (Ellison and Howard, 1981). In most nuclei a large fraction of each chromosome is curled into a series of loops or irregular helices with the telomeres lying at the opposite side of the nucleus from the chromocenter (Fig. 4a). Another striking feature of the models is the invariant confinement of each chromosome arm to its own topological domain; the arms never intertwine or knot around one another (Fig. 4c). This is true despite the extensive, complicated interfaces between them, indicating that the chromosomes are not wound through the nucleoplasm at random.

Quantitative analysis of nuclear models

It was quickly realized that simple visual inspection, even of rotated stereo models, would be of limited usefulness and could in fact be misleading. Because these nuclei are far from identical, any further search for common features requires translating the models into a form which can be examined objectively. By analysing various parameters that describe properties of the modeled chromosomes, one can extract their salient structural features. Derivation of these parameters and their plots is given elsewhere (Mathog, 1985). We describe here the important architectural features revealed by such an approach. These include

definable chromosome folding patterns, specific chromosome contacts with the nuclear envelope, and, less firmly established, a hierarchy of perferred chromosome arrangements within the nucleus. In all cases, these elements can be referred to specific cytogenetic sequences, making the investigation of structural organization at once more precise and more readily related to functional aspects of the nucleus.

Folding patterns of individual chromosomes

As the chromosome cable folds up in three dimensions, certain points which are well separated along the axis of the chromosome may approach each other quite closely in space. Such interactions can be visualized graphically in an intradistance map (Rossman and Liljas, 1974). The distances between the three-dimensional positions of all pairs of points on a chromosome are measured; these distances are plotted in a two-dimensional map. Distances larger than a cutoff distance of 8 μm are plotted as zero in the map. In these plots, both axes represent cytological position along the chromosome, the centromere being at the origin. An interaction between points which are not immediately contiguous along the arm will appear as a non-zero region located off the diagonal in the map (illustrated in Fig. 2d,e). Note that distance is measured from the chromosomal midlines defined by the model and that the chromosomes are, on average, 3-4 μm wide.

At first inspection, the intradistance maps of the same chromosome in different nuclei seem quite divergent. Nevertheless, common features in the set of six intradistance maps for a given chromosome arm are found when an appropriate statistical operation is performed on the collection. The operation we use calculates a generalization of the

median value, called the rank order value; the rank = n value is the n^{th} highest value in a distribution of values. The value for each point in a rank plot is derived from the distribution of values of the equivalent point in the original maps. In a rank = 4 plot, each non-zero patch marks an area of intrachromosomal apposition found in at least four of the six nuclei studied. Conserved regions are found throughout all of the arms. In Fig. 5, a rank-ordered intradistance plot of the X chromosomes shows a series of bars extending perpendicular to the diagonal. This kind of graphical feature is the hallmark of a loop in the model path and can be characterized by both its length and its location on the chromosome (Fig. 5b). A series of such loops is seen in the consensus structure of X. By evaluating such statistically ordered graphic signatures for each chromosome, it is possible to obtain an idea of their preferred configurations. The patterns are rather more complicated for the other chromosomes. The data indicate that a basal set of characteristic local conformations is available to each arm which is nonetheless compatible with considerable freedom in the global structure.

Spatial relationships between different chromosomes

In contrast to the above intradistance plots, pairwise comparisons between different chromosome arms (interdistance plots) reveal few, if any, specific interactions in this collection of nuclei. Only the 3L versus 3R diagram (at rank = 3) has an area of contact which is moderately conserved, centered at 72CE of 3L and 88AB of 3R (data not shown). The interdistance plots can still be used to obtain an idea of the nearest-neighbour relationships of the five chromosome arms for each

nucleus. This is done simply by counting the number of close approaches in each pairwise comparison plot. Certain arrangements, although not unique, are seen much more frequently than others. The clearest examples are: the arms of a given metacentric chromosome are usually next to each other, 3L is always far away from 2R except at the telomeres, and most of the X is well separated from 3R.

It appears that the chromosomes are packaged nonrandomly within the nucleus but without a determined set of pairwise interactions with specific sites on their nuclear neighbours. A caveat to this interpretation is that we have implicitly equated specific 'apposition' with 'interaction'. While this is probably valid in most instances, it does dismiss longer range and indirect interactions. For example, it is well known that ectopic fibres can sometimes reach enormous lengths, particularly in Chironomus where fibres as long as 45 μm have been observed in unsquashed nuclei (Quick, 1980).

Arrangement of chromosomes in relation to the nuclear surface

The role of the nuclear envelope has been emphasized in several models of nuclear organization (Comings, 1968; Brash and Setterfield, 1974; Vogel and Schroeder, 1974). Evidence supporting these models includes surface associations of chromosome ends (Boveri, 1888; Dupraw, 1965), ectopic fibres (Quick, 1980), and replication complexes (Comings, 1980). Accordingly, we were interested in determining how the chromosomes in our models were positioned with respect to this structure.

The chromosomes are intimately associated with the nuclear envelope at many points over its entire inner surface; this can be verified

directly using phase or Nomarski optics or by specifically staining the envelope. The parts of the chromosomes closest to the envelope thus define a convex boundary equivalent to the inner surface itself. This boundary is evident in Fig. 3. A close approximation to this surface can be constructed from several hundred planes which are tangential to the model (Mathog, 1985). This is equivalent to inscribing the model within a multifaceted polyhedron. The minimum distance from this surface to each point a chromosome is then calculated and plotted (Fig. 6). Figure 6a and 6b, for example, shows the plots of the six corresponding 2L and X chromosome arms, respectively. There are many regions that vary quite freely. On the other hand, points that show a close convergence of lines indicate a nonrandom relationship of the loci to the nuclear surface. These relatively fixed points are almost all located on the nuclear surface and are nearly all at loci which have previously been singled out for several structural peculiarities. These special features, collectively referred to as intercalary heterochromatin, include frequent ectopic pairing, late replication, a strong tendency to split or break in squash preparations, and a proclivity for chromosome rearrangement (Kauffman and Iddles, 1963; Zhimulev et al., 1982). Figure 7 summarizes these contact sites and compares them with regions of the chromosomes containing intercalary heterochromatin. There is a strong correlation between the conserved surface sites and the intercalary heterochromatin regions. The surface contacts may result from the formation of particular chromosome configurations, or they may actively determine these configurations; we cannot distinguish between these alternatives on the basis of our data.

When one compares the plots of one particular arm from different nuclei, some regions (as much as two-thirds of the total length) often show strikingly similar relationships to the envelope; Fig. 6c and d give two examples of this. The simplest explanation for such strong pathway homologies between segments of chromosome arms in different nuclei is that there is a small set of folding conformations which can be assumed by particular segments; thus in any group of nuclei several different but nonrandom patterns will be observed. In any case the plots do show that many parts of the chromosomes do not haphazardly contact the membrane.

DISCUSSION

The difficulties encountered in determining the three-dimensional structure of biological objects from serial sections are more often technical than theoretical. Given an appropriate sample, the techniques for data collection outlined in this paper are applicable. Others have observed that optical sectioning presents a rapid and accurate method for probing a sample (Skaer & Whytock, 1975; Agard & Sedat, 1983). We have found that the application of computer control to the process of optical sectioning greatly increases the speed and precision with which these sections can be made. The use of video cameras allows rapid collection of high quality pictures from each focal position. We have also found that nuclei can be successfully modelled without using two or more tilted sets of serial optical sections as was done in a previous study (Skaer & Whytock, 1975).

While the images used in the model building and analysis were derived from serial optical sections, they need not have been. Serial

electron micrographs, CAT scan sections, or even planes of electron density from X-ray crystallographic studies would have served equally well. The modelling system which was implemented requires only that a stack of aligned images be presented to it. Because of this, the approach described here can be simply applied to numerous other fields of study.

From the data presented here, a detailed three-dimensional picture of an interphase nucleus, with features down to the level of the specific cytogenetic banding pattern, begins to emerge. Overall, the architectural arrangement retains a significant degree of flexibility, but at the local level the configurations and dispositions of the chromosomes are quite narrowly circumscribed. Chromosomes fold up in highly characteristic ways, usually in a series of specific loops of definable length and position which often form roughly helical structures. Their centromeres, fused into the chromocenter, appose the nuclear surface while their telomeres tend to congregate around the opposite nuclear pole. The curling and twisting arms respect strict topological boundaries with respect to one another, in no instance wrapping around a neighbour. Some preference for certain nearest-neighbour arrangements is also seen. Finally, several nonrandom contacts with the inner nuclear surface are made by chromosomes as they pack into the outer regions of the nucleus.

The confinement of chromosome arms to separate topological domains is a striking result that does not necessarily follow from the other features of order which we have found. How might this strict separation be maintained? The way in which the individual arms fold up, perhaps involving ectopic fibres, may preclude their interweaving. Another

possibility is the specific scaffolding of individual arms within the nuclear sap to a protein matrix or to the nuclear envelope. Perhaps the domain restrictions can be best understood as a stable arrangement of the chromosomes established shortly after the completion of the last embryonic mitosis. The Rabl orientation is generally thought to reflect the configuration of the chromosomes in the preceding telophase (Fussell, 1975). The topological independence of the chromosome arms can be viewed as a natural extension of this data. There are several precedents for the limitation on interphase chromosome movement that would be required by such an interpretation (Sperling and Luedtke, 1981; Zorn et al., 1979; Herreros and Giannelli, 1967).

The most frequent chromosome-envelope touchpoints almost all map to sites of intercalary heterochromatin (Zhimulev, et al., 1982)(Fig. 7). Heterochromatin is known to aggregate near the nuclear surface in certain tissues. Skaer et al. (1976) noted that the patches of heterochromatin are tightly attached to the nuclear membrane. It is possible that the sites catalogued here may also serve as specific anchor points to the nuclear envelope. ~50% of the sites of strong ectopic pairing (≤3 bars in Fig. 7), neglecting the extreme proximal regions of each arm, are found to make frequent surface contacts. Why one subset of intercalary heterochromatin sites should be preferentially on the surface while the rest are not is unknown. Because of the limited number of nuclei included in this study we cannot distinguish by our criteria between sites which are not strongly conserved and sites which are not conserved at all.

From the intradistance plots, conserved regions of folding can be observed within each of the individual arms, the most common motif being

the loop. The loops could be the consequence of ectopic fibre connections or simply the mechanical characteristics of the synapsed chromosomes themselves. The pattern of attachment points on the envelope may also be important.

A basic assumption made in this study is that all the cells in the gland are in equivalent states. However, if chromosome conformations are very labile, we may have caught the different nuclei of the sample at various points in a spectrum of conformations. To test this, a living gland (by the criterion of trypan blue exclusion at the end of the test period) was continuously viewed by phase contrast optics over several hours. Pictures were taken at regular time intervals. No change in position of any chromosome region could be detected when the frames were compared (data not shown). Neither could any disruption of the nuclear contents be detected over a long period of time in the buffer conditions used to collect the image data. Moreover, these glands have not been fixed and thus are not subject to the well documented artefacts which fixation regimens can create (Skaer and Whytock, 1976).

The conclusions one draws from such models do not depend on who constructs them even though different model builders' placement of points within the 3-4 μm-thick chromosomes may vary slightly. One nucleus was modelled independently by two of us. The resulting reconstructions differed in only trivial ways from one another, and more importantly, the resulting quantitation plots were virtually indistinguishable.

A more difficult problem in this analysis concerns the small sample size. There is no good foundation for predicting a random set of

conformations as a statistical control, as we know very little about the boundary conditions. The restricted volume of the nucleus, exacerbated by the excluded region occupied by the nucleolus; the centromeric fusion of all the arms; limits on the mechanical deformation of the chromosome cable; and other constraints all restrict the ways in which the chromosomes can fold. Defining these boundary conditions is, of course, a major goal of our analysis. We are analysing more data both for this purpose and for reducing the problem of limited sample size.

There are several means by which a nonrandom chromosome organization within the nucleus can be rationalized (Comings, 1968; Comings, 1980). As discussed above, at least certain aspects can probably be best understood as relics of the last embryonic mitosis of these nuclei. Also, certain folding patterns and chromosome arrangements may simply fit more easily into the confined space of the nucleus. An additional coercive force on interphase chromosome arrangement could be the requirement that chromosomes in germ-line tissues be able to pair with their homologues during meiosis (Comings, 1968; Franke, et al., 1981; Avivi and Feldman, 1980; Finch et al., 1981). maintaining a defined spatial arrangement of chromosomes would greatly facilitate the orderly pairing and segregation of homologues, and somatic tissues could conceivably bear vestiges of this order. Certainly the somatic nuclei of the Dipterans, with their tightly paired homologues, attest to this possibility. Nonrandom arrangements of homologues and non-homologues is now supported by a wealth of cytological data in a variety of species (Cohen and Shaw, 1964; Avivi and Feldman, 1980; Becker, 1969), although the evidence in mammals remains controversial (Zorn et al., 1979; Coll et al., 1980).

A more radical rationale for determined configurations of chromosomes in the nucleus is that they are involved in gene expression. As few tools have previously been available to test this idea, the evidence is rather scant. We can now identify a large number of loci in their unperturbed three-dimensional context, providing a means of studying this problem. One straightforward approach would be to analyse the locations of known active loci as a function of developmental time. The glue protein genes and the ecdysone-induced puffs would be the first choices in such experiments. Indeed we have begun to measure the spatial relationships of the latter group in the present data set.

FIG. 1. Schematic diagram of the hardware on which the CAMA system has been implemented. Arrows indicate data paths. AP: array processor; IP: image processor; TTY: terminal; PET: Commodore PET microcomputer; FA: microscope focus drive; TD: microscope tilt stage drive; C1: SIT camera; C2: Chalnicon camera; S1: coaxial switch; M1,2,3: video monitors; Dunn: Dunn Industries colour camera system. See text for more detail.

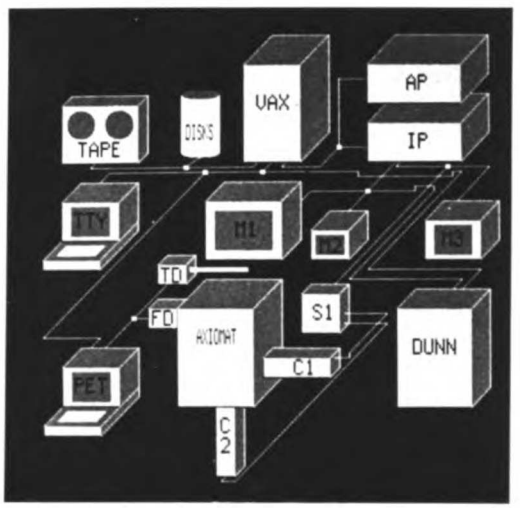
TAPE
DISKS
VAX
AP
IP
TTY
M1
M2
M3
TQ
FQ
AXIOMT
S1
DUNN
C1
PET
C2

Fig. 2. The overall scheme of the study. The structural information of each nucleus was analysed in situ. a) The sample gland: open circle, nuclei for which data were collected and preliminary models build: filled circle, nuclei used in this study. Fluorescently stained chromosomes were imaged using a high resolution objective lens with a shallow depth of focus. Incrementing the focus in regular steps through a nucleus effectively sliced it into a stack of images. b) The pathways of the different chromosomes were then traced using the program IMP, which moves a cursor within the data stack and uses it to place points along each arm. c) The vectors connecting these points defined a 'stick-figure' model. The model lines traced over the data set (see Fig. 3b) indicate to which path each piece of chromosme belongs, simplifying the cytological determination. Typically 25-35 bands, distributed all along the arm, were noted on the model. This was done for each arm. e) Chromosome pathways were then analysed for several properties, which are represented in a series of graphs. After the axes were normalized to the known banding pattern, these graphs were used to compare chromosomes from different nuclei. A cross-hair (shown in e) marks the positions in this plot which correspond to locations on the model. The regions in the model which gave rise to the targeted feature are marked in d by the two dots. CC, Chromocentre; T, telomere.

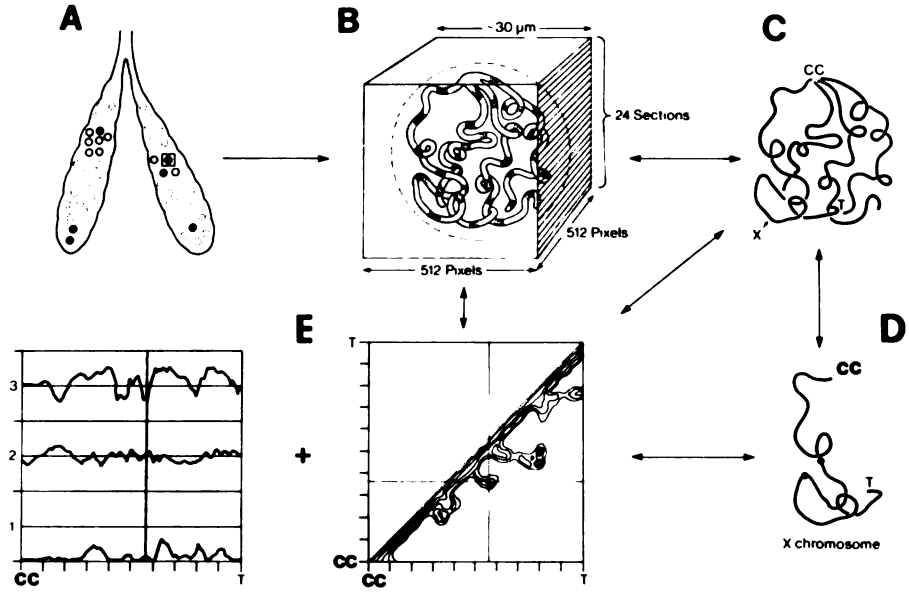
A
B
~30 µm
24 Sections
512 Pixels
512 Pixels
C
CC
T
X
D
CC
T
X chromosome
E
T
CC
CC
T
+
3
2
1
CC
T

Fig. 3. Two sample frames from the original data sets. Each represents the averaged digital image (512x512 picture elements of pixels) of 256 video frames. Twenty-four such images, conprising 24 successive focus steps through a nucleus, make up the image stack. The chromosome banding patterns visible in these preparations are virtually the same as those seen in unstained squashes. It is possible to roughly stage this gland at about PS7 or PS8 using the well established puffing sequence which characterizes the late third-instar/prepupal stages of development (Ashburner, 1972). a) A frame near the top of an image stack from a nucleus. At least partially visible in this plane are two telomeres (T). b) A frame in the middle of a stack from another nucleus: the chromocentre (CC) and part of the nucleolus (Nu) are visible. Some cytogenetic loci are indicated. Lines along the chromosomes indicate the model paths.

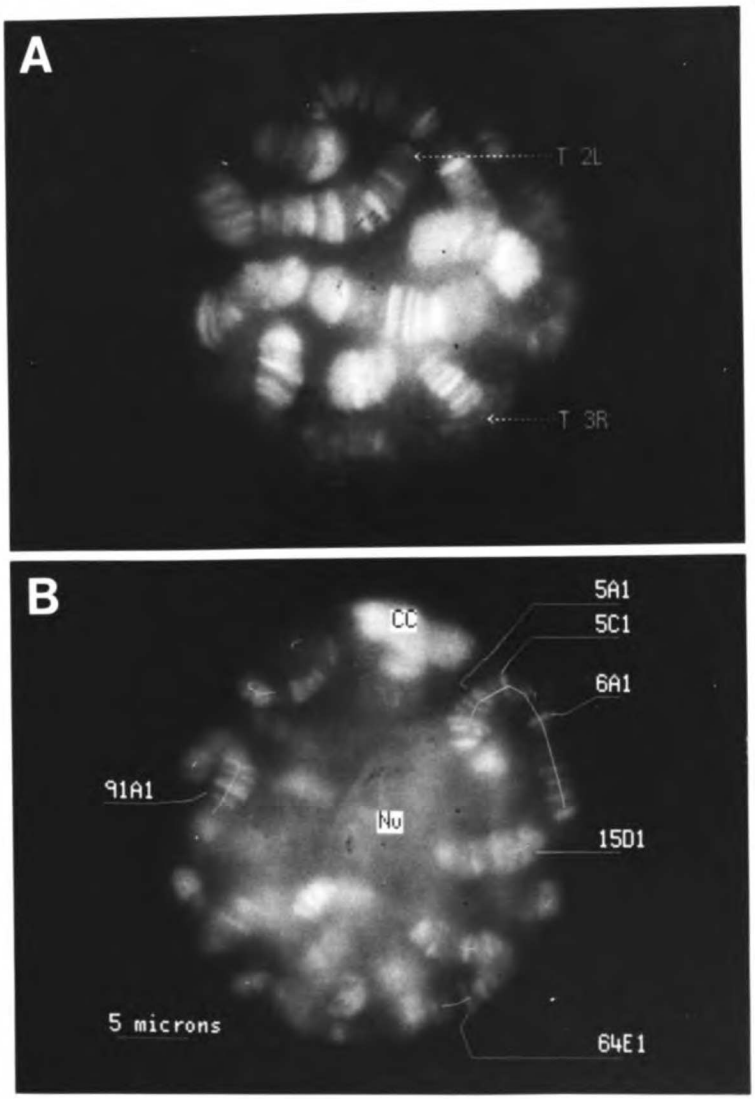
A
T 2L
T 3R
B
5A1
5C1
CC
6A1
91A1
Nu
15D1
5 microns
64E1

Fig. 4. a,b) Stereo pairs of two of the nuclear models. (Note that stereo glasses will reverse the handedness.) Corresponding chromosomes in the different models are assigned the same colour (green=X, orange=2L, blue=2R, purple=3L, light blue=3R). Models can be manipulated in several ways for visual inspection including rotation in near real time, selective blacking-out of sectors and chromosomes, and marking of cytological features. In a the telomeres (□) and chromocentre termini(+) are indicated to highlight the Rabl orientation (Rabl, 1885). In b the active puff sites for glands at this developmental stage have been indicated by small squares (Ashburner, 1972). c) The 3L and 3R chromosomes from b are shown with all cytologically identified sites marked with small squares. Confinement of individual chromosome arms to separate topological domains is illustrated in this view; while the chromosomes press together quite closely they do not wrap around one another.

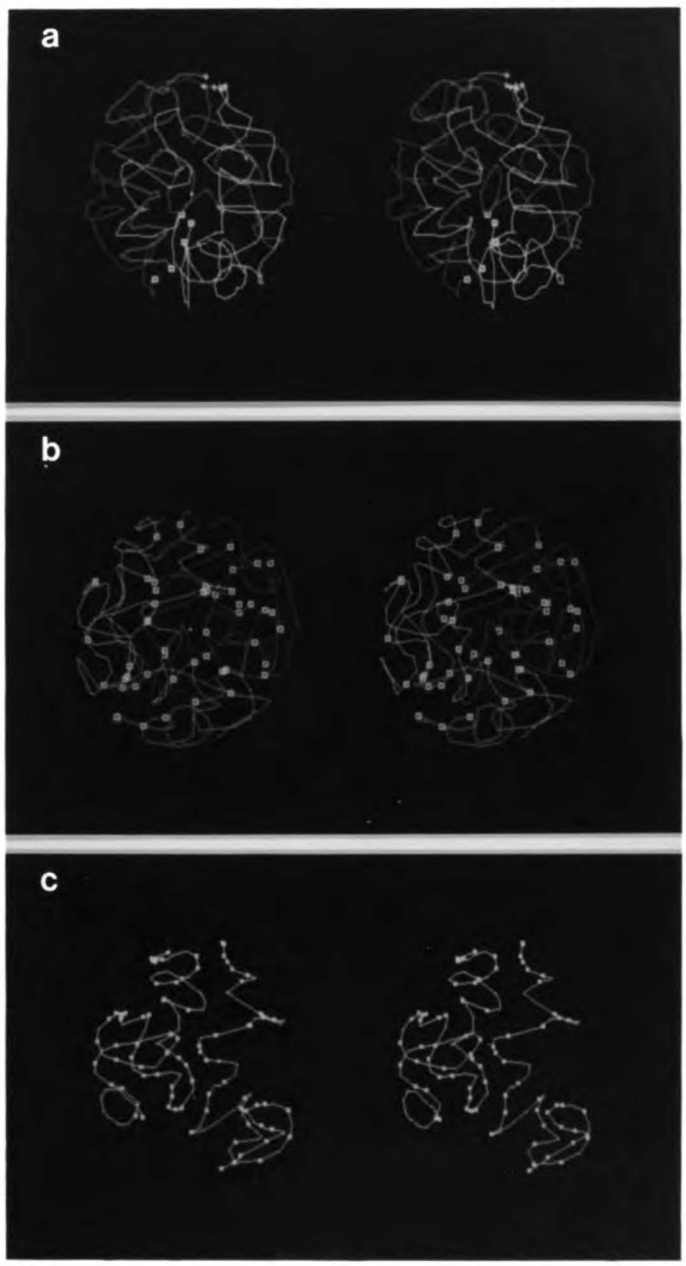
a
b
c

Fig. 5. The most comomon folding motifs which characterize the packaging of the X chromosome in the nuclei. Plot a was derived as follows. First, the intradistance plot (Rossman and Liljas, 1974) for each of the six X chromosmes was determined from its three dimensional model. The ordinate and abscissa are identical, representing cytological position along the chromosome, the centromere at the origin; what is displayed is the distance in space between each pair of points on the chromosome, distances larger than 8 um being plotted as zero. Contour lines were drawn immediately at every step of 1 µm up to a maximum at 8 µm. Points immediately contiguous along the axis of the chromosome are necessarily close together in space; these together form the diagonal region in the plot. Non-zero areas off the diagonal represent regions on the chromosome which are close in space and thus indicate the chromosome's folding pattern (see Fig. 2 d,e for example). The second step was to consider the plots for all of the X chromosomes together in order to find their common features. The values at each position in the 6 original intradistance plots were sorted in order of ascending value. The largest value was given a rank = 6, the smallest a rank = 1. A "rank-ordered" plot was thus constructed. The plot shown uses the rank = 4 values for all positions in the graph, thus in four out of six nuclei, the chromosome points represented at each position are as close as or closer than shown in the plot. The bottom part of the figure (b) represents our interpretation of the rank-ordered plot for the X chromosome, showning the location of folding features. Feature centre (v), interior (---), ends (###). The features centered at the start of numbered divisions 3,5,9 and 12 are typical loops or foldbacks. Note that some, but not all, of them overlap.

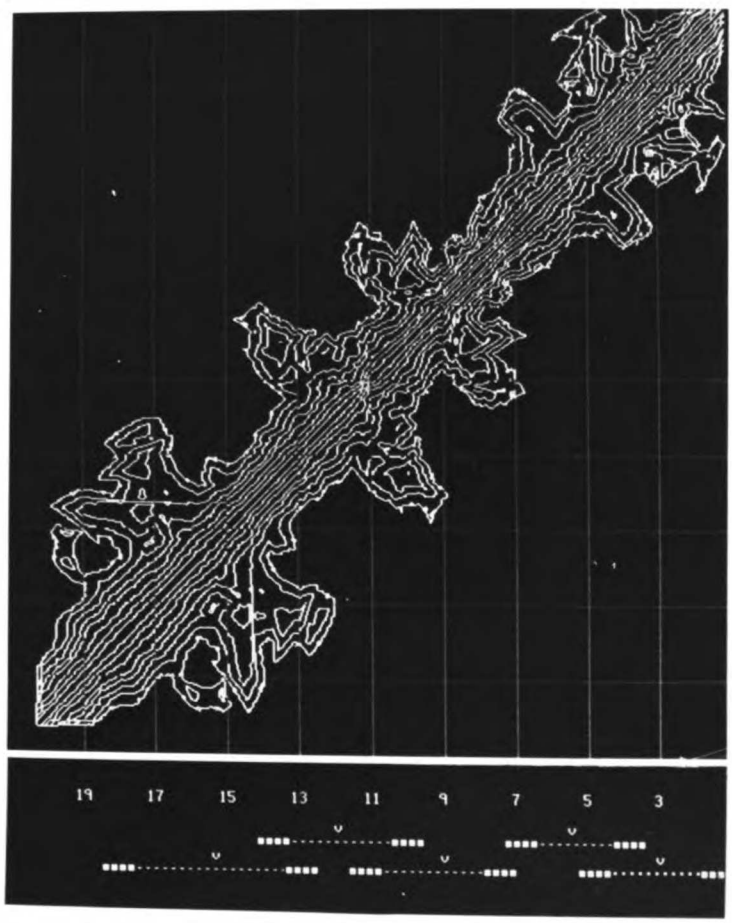
19
17
15
13
11
9
7
5
3

Fig. 6. A-D, Plots of the distance from cytological points along a chromosome to the nuclear surface. Full scale on the vertical axis is 10 μm. Each horizontal division corresponds to two numbered cytological divisions, with the chromocentre at the left. Conserved contacts are indicated by arrows. A) Superimposed graphs for the six 2L arms. B) Superimposed graphs for the six X chromosomes. C,D) Several of the contributing X chromosome plots are shown individually. The underlines indicate regions with strong similarities. The surface is represented by a convex polyhedron tangential to the model at each of its facets, as described in the text. A simple algorithm for generating the facet planes is described by Mathog (1985). The distances plotted here were measured from each point along the chromosome arm to the closest point on the polyhedral surface.

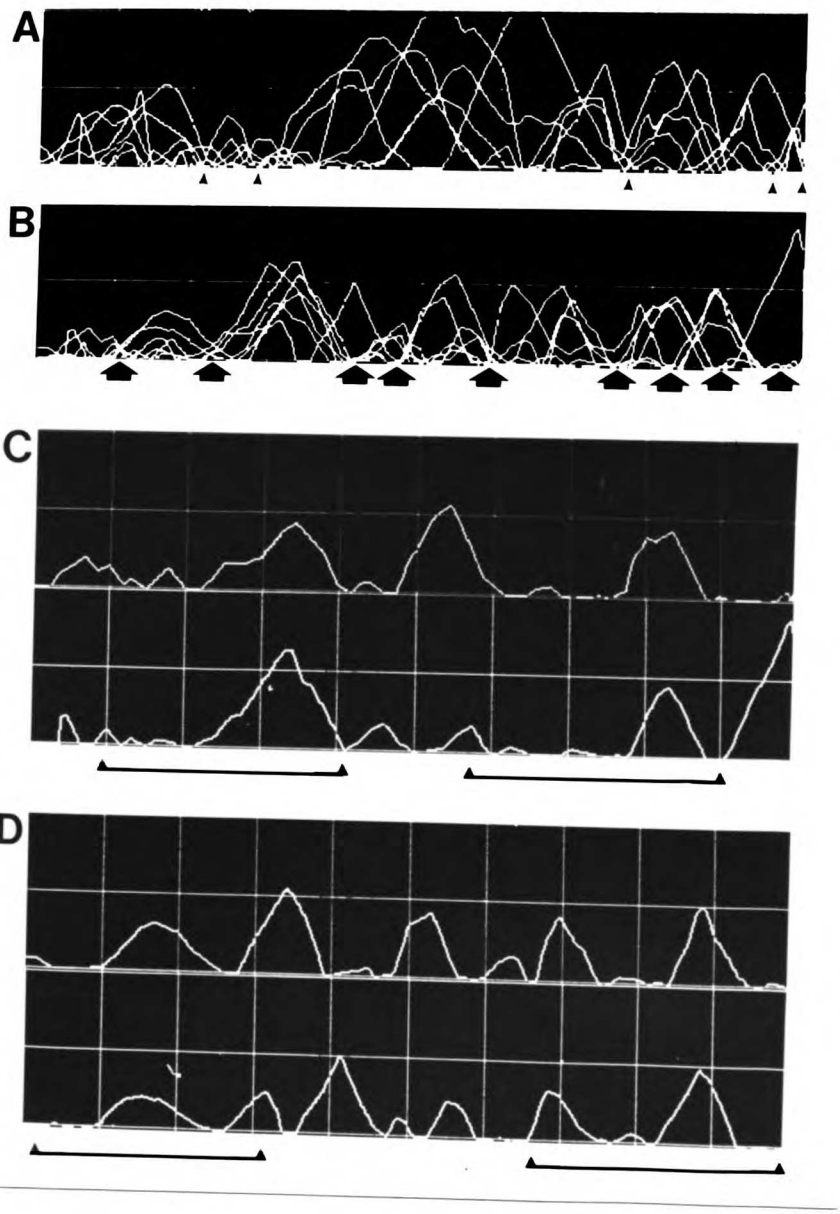
A
B
C
D

Fig. 7. Features characteristic of intercalary heterochromatin compared with conserved surface contact sites. Each horizontal scale is divided into the 120 lettered cytological subdivisions for each chromosome arm; the first square of each numbered division is filled. Weak points (W) and ectopic pairing points (E) are shown on top scale. Their frequencies of observation have been binned here into steps of 10% (W) and 1% (E) (intermediate values rounded to next highest bin). Grey bars indicate regions where they made no observation. Our surface contact sites are shown on the corresponding bottom scales. Large solid bars indicate surface apposition in six out of six nuclei, small solid bars in five out of six nuclei with the sixth at a peak in the distance to surface plot, and large broken bars mark all other cases of five out of six. The pair of small broken bars at 3C and 4D indicates that either site is on the surface to the exclusion of the other. The chromocentre (CC) and telomeres (T) are marked. The resolution of the surface sites is about one lettered subdivision. Data for the 2L and X chromosomes are shown in Fig. 6a,b.

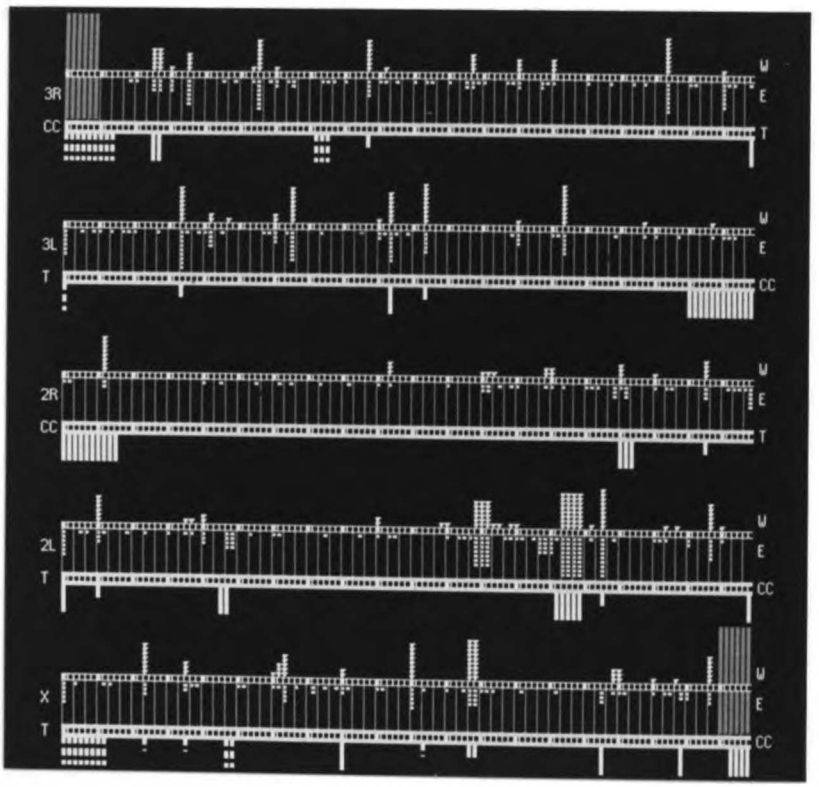
3R
W
E
CC
T
3L
W
E
T
CC
2R
W
E
CC
T
2L
W
E
T
CC
X
W
E
T
CC

Chapter 2

The Spatial Organization of Chromosomes in the Salivary Glands of *Drosophila melanogaster*

ABSTRACT

Using a computer-based system for model building and analysis, three-dimensional(3-D) models of 24 Drosophila melanogaster salivary gland nuclei have been constructed from optically or physically sectioned glands, allowing several generalizations about chromosome folding and packaging in these nuclei. First and most surprising, the prominent coiling of the chromosomes is strongly chiral, with right-handed gyres predominating. Second, high frequency appositions between certain loci and the nuclear envelope appear almost exclusively at positions of intercalary heterochromatin; in addition, the chromocenter is always apposed to the envelope. Third, chromosomes are invariably separated into mutually exclusive spatial domains while usually extending across the nucleus in a polarized (Rabl) orientation. Fourth, the arms of each autosome are almost always juxtaposed, but no other relative arm positions are strongly favored. Finally, despite these non-random structural features, each chromosome is found to fold into a wide variety of different configurations. In addition, a set of nuclei has been analyzed in which the normally aggregated centromeric regions of the chromosomes are located far apart from one another. These nuclei have the same architectural motifs seen in normal nuclei. This implies that such characteristics as separate chromosome domains and specific chromosome-nuclear envelope contacts are largely independent of the relative placement of the different chromosomes within the nucleus.

INTRODUCTION

Eukaryotic cells contain enormous lengths of DNA which must undergo considerable packing to fit inside the interphase nucleus. The packing is accomplished through multiple foldings of the DNA molecule within each chromosome and the folding of the chromosomes themselves inside the nucleus. This hierarchy of foldings is under several general constraints. First, the DNA must be available to regulatory factors and transcriptional machinery in such a way that readout of the genome can be precisely controlled. Second, the resident copies of DNA must be faithfully duplicated and repackaged with histones and other proteins; in dividing cells, the daughter helices must also be topologically resolved. Finally, nuclear division depends on a number of tightly orchestrated events: condensation of chromatin into compact chromosomes, dissolution of the nuclear envelope, movement of chromosomes to a central plate with subsequent splitting of daughter chromatids toward opposite poles, decondensation of daughter chromosomes, and reassembly of the nuclear envelope around them.

Despite the interest in elucidating the means by which cells accommodate these constraints and package their genomes, only a meager sketch of higher order structures can currently be claimed. Beyond the level of the 10 nm nucleosomal fiber, little consensus has been reached. This is particularly true of the highest level of chromosome organization, the 3-D arrangement of chromosomes in the interphase nucleus. For reviews, see refs. 13 and 21.

The giant polytene nuclei of the Drosophila salivary gland provide a convenient model system for analyzing the folding patterns of interphase chromosomes by direct optical methods. These cells can be considered to be in interphase by several criteria (Pearson, 1974). The

basic question addressed in the present work is how a set of chromosomes, which are over 800 μm in total length and average 3-4 μm in width, is packaged within a nucleus that is some 30 μm in diameter. By studying this system with a combination of fluorescence optical sectioning microscopy, 3-D modeling and quantitative analysis, we have been able to discover quite a number of consistent organizational motifs that characterize salivary gland nuclei in vivo.

This report represents a continuation of work begun several years ago (Agard and Sedat, 1983), and a preliminary account of a portion of the current data was described previously (Mathog et al., 1984). In the latter report, we drew several conclusions about the folding patterns of polytene chromosomes based on six nuclei from a single salivary gland. Four more nuclei in this gland were modeled and were discussed in a report on the spatial distribution of transcriptionally active sites (Gruenbaum et al., 1984). Here we discuss the results from a total of 24 reconstructed nuclei from 5 glands: 10 from the original gland analyzed, 7 from another gland of the same inbred stock which had been embedded in epoxy resin, and 7 from larvae of a different wild-type stock. The expansion of the data base as well as several additional methods of model analysis allow a number of new conclusions about nuclear spatial organization to be made. Most of the present results are in general agreement with our preliminary reports, but several of the earlier interpretations had to be changed. A hierarchy of organization that includes features strictly conserved among the nuclei to aspects that are widely divergent is described.

MATERIALS AND METHODS

Salivary gland samples

The method of sample preparation for optical sectioning was essentially the same as described by Mathog et al.(1984). The buffers used in this study were buffer A (Burgoyne et al., 1971) and the physiological buffer of Shield and Sang (1970). Buffer A was made with either 15mM PIPES or 15mM HEPES, 0.15mM spermine, 0.5mM spermidine, 60mM KCl, 15mM NaCl, pH 7.4. The OR-isoX stock (obtained from S. Beckendorf) is a wild type stock that has been made isogenic for the X chromosome. The other stock used is a highly inbred Oregon R stock.

The gland which had been embedded and sectioned was initially part of a uridine pulse-labeling experiment (Gruenbaum et al., 1984). Glands were dissected into Shield and Sang medium and, after the pulse-chase regimen, transfered to buffer A containing 3.7% formaldehyde (freshly prepared from paraformaldehyde (Kodak)). After fixing for 15 minutes, the glands were washed, stained with 3 µg/ml DAPI (4',6-diamidino-2-phenylindole) and refixed for 60 minutes. After washing, the glands were stepped into DMSO, and finally embedded in Spurr epoxy resin (Polysciences). Polymerization was performed overnight at 65°C. Blocks were serially sectioned with a glass knife, and the 0.5 µm thick sections were collected on coverslips. After mapping the location of well preserved nuclei, the sections were photographed on the Axiomat microscope using epifluorescence optics, the images being stored on a computer disk. Sections were aligned computationally (Agard and Sedat, 1983).

For optical sectioning into the partially sectioned Spurr block, a special plexiglas holder was made to hold the block on the stage of the Axiomat. A drop of oil was placed directly on the clean face of the

block for use with a 100X/1.3NA oil lens. 24 serial optical sections were taken for each nucleus using a step size of 1.3 μm, exactly as was done with glands observed in aqueous buffer.

To observe the salivary glands within the living animal, third instar larvae were washed in buffer and placed on clean slides; an 18x18mm no.1 cover slip was taped firmly over each while making sure the ventral aspect of the larva faced toward the cover slip. The larva cannot crawl away, and the obstructing fat body is often pushed out from between the salivary gland and the body wall, exposing the gland for viewing. A 100X/1.3NA Planapo objective lens was used, and the field diaphragm was closed down almost completely. Banded chromosomes are readily followed under these conditions.

Microscopy and model building

The computered-controlled Zeiss Axiomat microscope for serial optical sectioning of polytene nuclei was as described (Mathog et al., 1984; Mathog et al., 1985). Some hardware changes have been made. The Commodore Pet microcomputer that was used to control the focus stepping motor has been replaced by a Z8 microcontroller (Micromint). The focus-stepping motor itself has been replaced by a microstepping motor (Compumotor). A lamp shutter, also controlled by the Z8, has been added to minimize unnecessary exposure of the sample.

The model building and analysis program IMP has also been delineated (Mathog et al.,; Mathog, 1985; Mathog et al., 1985), although its capabilities have been expanded. None of the images from the aqueous samples were processed computationally. We found it helpful to apply Fourier filtering and out-of-focus removal algorithms to the

blurrier images obtained from the optically sectioned embedded gland (details in Gruenbaum et al., 1984).

Quantitative analysis of models

The histograms of triple product values (Fig. 3) were derived as follows. The model arm is divided into 512 evenly spaced points. Beginning at one end of the arm, a set of 3 consecutive vectors is placed on the model to connect points at 7 μm intervals. The triple product of their unit vectors, T=A•(BxC), is then calculated (Mathog, 1985). "•" is the inner product, "x" the cross product. The value is assigned to the midpoint of the model path between the outer ends of the 3 vectors, i.e., 10.5 μm from the model's end. The set of vectors is then shifted along the model path by one point and the calculation is repeated. This entire procedure is continued until the leading end of the vectors reaches the other model endpoint. The range of triple product values so produced is then divided into 100 intervals, and the values are histogrammed. This was done in all 24 nuclei for each chromosome arm; each histogram in Fig. 3 thus represents the distribution of triple product values summed over 24 chromosome arms.

A point on a chromosome model that falls within 1 μm of the nuclear surface was defined as a nuclear envelope contact. To test the association between such contacts and loci containing intercalary heterochromatin, each chromosome was divided into intervals of 3 letter subdivisions (e.g.12A-C), and any interval in which the contact frequency (Fig. 5) was at or above the $p' .05$ cutoff (see Results) was counted in the tabulation. Only weak points present in at least 20% and

ectopic fiber sites present in at least 15 out of 550 of the squashes of Zhimulev et al. (Zhimulev et al., 1982) were counted as intercalary heterochromatin loci. The last four intervals (2 divisions) closest to the chromocenter were not used. The χ^2 formula is

$$\chi^2=n(ad-bc)^2/((a+b)(a+c)(b+d)(c+d))$$

where a= the number of intervals with both a high frequency contact and intercalary heterochromatin, b= number of intervals with no contact but intercalary heterochromatin, c= number of intervals with a contact but no intercalary heterochromatin, d= number of intervals with no contacts and no intercalary heterochromatin, and n= a+b+c+d. The same statistic was used to evaluate the correlation between the high frequency surface contacts in the different contributing data sets used in this study. In these cases, a 0.5 μm limit was used to generate the frequency plots. The frequency cutoffs for the different sets were as follows: nuclei with split chromocenters (see Results), 4-5 out of 5; nuclei from the embedded gland, 5-7 out of 7; and nuclei from the original unfixed gland, 7-10 out of 10.

The Monte Carlo procedure used to estimate the random probability distribution for surface contact frequencies for a chromosome arm works as follows. Distance-to-surface plots, which plot the minimum distance between each cytological position and the nuclear surface versus cytological position (e.g., Fig. 6 in ref. Mathog et al., 1984) provide the set of input distance values. One distance value is randomly chosen from each of the 24 plots for a chromosome arm. The 24 selected values are then compared to the cutoff value of 1 μm used to generate the surface contact frequency plots, and the number of values less than or equal to the cutoff is counted. This entire procedure is reiterated 10^6

times. The final result is a tabulation of the frequencies with which 0,1,...24 out of 24 randomly selected values fell within the cutoff distance.

Chromosome intradistance plots (Fig. 7) were generated as described previously (Mathog, 1984). To generate a set of control intradistance plots with intradistance values randomly displaced with respect to position on the chromosome, the values in each of the original plots were shifted by a random amount in a direction along the diagonal (see Fig. 7); the magnitude of the shift is different for each plot. The shift causes a portion of the distance values to roll off the right side of the plot; this is then patched back onto the bottom. The entire transformation can be visualized as follows (see diagram). An isosceles right triangle placed on its side (=intradistance plot), originally superimposed over a second (Agard and Sedat, 1983), is displaced by some amount along the diagonal (Appels et al, 1979). The region of overhang where the top triangle no longer overlaps the other (indicated by cross-hatching) is cut off and pasted to the exposed portion of the bottom triangle. This involves a 90° counterclockwise rotation in the plane of the paper and a reflection across the x-axis. This method introduces a discontinuity at the border of the patch but retains all the distance information from the original plot; moreover, the displaced intradistance values remain at their original distances from the diagonal despite being in new places with respect to cytological position (this is illustrated by the shaded section in the diagram). The mean and standard deviation of the randomly superimposed distance values at each point are then calculated as before.

RESULTS

The approach we have taken to describe the spatial arrangement of chromosomes is direct and in principle quite simple. The specimen is stained with a DNA-specific fluorescent dye and prepared for microscopy. Fluorescence images from serial sections of nuclei are collected, and from such image stacks, the paths of the five major chromosome arms are traced using an interactive modeling program (IMP; Mathog et al., 1984; Mathog, 1985; Mathog et al., 1985). Subsequently, quantitative properties of the resulting stick figure models are measured and displayed. The models and quantitation plots are used to derive a detailed structural description of chromosome folding. Details of methodology are published elsewhere (Mathog et al., 1984; Mathog, 1985; Mathog et al., 1985), and any modifications are noted under Materials and Methods.

Orderly large scale organization of chromosomes

Several general organizational features discovered by Mathog et al. (Mathog et al., 1984) by inspecting stereo-pair models of nuclei have been further documented in the present study. First, the chromosome arms are always maintained in separate spatial domains within the nucleus, with no arm looping around another even though the chromosomes are highly contorted and closely packed (Figs. 1,8). Second, the centromeric regions of salivary gland chromosomes, which are usually aggregated together to form an amorphous mass called the chromocenter, are always positioned against the nuclear envelope. Such an invariant association between centric heterochromatin and the nuclear envelope recalls a similar situation documented in Drosophila early embryos

(Ellison and Howard, 1981; JWS, unpublished). In early embryos the chromocenter is always at the edge of the nucleus closest to the topological exterior of the embryo. In contrast, the chromocenter in salivary gland nuclei is found in a wide range of positions relative to the gland lumen; our earlier inference of a very limited range (Mathog et al., 1984) is therefore not generally true. Finally, a related motif of chromosome organization that is observed is the Rabl orientation (Rabl, 1885; Foe and Alberts, 1985; Fig. 1). This is the grouping of centromeres near one pole of the nucleus with the telomeres arrayed in the opposite hemisphere. 80% of the chromosome arms have configurations that fulfill this criterion.

Preferred relative arrangements of chromosome arms

Considerable effort has been directed toward determining whether there are any favored relative arrangements of chromosomes within the nucleus (4). Perhaps the best evidence for nonrandom chromosome positions has been reported by Bennett (1983), who looked at centromere positions in thin-sectioned mitotic plant cells. Coates and Smith (1984), however, employing the same method of analysis as Bennett, came to the opposite conclusion for hybrid grasshopper cells. We find that the relative arrangement of the major chromosome arms in salivary gland nuclei is not entirely arbitrary. Because the bulk of each arm is generally situated between only two neighboring arms and the arms lie in noninterwoven domains (analogous to the sections of a grapefruit), it is usually straightforward to determine their relative arrangement. Fig. 2 shows the the different arrangements in schematic fashion; in one of the nuclei the relationships cannot be uniquely assigned and are therefore not included. As can be seen, 2L and 2R are almost always next to each

other; the same is true for 3L and 3R (21/23 in both cases). Besides these, the strongest preference for particular arrangements of arms is seen if one groups the nuclei according to whether the right arms of the autosomes and/or the left arms are next to each other ("cis") or are in the complementary arrangement ("trans"). The cis constellation is seen more than twice as often as the trans. It remains possible, however, that this is a sampling effect; even if a 1:1 ratio of these two types actually exists, such a bias in a sample of this size is not significant (χ^2=1.45, P>.20). Other small biases in the relative frequencies of nearest neighbor pairs pointed out previously (Mathog, 1984) may also have been due to sampling. The X chromosome, for example, while almost always between the two autosomes, is not preferentially positioned next to any particular arm. In only one nucleus were the arms from autosomes 2 and 3 interdigitated (but not entangled).

Relative positions of chromosome arms can be assessed in several additional ways. One is to calculate the center of mass of each arm and measure the distances between them. Another is to look at the interdistance maps for each pair of arms in each nucleus and find which pairs have the highest number of close sites. Both methods yield the same qualitative conclusions just described (data not shown). Thus, it appears that the arms of each autosome remain close together in the nucleus, whereas other relative arm positions vary considerably.

Chromosome coils are right-handed

It is evident from the models (Figs. 1,8) that a dominant folding motif of the salivary gland chromosome is the coil. What is more striking, however, is that these coils almost always appear to be

right-handed (see also Fig. 3 in Gruenbaum et al., 1984; Mathog et al., 1984). This is a surprising result as no such chirality has previously been reported either in mitotic or polytene chromosome coiling (Beerman, 1962; Manton, 1950). To demonstrate the asymmetry by an independent and more quantitative method, we have employed the triple product, a standard vector operation, which has been used previously to analyze helices in proteins (Braun, 1983). The triple product, A•(BxC), where A,B,C are successive vectors along a path, yields a scalar value whose sign depends on whether the vectors' relative orientations in space follow a left or right handed screw. A positive value indicates a right-handed screw, a negative value a left-handed one. Here we use a set of three unit vectors connecting points located at 7 μm intervals along the model arm. The set of vectors is slid along the model path and their triple product is calculated at each of 512 equally spaced points (Mathog, 1985; Materials and Methods). Fig. 3 displays histograms of the triple product values for the five major arms gathered from all 24 nuclei; zero is at the center. The distributions are all strongly skewed to the right, with the ratio of positive to negative values ranging from 2.0-2.7. This demonstrates that the direction of coiling along each chromosome is indeed predominantly right-handed.

Two comments need to be made about these plots. First, the selection of a particular vector size acts as a filter for curves in that size range. Vectors spaced at 7 μm intervals were chosen because the patent coils seen in the models are some 15-30 μm long; this set of 3 vectors samples the pathway in the desired range (3x7μm=21μm). Use of other sizes, however, yields qualitatively similar plots as long as they are not extremely small or large. Second, there are certainly segments

of some chromosomes that are not particularly coiled. These, along with coils of little or no pitch, will contribute to a set of triple-product values at or close to zero; also, although almost no clearly coiled regions are left-handed, some stretches, especially around sharp bends, do yield negative triple product values.

Preliminary evidence suggests that a chromosomal region need not be homologously paired for it to display a right-handed chirality. We have found an example (Fig. 4) of a 3L chromosome arm that has an asynapsed region stretching from about 63A to 69A, over a third of the arm's length. The coils in the thinner, unpaired homologs are smaller than in the synapsed regions, but they are still right-handed. This is confirmed in their respective triple product plots (not shown).

A set of loci regularly contact the envelope

Previously, we tabulated a set of loci which were almost always positioned against the nuclear envelope in the six nuclei examined (Mathog et al., 1984). Now, having 24 reconstructed nuclei from five larvae of two different stocks, we can make a statistically more meaningful statement about which loci are frequent surface contacting sites. The individual data sets were first examined separately. We observed a certain amount of variation between them which may be stock or larva specific; for example, the 5F/6A site is on the surface in 10 out of 10 nuclei in the original gland but is rarely there in all the other nuclei examined. However, the majority of high frequency surface contact loci are the same among the different sets of nuclei (see below). While the variations may have significance, we do not yet have enough data to evaluate them properly. Consequently, we have pooled the

surface contact frequencies for all 24 nuclei, thereby concentrating on the contacts preserved in all data sets.

Pooled envelope contact frequencies for the 5 major arms are shown in Fig. 5. Each arm is divided into 512 evenly spaced points; when a point falls within 1 μm of the nuclear surface, the point is counted as a contact site. As described previously (Mathog et al., 1984), cytological bands on the chromosomes are identified and used as fiducial marks when comparing the same chromosome in different nuclei. The frequency with which a locus apposes the nuclear envelope in this set of nuclei varies markedly along the length of each chromosome arm. Some regions are on the surface in almost every nucleus examined, others in a majority of cases. However, to judge the significance of the frequency peaks (and valleys) it is necessary to determine how often one would observe such frequencies if surface contacting regions were located randomly on each chromosome arm. Rather than assume a particular type of random frequency distribution, a Monte Carlo procedure was used to generate one from the input data so that the random distribution would match the real data in the percentage of the arm in each nucleus that was in contact with the surface. The procedure is described in Materials and Methods.

All frequency peaks whose probability of occurring randomly is less than 0.05 (probability of occurring this many or more times) are marked with arrows in the plots. This cutoff is somewhat arbitrary. It was chosen so that only peaks with a relatively low probability of representing random juxtaposition would be considered, but it is not low enough to eliminate this possibility. By this criterion, at least 15 loci along the chromosomes are on the nuclear envelope with frequencies

that are unlikely if contacts were only made randomly (see figure legend). However, additional information is needed to verify whether the indicated peaks are specific for particular chromosomal loci.

We searched the literature for evidence of any structural peculiarities common to these loci (Mathog, 1984). A comparison of our persistent envelope contacts to the positions of intercalary heterochromatin mapped by Zhimulev et al. (Zhimulev et al., 1982) reveals a very strong correlation between the two. intercalary heterochromatin is a term for sites along the chromosomes with properties typical of centric heterochromatin from either polytene or diploid cells. These include frequent ectopic fibers, constrictions in polytene squash preparations, late replication, frequent breakage from irradiation, and certain chemical (Barr and Ellison, 1972) and genetic properties (Spofford, 1976).

In Fig. 5, 14 of the 15 regions marked with arrows are centered on loci which show frequent ectopic pairing and/or weak point behavior, two of the most stringent criteria for the presence of intercalary heterochromatin. The degree of association was evaluated from a 2x2 contingency table with a chi-square statistic and was found to be highly significant (χ^2=23.7, P‘‘.001; see Materials and Methods). An examination of intercalary heterochromatin sites in section images suggests this correlation may indeed be relevant (Fig. 6). These sections show intercalary heterochromatin bands that appear to be pulled out toward the nuclear surface, suggesting a physical connection. A section with chromocenter material pressed against the surface is also shown. To summarize, three sets of observations argue that specific loci are involved in frequent chromosome-envelope interactions: 1) a set

of loci are on the surface with high frequency 2) almost all of these loci coincide with intercalary heterochromatin positions; and 3) these sites often appear in physical sections to be attached to the surface. It should be noted that although some of the lowest dips in Fig. 5 are as statistically unlikely as some of the peaks, there is no correlation with intercalary heterochromatin (χ^2=1.68, P>.10), again using a P<.05 cutoff; we have not yet found any other structural correlates to these sites, so their biological significance remains unknown.

Chromosomes assume a wide variety of configurations

Several studies have shown a restricted spatial distribution of certain DNA sequences in the nucleus (Hammon and Laird, 1985; Lifschytz and Haravan, 1982). Some authors have suggested that the configurations of chromosomes within the interphase nucleus are under specific genetic control (Steffenson, 1977; Sved, 1976). In a direct approach to these problems, we have been analyzing chromosome folding patterns with the aid of "intradistance" plots (Rossman and Liljas, 1974; Mathog et al., 1984). For such plots, the absolute distances between all pairs of points on a chromosome model are measured (the model path is traced through the approximate center of the 3-4 μm thick arm) and then plotted on a two-dimensional map in which each axis represents cytological position along the arm. The pattern of intensity values is therefore a mapped representation of the 3-D folding of the chromosome.

Fig. 7a shows a sample intradistance plot of chromosome arm 2L from one nucleus. The contoured set of distances are displayed as intensity values, the darkest regions representing pairs of chromosome points that are closest together in space. Contour steps are 2 μm, and

intradistance values larger than 10 μm are not displayed. This representation of the arm's configuration reveals a variety of appositions between loci. When such maps are compared for the same chromosome in different nuclei, common contacts and configurations should be apparent if they are present.

One way to compare all the nuclei with a data set of this size is to generate a mean intradistance plot. Such a plot is shown in Fig. 7b for chromosome 2L that is derived from the 24 individual 2L intradistance plots. Loci that are consistently paired in the different nuclei would appear as dark areas off the diagonal. In none of the mean plots for the 5 major arms are such areas present. When the standard deviations of the intradistance values between each pair of loci are plotted in a 2-D map (Fig. 7c), they show a general increase with distance from the diagonal. In fact, they increase roughly linearly with the corresponding mean intradistance values, although several areas in Fig. 7c show small standard deviations in places where the mean values are relatively high.

These plots therefore appear to provide little evidence of closely circumscribed 3-D chromosome configurations. This view is strengthened by the following control experiment. As described in Materials and Methods, intradistance values were randomly displaced relative to cytological position by a different amount in each of the 24 plots, and these randomly shifted plots were then compared. The shifts scramble the distance information, and the resulting mean and standard deviation plots reflect only the random overlap of the original plots' features. The resulting mean plot for the randomly shifted data is shown in Fig. 7d. The similarity to Fig. 7b is striking: regular contacts are limited

to regions close to the diagonal and mean intradistances increase at a similar rate with distance from the diagonal. Likewise, the standard deviation plot for the randomized data is also qualitatively very similar to Fig. 7c, with standard deviation values increasing no more rapidly with distance from the diagonal and with several regions of low standard deviation off the diagonal (plot not shown). The simplest explanation for these results is that the observed interactions primarily reflect the confinement of the chromosome to a very restricted volume with no requirement for specific pairwise interactions between loci (see below).

It could be argued that several different well defined sets of interactions are present in the different nuclei, but by considering them all together this information is obscured. The issue has been tested in two ways. First, we studied printouts of the 24 individual 2L plots and attempted to sort them into groups according to shared folding features using their off-diagonal patterns of intensity (e.g., Fig. 7a). No two plots exhibit a similar set of off-diagonal contacts, so no two 2L chromosome arms can have very similar longer range interactions (i.e., interactions between loci separated by more than 1-2 cytological divisions). Second, the 24 plots were transformed into a set of 24 "rank order" plots (Mathog et al., 1984). The values that are ranked in ascending order are the 24 intradistance values recorded at each pixel. Thus, the original plots are reorganized into a set in which each pixel in the rank=1 plot contains the lowest intensity value (closest contact) recorded at that pixel in the original set of plots, each pixel in the rank=24 plot the highest. For instance, if a pixel in the rank=12 plot has an intensity corresponding to a 5 μm separation, then the pair of

loci denoted by that pixel are within 5 μm of each other in at least 12 of the 24 nuclei.

The off-diagonal features rapidly disappear as one goes up in rank (data not shown). By rank=6, 36D-38C are the only loci separated by more than about one cytological division (~7-8 μm) that are within 4 μm of each other. That is, no pair of widely spaced loci besides this one is closely apposed in even one fourth of the nuclei. No model sites separated by more than one cytological division come within even 5 μm of one another in 12 or more nuclei. So although there may be some similarities in the local bending of the arm in some of the nuclei, there is little support for a unique or small number of similar longer-range configurations. These results argue that the variation seen in the pooled data cannot be explained simply by positing the existence of a small number (say, 2-3) of classes of nuclei with different but uniform chromosome folding patterns.

That contacts between loci are generally not specific is further supported by performing the same ranking operation on the 24 randomly shifted intradistance plots described above. When the real and the randomized data are compared, it is found that the off-diagonal features disappear just as quickly in both as one goes up in rank (data not shown). The ranked features are also similar in shape and distribution, suggesting that in both cases they arise from the chance overlap of intensities. It therefore appears that no longer-range chromosome interactions are the same in more than a small number (at most 25%) of the nuclei examined; moreover, in the absence of additional information, the shared contacts in such small subsets of the data cannot presently be distinguished from random juxtapositions.

Chromosomes packaged similarly in nuclei with split chromocenters

From the reconstructions of several salivary gland nuclei from another wild type stock of Oregon R flies (here referred to as OR-isoX), it was discovered that the centromeric regions were occasionally split into two well separated chromocenters. Hence, they cannot be organized in the usual Rabl orientation. Such separation of the normally fused centromeric sequences seems to occur in a small fraction of nuclei as it has been observed now in a number of larvae. Both Appels et al. (Appels et al., 1979) and Hammond and Laird (Hammon and Laird, 1985) have reported examples of salivary gland nuclei with two separate hybridization sites to a chromocenter specific DNA probe, so the phenomenon may not be uncommon.

Nuclei with split chromocenters provide a natural test for the question of whether a major change in the relative positions of portions of the chromosome complement will affect other aspects of chromosome packaging. For instance, are chromosomes still kept in spatially distinct domains when the orientation of some of the arms is flipped relative to their neighbors? Two OR-isoX nuclei with single, intact chromocenters have been modeled and exhibit the same organizational motifs discussed above (nuclear envelope contacts were not evaluated since with only two nuclei, they could not be reliably analyzed). Hence, any differences observed in the nuclei with split chromocenters should not be due to stock variations.

We have been able to find five nuclei with split chromocenters to date. In 4 out of 5, the centromeric region of the second chromosome is found 15-30 μm away from the other chromocenter; in the fifth, chromosome 3 is split off. Fig. 8 is an example of a nucleus in which

separate chromocenters are on almost opposite sides of the nucleus (a neighboring nucleus shows a similar large split). Despite the reconfiguration, all chromocenters are still apposed to the nuclear envelope, the arms remain in domains, chromosomes coil into right-handed gyres, the arms of each autosome are usually close together, and most of the high frequency nuclear envelope contacts are the same. This last conclusion follows from a comparison with the 10 nuclei from the original gland; the correlation of high frequency contacts between the two data sets was evaluated from a 2x2 table as above and was shown to be statistically significant (χ^2=4.97, P‘.05; see Materials and Methods). As might be expected from the results presented above, the high frequency contacts in the nuclei with split chromocenters are also associated with intercalary heterochromatin loci (χ^2=8.44, P‘.01).

Different preparative procedures do not alter organizational rules

The gland yielding the first set of ten reconstructions and the OR-isoX glands were all viewed in an aqueous buffer optimized for chromosome structure preservation (buffer A) and were not fixed. However, the organizational rules described are independent of the preparative procedures used. A very different procedure was used for comparison (Gruenbaum et al., 1984; Materials and Methods). Glands from a late third-instar larva of the inbred wild-type stock were fixed, dehydrated, and embedded in Spurr's resin. After collecting a set of serial physical sections, optical section data were obtained from the unsectioned remainder of the embedded gland by focussing into the block. Two nuclei were reconstructed from aligned physical sections, five from the optically sectioned block. The glands were estimated to be in

puffing stage (PS) 5-6 (Ashburner, 1972); the glands in the other data sets were in PS 7-8.

The nuclei show all of the structural features exhibited by the other sets of nuclei (data included above). The high frequency contacts are similar to those in the original unfixed gland of the same stock (χ^2=5.48, P‘.02), and correlate strongly to intercalary heterochromatin loci (χ^2=9.98, P‘.01). Thus, the structural motifs we could observe in the unfixed, minimally processed glands are maintained in embedded and physically sectioned nuclei, even though the glands are slightly different in developmental (i.e., puffing) stage. These results and those of the previous section provide the justification for considering all 24 nuclei from a total of five female larvae together in the preceding results.

Controls

Although the aim of the present work was to determine the in vivo folding of salivary gland chromosomes, the glands were not actually observed in vivo, strictly speaking. It is therefore necessary to show that the chromosomes do not rearrange appreciably as a result of our manipulations. To this end, several control experiments were performed. First, the same nucleus was optically sectioned at both the beginning and the end of a data collecting session and the two data stacks were compared by visual inspection. No differences were noted. Second, glands were dissected into buffer A or physiological buffer and immediately mounted for viewing with bright field optics. The banded chromosomes are easily discerned under these conditions, and any

movement over a time period of minutes to hours would be detected. None was.

Our analysis is also based on the assumption that chromosome positions are relatively stable when the glands are in their normal milieu. To test this, salivary gland nuclei were viewed directly through the ventral body wall of living third instar larvae that had been immobilized between a cover slip and slide. Active movements within the body cavity continue, but it is not difficult to track particular banded regions in a single nucleus for several hours and thereby examine the relative positions and orientations of chromosome segments. No obvious repositioning of any chromosome region within the nucleus until histolysis was detected. During this latter period, cells become increasingly vacuolated and the chromosomes then do shift appreciably. Hence, since the glands we have examined are not histolysing, we are confident that our data describe the authentic in vivo configurations of chromosomes.

DISCUSSION

We have described a number of regular motifs that characterize the organization of salivary gland nuclei. They include: invariant association between the chromocenter and nuclear envelope, confinement of the arms to non-intertwined spatial domains, certain nonrandom relative chromosome arm positions, Rabl orientation of chromosomes, envelope contacts that are locus specific and correlate with intercalary heterochromatin, and a large predominance of right-handed chromosome gyres. On the other hand, chromosomes fold into a wide variety of configurations that bear few obvious similarities between nuclei.

Moreover, a gross relative repositioning of a portion of the genome in nuclei with split chromocenters does not alter any of the above motifs (except the Rabl orientation). In sum, a scheme of chromosome packaging can be described that contains both well ordered and apparently indeterminate features.

To interpret our results, it is useful to seek parallels with the organization of diploid nuclei. In what follows, much of the present data is rationalized through a consideration of the origin of the salivary gland as a diploid rudiment in the early embryo (Sonnenblick, 1950). This interpretation implies a high degree of positional stability of interphase chromosomes since many days have passed between the final embryonic mitosis and the stage at which we examine the gland. This is especially striking when one considers that in the intervening period the nuclei have increased in volume several hundred-fold and undergone 9-10 additional rounds of DNA replication. A stable intranuclear chromosome topology has been inferred from a number of different studies with diploid cells (Herreros and Gianelli, 1967; Sperling and Luedke, 1981; Zorn et al., 1979). Moreover, the retention of similar relative positions of chromosomes through an entire cell cycle has also been seen (Pera and Schwarzacher, 1970). We also know from our control experiments that at least in the last hours of third instar, salivary gland chromosomes are likely to be immobile.

The Rabl orientation has been repeatedly documented in diploid cells (Comings, 1980; Foe and Alberts, 1985; Fussell, 1975), where it is regarded as a relic of mitosis. It seems unlikely that it has a completely different cause in polytene tissues. The fact that the arms of each autosome are almost always close together (Fig. 2) is also

consonant with the retention of telophase chromosome positions during polytene interphase.

Normal telophase chromosomes are dense structures that are topologically separable from one another. It is tempting to view the nonintertwined chromosome arm domains in third instar salivary gland nuclei as a vestige of this mitotic condition. In other words, as the cell progresses into interphase, the unraveling of each chromosome takes place entirely within the boundaries presented by neighboring chromosomes and the nuclear envelope. Indeed, the orderly condensation and division of chromosomes in mitotic cells supply a possible rationale for maintaining stable, noninterwoven domains during interphase. Drosophila chromosomes must nevertheless find and synapse with their homologs since it is known from neuronal cells and cell culture lines that during metaphase and anaphase, homologs are not tightly paired (7,19); this requires local chromosome movement and fusion of homolog domains. A striking example of the strength of these pairing interactions comes from flies heterozygous for a whole X chromosome inversion; after completing mitosis with the centromeres of the two homologs aligned, a complete reorientation of one homolog relative to the other occurs, allowing the two to synapse (Becker, 1969).

The surface contact data (Fig. 5) reveal a number of preferred associations between the chromosomes and nuclear envelope. There are, however, additional peaks in the plots that fall below our statistical cutoff which may also be specifically positioned at or interacting with the nuclear surface. For example, a smaller peak is observed at 25EF on 2L that coincides exactly with an intercalary heterochromatin site. However, we can only discuss with confidence loci that have a very

strong propensity for making nuclear envelope contacts. Possibly, an intercalary heterochromatin locus's position within a chromosome may modulate its ability to reach the surface; small translocations which move a surface contacting locus to new positions should help answer this question. Finally, groups of individual distance-to-surface plots from different nuclei sometimes look quite similar over considerable stretches (see Fig. 6 in Mathog et al., 1984), and we are currently examining whether this can be interpreted in terms of discrete, alternate chromosome attachment patterns.

A plausible way to view these results is that as a cell emerges from mitosis, a large number of chance contacts with the nascent envelope occur, with a subset of loci making more stable associations. As the nucleus progresses into interphase, these associations tend to persist. It is also possible that the high frequency contact loci represent preferred nucleation sites for envelope reformation. The correlation of the contacts with intercalary heterochromatin suggests that the heterochromatic nature of these loci allows them to bind more tenaciously than other loci to envelope structures and may account for the selectivity. Such a contention is supported by the data in Fig. 6 as well the micrographs of Quick (1980) and Gay (1956), showing the adhesion of ectopic fibers or dense heterochromatic material to the nuclear envelope. The idea that nuclear envelope attachments are established relatively early in salivary gland development is lent credence by the fact that heterochromatic material is known to bind to the nuclear envelope in diploid nuclei (Comings, 1980). This may also explain, at least partly, the long term positional stability of interphase chromosomes discussed above.

The strong predominance of right-handed chromosome gyres over left-handed ones is a novel finding that is at odds with previous studies in which the direction of polytene chromosome windings was investigated (Beerman, 1962; Koller, 1935). This discrepancy is probably traceable to the complexity of folding, which makes it extremely difficult to follow the chromosome paths without the aid of reliable 3-D modeling and cytological mapping. Furthermore, the coiling is neither absolutely right-handed nor obviously localized to particular stretches of the chromosome.

The source of the coiling asymmetry is unknown. The extensive literature on the regular spirals seen in mitotic and meiotic chromosomes gives no indication of such a chirality (Manton, 1950; Ohnuki, 1968), so it seems unlikely that our finding can be explained as a vestige of mitotic coiling. It could arise from some chiral aspect of the association between the chromonemata making up the polytene chromosome, which, conceivably, may originate in the right-handed DNA duplex itself. A more speculative possibility is that some of the positive helical torsion engendered by unwinding DNA, e.g., during replication, can be partitioned into higher levels of chromosome folding where it is resistant to full relaxation.

The present results do not reveal any precise long range configurations of chromosomes. More exactly, the data show that no pair loci more than one or two cytological divisions apart is positioned close together in a large fraction of the nuclei examined. This result differs significantly from our preliminary account (Mathog, 1984), where we had suggested the existence of specific chromosomal loops extending over as many as five cytological divisions. It now seems likely that

such long range contacts coincide in only a small percentage of nuclei. The apparent conclusion is that the precise geometry of a salivary gland chromosome is not determined, and specific pairwise interactions between widely spaced genetic loci are not obligatory. More complicated combinatorial schemes, with different but specific interactions between multiple loci, have not been addressed in this study; ectopic fibers, for example, may connect sites in this way.

There remain a number of alternative explanations that are consistent with both our data and the possibility of determinate structural interactions between genetic loci. For instance, specific interactions may exist in distinct subpopulations of the gland's cells and/or in particular cell-positions in the gland. There is some evidence for heterogeneity in cell type within the salivary gland (Probeck and Rensing, 1974). Consequently, the wide variation seen between nuclei may not be due to random folding but to cell type-specific differences. We have not found any obviously related subsets among the intradistance plots (see Results), but a multivariate statistical analysis is being initiated to examine this point further. Another arguable possibility is that a particular chromosome configuration is only important during the diploid or early polytene stages of the gland's development, and when we look at it, it may no longer be constrained, even though the grosser organizational motifs are retained.

These alternative explanations imply a degree of folding complexity that will make the further study of chromosome geometry correspondingly more laborious. It will be recognized, for example, that if chromosome configurations, although specific, vary from one set of cells to the

next, then a direct investigation of their functional significance and the mechanisms by which they are established may be very difficult. Likewise, if specific chromosomal interactions occur early in gland development but are transient, it may be necessary to determine the 3-D structure of many nuclei from many time points in the gland's early development, including diploid stages; this is a formidable task. Examination of these possibilities will require the development of new methods that allow the rapid assessment of chromosome structures in many nuclei and/or in the same few cells from many samples.

The similarity between nuclei with split chromocenters and those with intact ones suggests that organizational rules such as chromosome domain separation and specific chromosome-nuclear envelope contacts are independent of gross chromosome placement within the nucleus. One implication, for example, is that the nuclear envelope structure(s) to which the specific intercalary heterochromatin loci and centromeric regions apparently attach is probably not uniquely configured relative to these sites, i.e., each particular chromosome attachment locus does not have a unique position on the nuclear envelope. Thus, it is unlikely that such interactions could contribute to a single defined geometry for each chromosome. Second, the preservation of domain boundaries in these nuclei strongly supports the notion that a direct physical impedence between chromosomal regions is responsible for their separation rather than some specific scaffolding scheme. Similarly, these nuclei provide prima facie evidence against obligatory pairwise interactions between loci on different chromosomes.

Several projects in progress in the lab will bear on the interpretation of the present results. A large number of nuclei are

being reconstructed from a single, physically sectioned salivary gland to determine whether any organizational features vary in a regular fashion from one region of the gland to another. Nuclei with ring and inverted chromosomes are also under investigation. Finally, we are examining several other larval tissues with polytene nuclei to learn which packaging motifs are tissue specific and which represent general properties of polytene nuclei.

Figure 1. A stereo pair model of a salivary gland nucleus. The figure shows the generally polarized orientations of chromosomes (3R is an exception) and the absence of any intertwining between arms. Chromocentral endpoints for each arm are marked with squares; telomeres are indicated with crosses. Note that the proximal heterochromatic portions of the arms that form the chromocenter are not modeled, so the arms of each chromosome are not connected. The color code of the arms is: X=green; 2L=red; 2R=blue; 3L=purple; 3R=light green. The diameter of the model is about 32 μm.

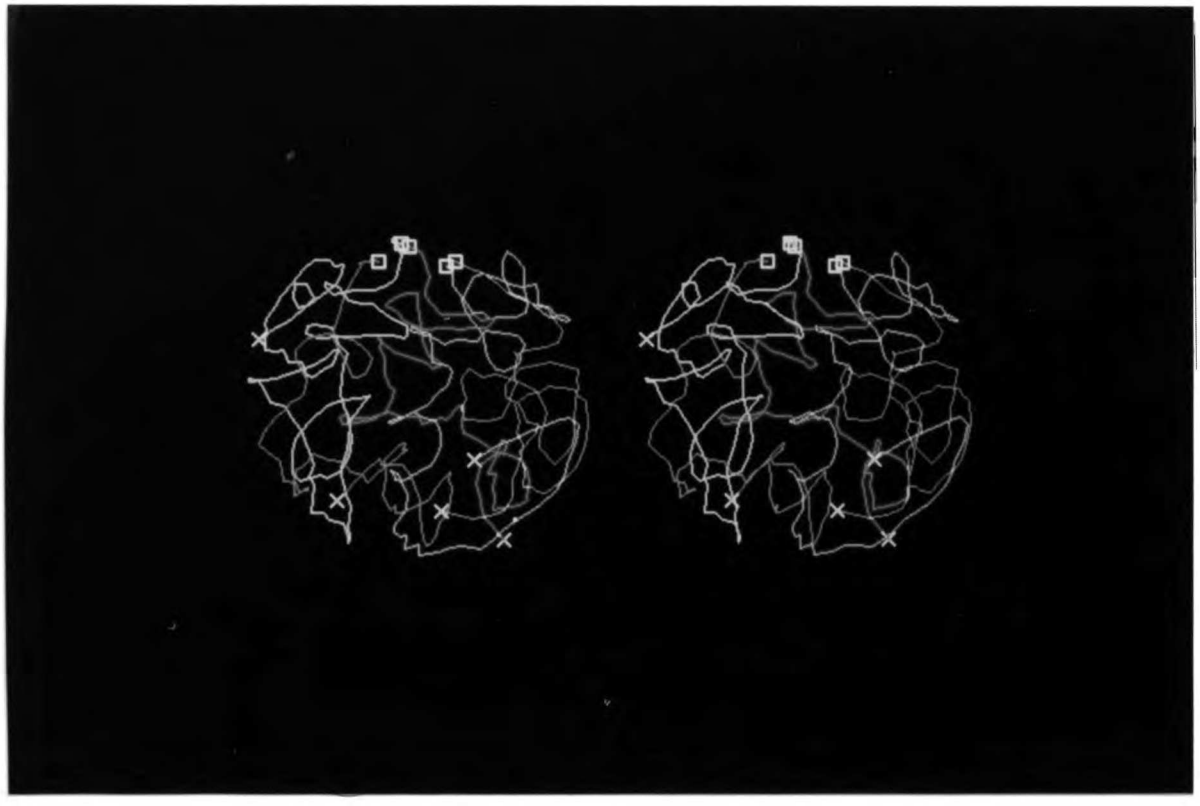

Figure 2. Relative arrangements of chromosome arms. In one nucleus relative arm positions cannot be assigned uniquely and so cannot be included in the figure. In another nucleus the arms from the different autosomes are interdigitated, and it is omitted here for clarity. 15 of the remaining 22 nuclei are in the cis arrangement, 7 in the trans (see text for definitions). The various positions of the X chromosome are shown with dashed lines. The number of nuclei in which it is in each position is noted.

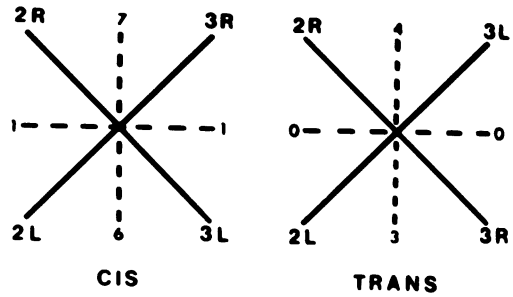
2R
7
3R
1
1
2L
6
3L
CIS
2R
4
3L
0
0
2L
3
3R
TRANS

Figure 3. Triple product value histograms for each major arm. Values are summed from 24 nuclei. See text for details. The vertical scale is arbitrary. The center line in each histogram is at the point of "zero handedness", i.e., the triple product value equals zero. All values to the right of this line are positive and indicate right-handedness, and the opposite is true of those values to the left of it. The ratios of positive to negative values using a 7 μm spacing between unit vectors are: X(2.0), 2L(2.0), 2R(2.5), 3L(2.2), and 3R(2.7). To avoid end effects when calculating the triple products, the calculation is terminated when any of the vectors reaches an end of the chromosome path.

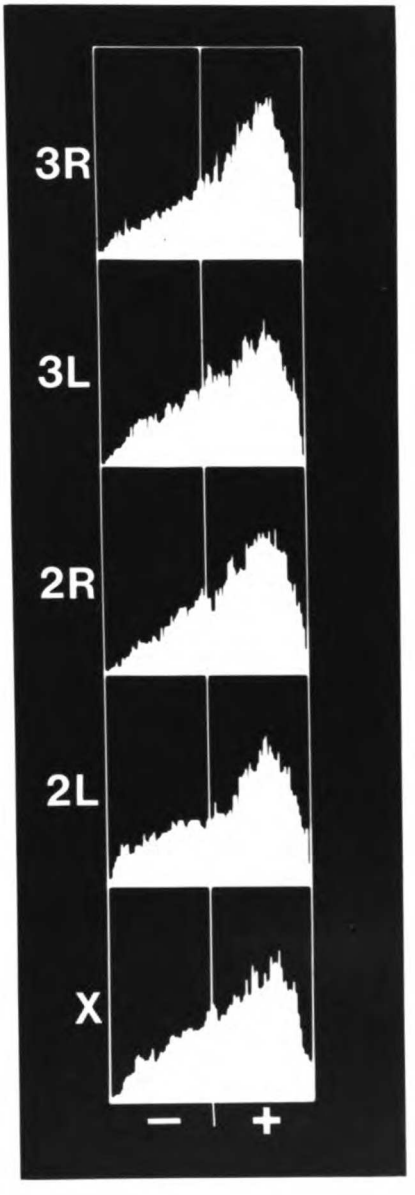
3R
3L
2R
2L
X
−
+

Figure 4. Asynapsed 3L chromosome arm. The region of asynapsis extends from about 63A to 69A (endpoints marked with arrowheads). Right handed coils are evident in both the synapsed and asynapsed portions of the arm, the latter having smaller radii. The scale is the same as in Fig. 1. The proximal endpoint is marked with a square, the telomere with a cross.

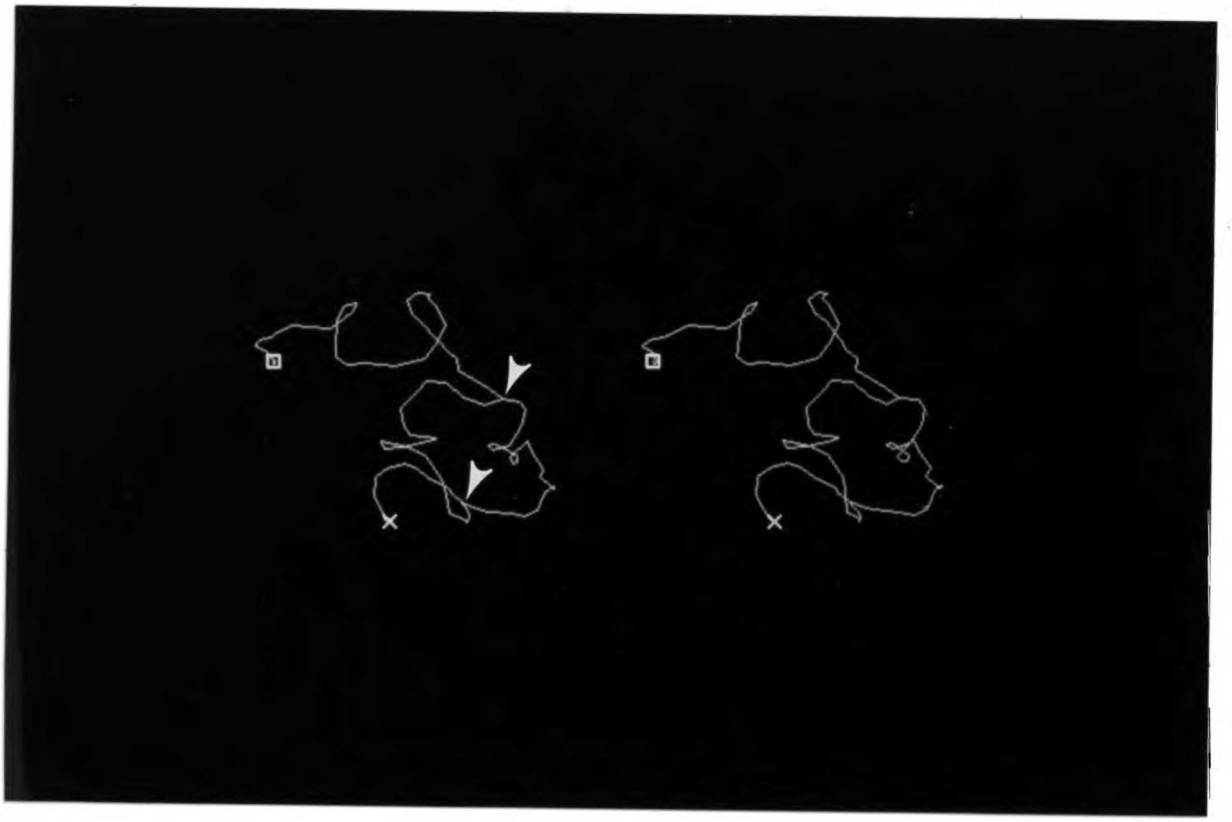

Figure 5. Nuclear surface contact frequencies for the 5 major chromosome arms. A locus is regarded as on the nuclear envelope if it is within 1 μm of the surface. The nuclear surface is approximated by a convex polygon in which the model is inscribed (Mathog et al., 1984). Cytological position is plotted along the abscissas of each plot, the chromocenter (CC) on the left, the telomere(T) on the right. The ordinate range is 0 to 24 (out of 24). Each horizontal division represents one cytological division (e.g., 1A-1F) in the respective arms (10,24). The values in the left-most division in each plot have been set to zero because the cytology is never followed into these regions. The data in the second division from the left of each arm is displayed but is not included in the analysis because cytological indentification is sometimes difficult close to the chromocenter. The telomeres in the 2R and 3R plots fall one letter subdivision short of the right end, so the rightmost ends in these two plots are set to zero. The average fractions of each model arm within 1 um of the surface are approximately as follows: X(.46), 2L(.46), 2R(.40), 3L(.47), 3R(.42). The arrows highlight regions where the frequency of contact is at or above the cutoff frequency for the arm (indicated by the dashed line). The cutoffs used are as follows: X(16 out of 24), 2L(16), 2R(15), 3L(16), 3R(15). Approximately 8% of each arm's plot is at or above the cutoff. The dark arrows indicate an overlap with a position of intercalary heterochromatin, while the open one means no intercalary heterochromatin is in that contact region.

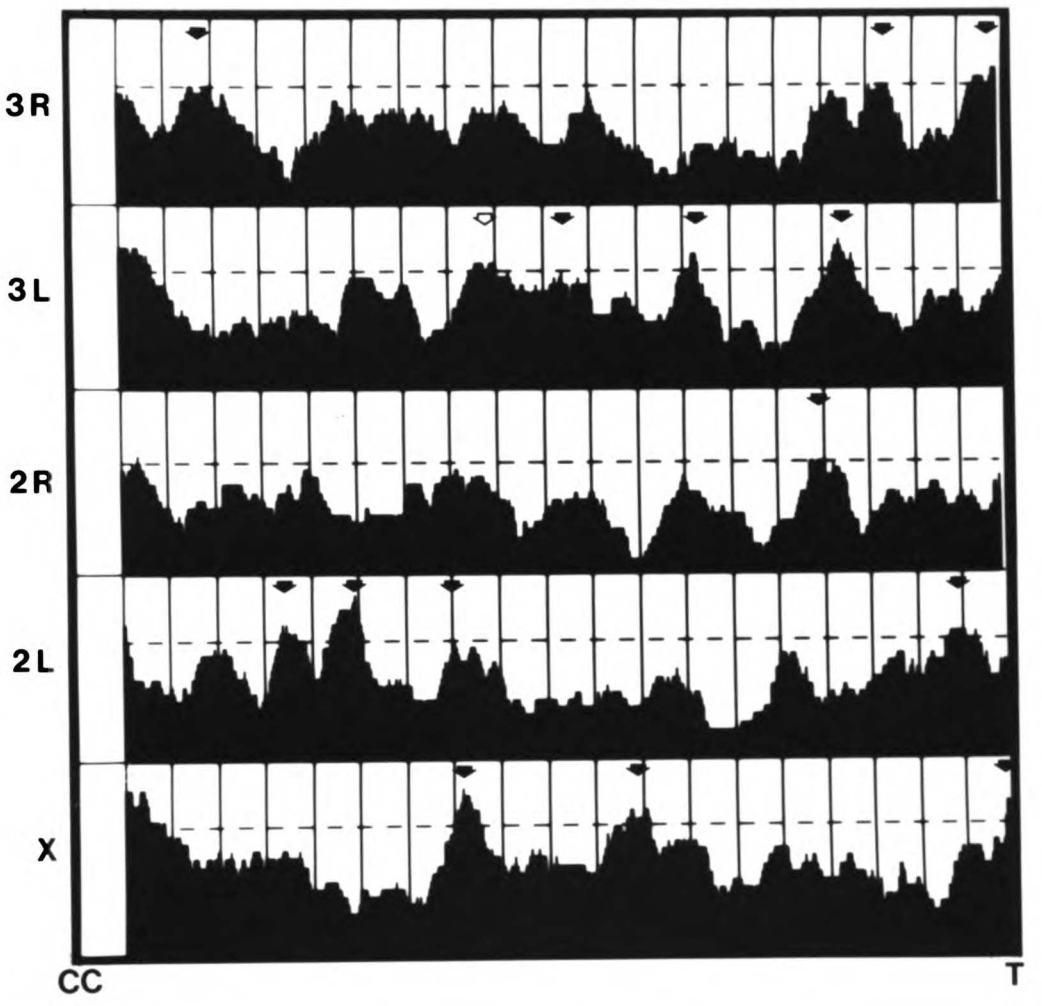
3R
3L
2R
2L
X
CC
T

Figure 6. Physical sections of DAPI-stained salivary gland nuclei. (a) Example of chromocenter material appressed to the nuclear surface (arrowheads). (b) A locus containing intercalary heterochromatin, 70C, apparently attached to the nuclear surface (arrow). (c) Another intercalary heterochromatin site, 71C, showing an apparent attachment (arrow). Sections (b) and (c) show the same 3L chromosome arm in successive 0.5 µm sections. The scale bar equals 2 µm. The cytoplasm fluoresces weakly in the embedded gland, so the nuclear border can be seen in the sections. To accentuate the cytoplasmic staining for display purposes, the section images were processed with a program that compresses the overall dynamic range in the image while providing local contrast enhancement (written by Andrew Belmont).

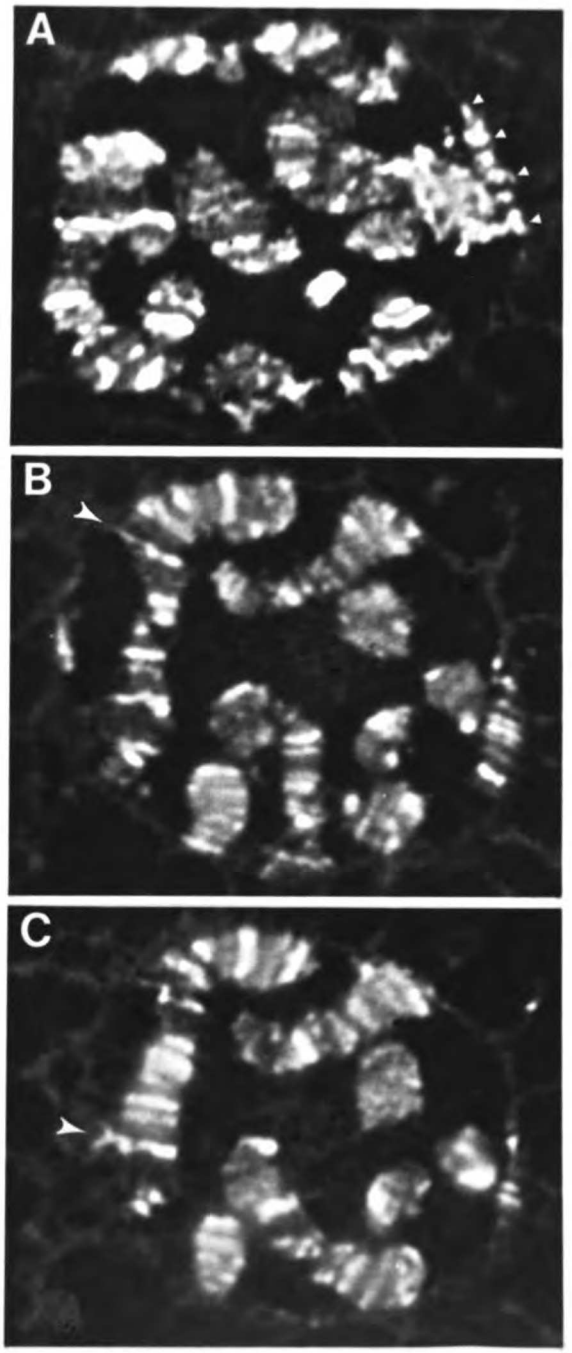
A
B
C

Figure 7. The 3-D folding of chromosome arm 2L. (a) A contoured intradistance plot for one 2L arm. See text for derivation. Cytological position is plotted along both abscissa and ordinate with grid lines separated by two cytological divisions. The telomere (T=21A) and the chromocentral endpoint (chromocenter=40F) are marked (the plot is actually never interpolated beyond 40A). The average length of the 2L model arm is 146 μm. The darkest regions mark pairs of loci closest together in space. Contour steps equal 2 μm. All distances greater than 10 μm are displayed as white. The arrowhead points to an apposition between 29B and 35E in the model; their separation is between 2 and 4 μm. (b) The mean intradistance plot for 2L (24 nuclei). The value at each point represents the mean distance between the pair of loci denoted by that point. Values are plotted as in (a). The bottom portion of the plot is truncated because the chromosome banding pattern could not be traced in every nucleus into this proximal region of the arm. (c) The standard deviation map for 2L. The value at each point represents the standard deviation of the distribution of distances between the pair of loci denoted by that point. The darkest values have the lowest standard deviations (‘1 μm); contour steps in this plot are at 1 μm intervals. (d) The mean intradistance plot for the set of 24 2L intradistance plots that had been randomly displaced relative to one another. The plot is displayed exactly as in (b).

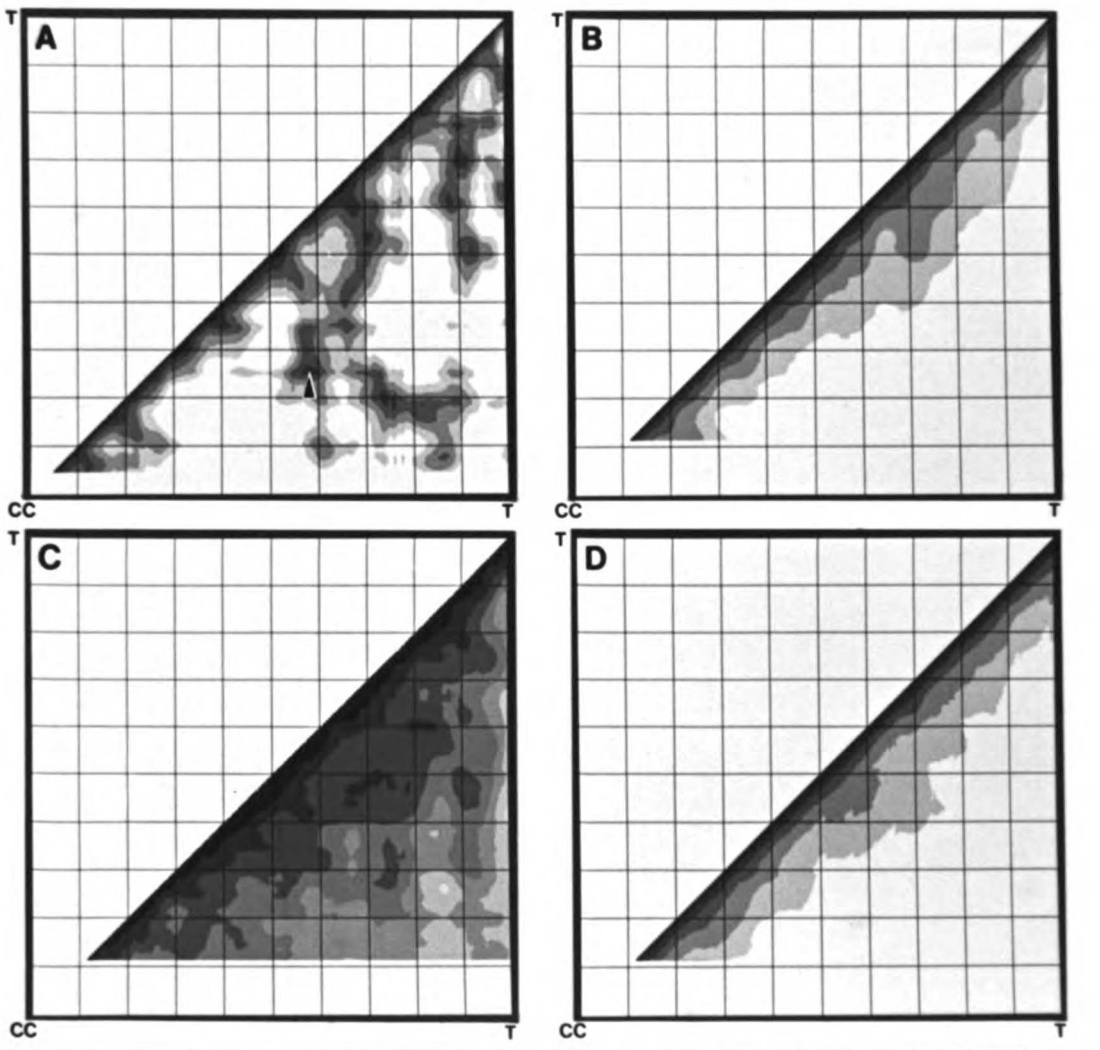
T
A
CC
T
T
B
CC
T
T
C
CC
T
T
D
CC
T

Figure 8. A stereo pair model from a nucleus with a split chromocenter. The two chromocenters are approximately 20 μm apart. Chromocentral endpoints for each arm are marked with squares; telomeres are indicated with crosses. Chromosomes 3 and X are attached to one chromocenter, while chromosome 2 is at the other. The color code and scale are as in Fig. 1.

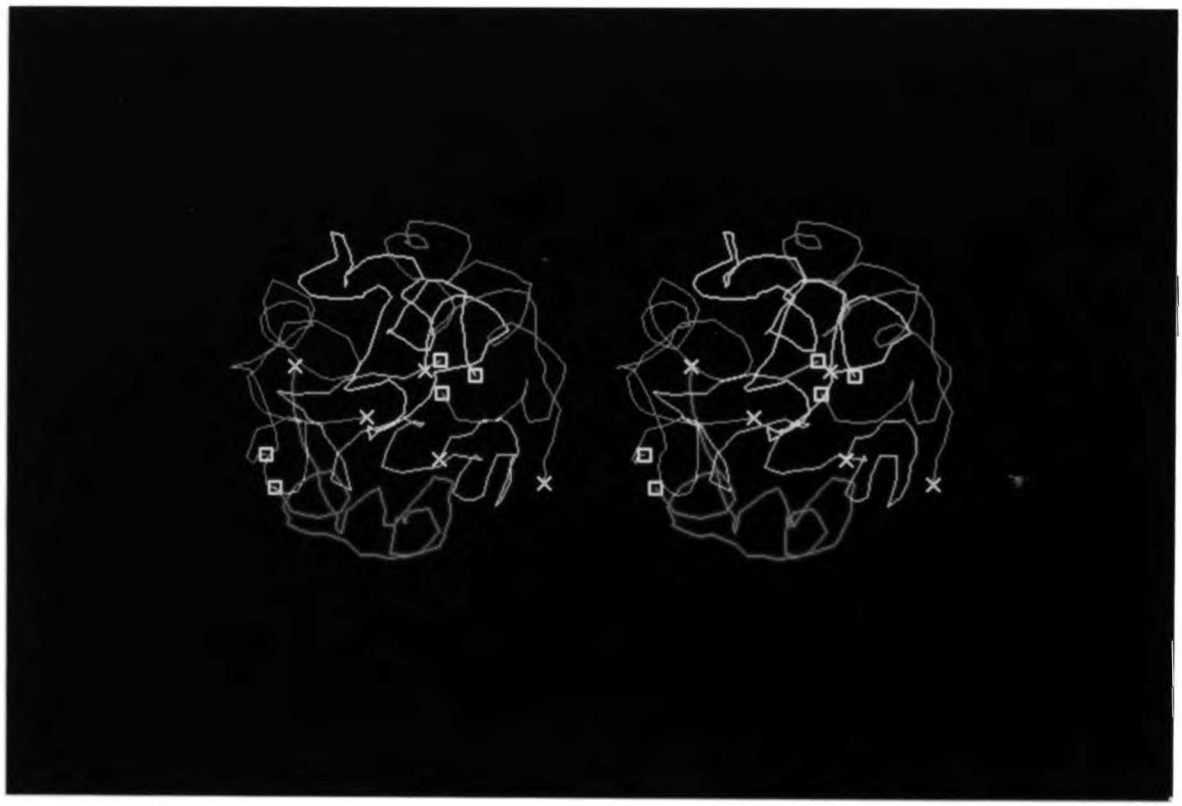

Chapter 3

Three-Dimensional Organization Of *Drosophila Melanogaster* Interphase Nuclei. I. Tissue Specific Aspects of Polytene Nuclear Architecture

ABSTRACT

An analysis of interphase chromosome organization in 4 different Drosophila melanogaster tissues, covering 3-4 levels of polyteny, is presented. The results are based primarily on three-dimensional reconstructions from unfixed tissues using a computer-based data collection and modeling system. A characteristic organization of chromosomes in each cell type is observed, independent of polyteny, with some packing motifs common to several or all tissues and others tissue-specific. All chromosomes display a right-handed coiling chirality, despite large differences in size and degree of coiling. Conversely, in each cell type, the heterochromatic centromeric regions have a unique structure, tendency to associate, and intranuclear location. The organization of condensed nucleolar chromatin is also tissue-specific. The tightly coiled prothoracic gland chromosomes are arrayed in a similar fashion to the much larger salivary gland chromosomes described previously, having polarized orientations, nonintertwined spatial domains, and close packing of the arms of each autosome, whereas hindgut and especially the unusually straight midgut chromosomes display striking departures from these regularities. Most surprisingly, gut chromosomes often appear to be broken apart in the centric heterochromatin. In vivo observations reveal severe deformations of midgut nuclei during gut contractions which may account for their unusual properties. Finally, morphometric measurements of chromosome and nuclear dimensions suggest several interesting properties of chromosome growth and provide boundary constraints on models of chromosome substructure.

INTRODUCTION

In a polytene interphase nucleus, chromosomes undergo repeated rounds of DNA replication without nuclear division. Moreover, the homologous chromatids remain in close lateral alignment, rendering chromosomes with distinctive banding patterns visible in the light microscope. These nuclei thus provide a useful model system for directly analyzing interphase chromosome organization. Previously, we were able to determine the spatial organization of chromosomes in a set of wild-type salivary gland nuclei, which have the highest level of polyteny in the larva (Mathog et al., 1984; Hochstrasser, et al., 1986). Characteristic packing motifs were found, including: a polarized (Rabl) orientation of chromosomes across the nucleus, separation of chromosomes into noninterwound spatial domains, nearest-neighbor packing of the metacentric autosome arms, high frequency contacts between a specific set of intercalary heterochromatin-containing loci and the nuclear surface, invariant apposition of the aggregated centromeric regions (the chromocenter) to the nuclear surface, and a striking right-handed coiling chirality that does not require homolog pairing. Despite these nonrandom features, precise three-dimensional chromosome configurations appear not to be specified. Thus, while the folding of chromosomes is not identical in every salivary gland cell, several other facets of their organization are quite well defined.

To what degree the properties of the large, densely packed salivary gland nuclei reflect structural features of all polytene nuclei or, instead, are a function of ploidy or cell type is unknown. Many tissues in D. melanogaster larvae are polytenized but generally not to the same high level as in the salivary glands. It would be possible to address

several issues raised by the salivary gland data in a comparative analysis of chromosome organization in different tissues. Important issues include whether a tissue-specific set of loci localizes to the nuclear surface in each differentiated cell type and whether a right-handed chirality typifies the coiling of all polytene chromosomes. In addition, chromosomes in other tissues may have more regular spatial configurations than in the salivary gland, particularly since variable cell types could not be rigorously ruled out in the latter tissue. An analysis of lower polyteny nuclei should also help clarify to what degree one may extropolate from the polytene condition to differentiated diploid cells. Finally, correlations of specific organizational features with cell type can provide clues about their possible functional significance.

Such a comparative analysis has now been done. It was first necessary to systematically search for other tissues with sufficient polyteny and optical clarity to permit a three-dimensional analysis. In addition, we had to refine existing cytological methods so that less-polytenized nuclei could be studied. Three wild-type larval tissues that have been subject to little or no previous study provided the material on which the present work is based. The data described here should therefore be of general utility to cytologists interested in comparing chromosomes in different D. melanogaster cell types.

In this report, nuclear architecture in salivary gland, prothoracic gland, hindgut, and middle midgut nuclei is compared. First, global properties such as chromosome size, packing density and coiling, and aspects of chromosome and nuclear growth inferred from them, are described. This is followed by a comparison between cell types of local

regions of the genome, in particular centric heterochromatin and nucleolar chromatin. Finally, from the similarities and differences between cell types, we make inferences about the mechanisms and physical properties of chromosomes and nuclei that result in the organizational motifs observed. The accompanying report focuses on aspects of chromosome spatial organization that have been hypothesized to be involved in the tissue-specific pattern of gene expression. Together, the results provide a precise description of interphase chromosome organization based largely on three-dimensional reconstructions of unfixed, unembedded nuclei. The data thus provide a structural framework for models of nuclear architecture and the functional organization of the genome.

MATERIALS AND METHODS

Tissue preparation

Either of two wild-type Oregon-R stocks were employed. One, obtained from S. Beckendorf, had been made isogenic for the X chromosome (referred to as OR-isoX in Hochstrasser et al., 1986); the other was provided by T. Kornberg. All of the three-dimensional reconstructions made from prothoracic glands and hindgut were from OR-isoX larvae, while both stocks were used for midgut (and salivary gland) nuclei reconstructions. Flies were raised on standard cornmeal food supplemented with yeast in uncrowded bottles; the bottles were either left at 16°C for the entire period to third instar or were transferred to 16°C after allowing egg-laying for several days at 25°C. Growth at low temperature increases the fraction of nuclei that reach the higher

levels of polyteny (Hartmann-Goldstein and Goldstein, 1979); it does not alter chromosome organization since the salivary gland nuclei from Hochstrasser et al. (1986) that were from OR-isoX larvae raised at 16°C during the larval period did not differ in any measure from those of larvae raised at 25°C, including average chromosome dimensions.

Tissues were prepared for optical-sectioning microscopy as follows. After rinsing larvae in dissection buffer, the anterior end was removed by grasping behind the mouthhooks with a pair of jeweler's forceps and pulling away the anterior tissue with another. Part of the viscera was ejected through the opening created; the rest was gently pushed out by running lightly clamped forceps along the body from the posterior tip. The interconnected organs were then gently cut and teased apart with needles to isolate the desired tissue. Most of the gut is knotted together by tracheal tubes, and some must be severed to get at the "large cells" of the middle midgut; these are located right at the bend between the Ia and Ib segments of the midgut (Strasburger, 1932). The midgut was cut in positions far from the bend, and the loop of intestine was carefully removed. The hindgut usually hangs free of most of the convoluted gut and could be viewed without cutting it free. For schematic illustrations of the larval gut see Poulson and Waterhouse (1960) and Filshie et al. (1971). To minimize perturbations, ring glands were examined without separating them from the cephalic complex of tissues, which includes the brain hemispheres, ventral ganglion, and imaginal disks. Aggarwal and King (1969) provide drawings of the ring gland and the location of prothoracic cells within it.

Buffer and staining conditions

Gut tissues were transferred directly to a drop of buffer containing 3-5 ug/ml of the DNA-specific fluorescent dye 4',6-diamidino-2-phenylindole (DAPI) on a 40x22 mm no. 1.5 coverslip that had been taped to a C-shaped steel mount. Ring glands were stained for 10-20 minutes in 20 ug/ml DAPI and mounted in DAPI-free buffer. DAPI is a nonintercalating dye that does not appear to perturb chromosome structure; different staining protocols were used in the different tissues because of differences in the rate of dye uptake. Supports fashioned from coverslips were placed on either side of the drop, and another coverslip was placed across these. The coverslip sandwich was sealed with paraffin oil, and the assemblage was immediately mounted on a computer controlled Zeiss Axiomat inverted microscope. Optical sections of nuclei were collected exactly as described previously (Mathog et al., 1984; Hochstrasser et al., 1986). After the initial 256-frame video averaging of the fluorescent images to reduce the effect of camera noise, no image processing of any kind was used on any of the nuclei discussed in this report.

The buffer used with the gut tissues was the following formulation of Buffer A (Burgoyne et al., 1971; Sedat and Manuelidis, 1978): 15 mM Hepes, 0.15 mM spermine, 0.5 mM spermidine, 80 mM KCl, 15 mM NaCl, 0.1 mM EGTA, 0.5 mM EDTA, 15 mM 2-mercaptoethanol, pH 6.8; all other buffers tried, including physiological ones, lead to severe shortening of the gut that resulted in all the nuclei being compressed into flat crescent shapes. In the serum-free physiological D22 medium of Echalier and Ohanessian (1970), this contraction occurs but is gradual; the initial appearance of nuclei in this case is the same with regard to nuclear shape and general chromosome layout as those in Buffer A. If the

chelators are omitted from Buffer A, the guts will often continue to undergo peristaltic contractions for 10-30 minutes. The prothoracic glands were isolated and mounted in D22 medium. Buffer A was not suitable in this case because the chromosomes tended to contract toward the nuclear surface with time, whereas in the D22 medium, their positions were stable for many hours. For both midgut and prothoracic glands, examination of nuclei in living larvae (see below) indicated that the chromosome organization described for these tissues reflects the in vivo situation.

Histological assays

To verify that the middle midgut cells studied here were indeed the "large cells" (Poulson and Waterhouse, 1960) and not the copper accumulating calycocytes located just anterior to them, larvae fed on food mixed with copper sulphate were dissected and their intestines were subjected to a simple histochemical assay for copper using diethyl dithiocarbamate (Filshie et al, 1971). The distinctive group of cells immediately proximal to the Ia/Ib bend developed a characteristic yellow-brown precipitate because of copper uptake; however, the large cells described in this report, which are right at the bend, did not.

Approximate cell counts were made as part of the characterization of midgut and prothoracic gland tissues from the stocks used in this study. 12-16 "large cell" midgut nuclei could be counted in DAPI-stained whole mounts and 35-41 prothoracic gland nuclei were counted in orcein-stained preparations. These are comparable to published values: 14-18 (Poulson and Waterhouse, 1960) and 40 (Holden and Ashburner,

1978), respectively. All the tissues studied here undergo histolysis well after the stage at which they were analyzed (Robertson, 1936).

Model building and mapping of cytology

The three-dimensional paths of chromosomes were traced as desribed previously using the interactive modeling program IMP (Mathog et al., 1984; Mathog et al., 1985; Mathog, 1985). Because midguts occasionally move slightly on the slide due to residual muscle activity, data from the same nucleus were taken at different times to test for possible changes in chromosome dispositions. From the models made from each data stack, it could be shown that despite a slight reorientation of the nucleus relative to the objective microscope lens between sets, they were essentially identical as measured by all the quantitative parameters described in this and the accompanying paper.

Identification of the cytological banding pattern in intact nuclei from the non-salivary gland tissues first required preparing montages of photographs of squashed, orcein stained chromosomes from each tissue. The general banding pattern is very similar between tissues, but there are considerable differences in puffing, relative band spacings and the distribution and appearance of cytological landmarks. These differences made it extremely difficult, at least initially, to correctly identify the banding throughout the euchromatic complement in whole tissues without the montages. Details of this work will be published elsewhere (Hochstrasser, in prep.).

The surface of the single large nucleolus in prothoracic gland cells could be traced. This was done in either of two ways. In the first, the modeling program was modified so that the outline could be

represented by more than the 512 points used for each chromosome arm; thus, when the nucleolar outlines are traced in each section and are connected into a set of linked ellipses, the nucleolar surface will be adequately sampled. In the second, the nucleolus is approximated by a set of interpenetrating disks, each the thickness of an optical section (Mathog and Sedat, submitted; Fig. 3a). Both methods yield the same result when measuring the distances between chromosome loci and the nucleolus, but the latter also allows one to measure conveniently nucleolar volume.

Morphometric measurements and model analysis

Chromosome widths were measured at ten prominent reference bands, two from each chromosome arm, that were unpuffed in the different tissues (8E1, 13B1, 22A1, 29E1, 45A1, 55A1, 63A1, 67F1, 87B1, and 89A1; 67F1 was slightly puffed in a few of the salivary gland nuclei). A minimum of 7 and generally 8-9 of these bands could be measured in each nucleus examined. The 15 salivary gland nuclei were from the unfixed nuclei discussed in Hochstrasser et al. (1986). It should be noted that the prothoracic gland polyteny levels inferred from band width measurements (see Results) are somewhat higher than Welch's (1957) values from Feulgen cytophotometry. His calculations for other tissues also appear to be systematically lower than in other studies (e.g., Laird et al., 1980). In addition, we always select the largest nuclei in the tissue, so our values will be strongly biased toward the highest levels. Finally, levels of polyteny can vary with genetic background (Welch, 1957).

Euchromatic chromosome arm lengths were measured between the following endpoints: X (1A-20A), 2L (21A-40A), 2R (60F-42A), 3L (61A-80A), and 3R (100F- 82A) (Bridges, 1935). Chromosome volumes were approximated by the volume of a cylinder whose width equaled the average width of the set of reference bands and whose length equaled the sum of the model lengths of the five major arms. The small fourth chromosome could frequently be modeled but was not included in any of the size calculations. Nuclear (and nucleolar) volumes were calculated by placing a cube of the smallest possible size around the model and picking 10,000 random points within the cube; by multiplying the known volume of the cube by the fraction of the points that fell within the surface of the model, the nuclear volume was obtained (Mathog and Sedat, submitted). Very similar values are obtained if the number of random points is increased 10-fold. The surface of the model is defined by a multifaceted polyhedron in which the model is inscribed (Mathog et al., 1984); because the models are drawn roughly down the center of the chromosomes, the calculated volume is significantly less than the actual volume. To correct for this, each facet in the polyhedral model surface was computationally moved outwards by a distance equal to the average chromosome radius determined from the band width measurements.

Midgut nuclear shape is generally that of a very flat oblate ellipsoid. A measure of this flatness was made from the ratio of the maximum diameter measured on the displayed model to the maximum distance between any two model points along the direction in which the model is flattest, the two axes being roughly orthogonal. The latter distance was found by rotating the model so that the short axis of the nucleus (pointing toward the gut lumen) was directed in the +x direction. The

resulting rotation angles were used to deduce the original orientation vector. The largest of the dot products between this unit vector and the vectors between every pair of model points could then provide the short axis length; however, to avoid computing the distances between 512x5 model points, the program only considered points that fell within 0.1 μm of the model surface. The average chromosome width was added to both long and short axis values in Table 1.

Logarithmic plots of nuclear volume vs. chromosome volume were analyzed by linear regression (Table 4). The linear correlation coefficients were 0.88 (prothoracic gland), 0.77 (midgut), and 0.92 (salivary gland). All represent statistically significant correlations. The slopes of the regression lines were compared by covariance analysis, and mean values of different measurements were compared with Student's t-test (Sachs, 1983).

Triple product and unpacking ratio calculations were done as previously described (Mathog, 1985; Hochstrasser et al., 1986). In this paper, we have summed the values from either of these two metrics over all chromosome arms in the nucleus because there were no major differences between arms. Also, an analysis of these parameters at each point along the chromosomes did not reveal any well-defined local regularities.

In vivo observations of DAPI-stained tissues

Third-instar larvae, either crawling at the edge of or in the food layer, were washed in saline, etherized, mounted on double stick tape, and then microinjected throught the posterior end with an estimated 1-3 microliters of a solution of 200 μg/ml DAPI in insect saline. Glass

capillary tubes (1 mm O.D., extruded fiber, from Frederick Haer, Inc.) were pulled out on a Narishiga needle maker to give a inner tip bore of ~10 um. Injected larvae were mounted on a glass slide under a firmly taped 18x18 mm cover slip.

Injected larvae were viewed with minimal irradiation on a Zeiss Universal microscope connected to a Chalnicon camera (DAGE-MTI) and a Sony videocassette recorder; the lamp aperture was reduced and the camera was operated at high gain. Prolonged exposure of midgut cells even at these low levels appeared to lead eventually to reduced gut contractions and pycnosis of nuclei; therefore, nuclei were generally examined for only a few minutes. For visual tracking of nuclei in explanted midguts for longer periods, a high sensitivity SIT camera (DAGE-MTI) was employed. Photographs were taken from stop-frame video images on an RCA television monitor.

Electron microscopy

The same buffers as above were used for tissue dissections. Tissues were either fixed at room temperature for 1-2 hours in 3.7% formaldehyde prepared from paraformaldehyde, (Polysciences) followed by 2% glutaraldehyde (Polysciences) for four hours or were fixed for 2-4 hours in 2% glutaraldehyde at room temperature and then overnight in fresh fixative at 4 C. In the latter case, tissues were also postfixed for two hours in 2% osmium tetraoxide. All fixatives were in Buffer A. Dehydration through a DMSO series was followed by embedding in Spurr's resin (Polysciences). Blocks were sectioned with glass knives on a Sorvall MT2-B ultramicrotome, and random or serial ~gold sections were collected on 100-150 mesh copper grids that had either been coated with

or rapidly dipped in Formvar (Zelechowska and Potworoski, 1985). Sections were stained with 2% uranyl acetate (either aqueous or in 50% ethanol) and ~0.5% lead citrate. Specimens were viewed at 80 kV with a 30 µm objective aperture in a Philips EM400 microscope.

RESULTS

It is generally held that the only wild-type D. melanogaster tissue of sufficient polyteny for routine cytogenetic analysis is the salivary gland (see Ashburner and Berendes, 1978). The single detailed study of polytene chromosomes in another wild-type tissue is by Richards (1980), who analyzed part of the fat body. Unfortunately, the cells are almost completely opaque in whole mounts. Other species of Drosophila such as D. hydei do have larger polytene chromosomes in other tissues (Ashburner and Berendes, 1978). On the other hand, because of the wealth of cytological and genetic information available for D. melanogaster and because all our previous work was done in D. melanogaster salivary glands, it would be of great advantage if a comparative analysis of polytene chromosome folding could be based in this species. We therefore undertook a systematic search in several stocks for candidate tissues with suitable optical properties and levels of polyteny (Hochstrasser, in prep.). Cells within several larval tissues proved to have high levels of polyteny: the so-called "large cells" of the middle midgut (Poulson and Waterhouse, 1960), the hindgut, and the prothoracic gland.

The prothoracic gland forms part of the larval ring gland and is the site of alpha-ecdysone synthesis; this steroid is the immediate precursor of the growth and moulting hormone, 20-hydroxyecdysone (Aggarwal and King, 1969). The "large cells" of the midgut are of

ill-defined function. These cells are thought to develop from the tip of the endodermal posterior midgut invagination (Poulson and Waterhouse, 1960). It is thought that ingested food undergoes acid hydrolysis in this region (Filshie et al., 1971). The role of the hindgut, the final segment of the intestinal tract, is also not well understood, although in some insects a general secretory function has been ascribed to it (see Strasburger, 1932); it forms from the proctodaeum, an ectodermal rudiment.

General description of nuclei from different tissues

Three-dimensional chromosome models have been constructed from stacks of optical sections of unfixed, unembedded, DAPI-stained nuclei from the different tissues. 25 middle midgut nuclei from 15 female and 2 male larvae have been reconstructed; the majority of these nuclei are from the 2-4 cells right at the Ia/Ib bend. 11 prothoracic gland nuclei, most located near the corpus allatum, from 7 female larvae and 4 nuclei from a patch of distal hindgut cells in one female larva provided the other reconstructions described in this report. Examples of unprocessed optical sections of nuclei from each tissue are displayed in Fig. 1 (for a comparison with salivary gland nuclei, see Mathog et al., 1984).

Nuclei from each cell type have a characteristic appearance. Prothoracic chromosomes are tightly coiled and twisted within a generally spheroidal nucleus ~22-25 μm in diameter; a large nucleolus usually occupies the central zone of the nucleus. Hindgut chromosomes are also tightly coiled in many regions, although long straight stretches are not uncommon; nuclei are also usually spheroidal or

slightly ellipsoidal with similar diameters to prothoracic gland nuclei. In marked contrast, the "large cell" nuclei of the midgut form extremely flat ellipsoids; the long axis can exceed 50 μm in length and, on average, is 2.3 times longer than the short axis (Table 1). Midgut chromosomes are also unusually straight, often with only a few true gyres in the entire nucleus. For comparison, the nuclei of the salivary gland are usually around 35 μm in diameter and contain densely packed, coiled chromosomes (Mathog et al., 1984; Hochstrasser et al., 1986).

Chromosome size and packing density in different tissues

With the ability to identify the specific chromosome banding pattern in intact tissues, it has been possible for the first time to obtain measurements of chromosome dimensions under approximately in vivo conditions. Fig. 2 is a histogram of mean chromosome widths measured in 55 nuclei, none of which had been fixed or embedded; the same ten reference bands were measured in each nucleus (Materials and Methods). Tables 2-3 provide values for several other nuclear size parameters.

Studies comparing (squashed) chromosome band width to DNA content in polytene tissues (Hartmann-Goldstein and Goldstein, 1979; Laird et al., 1980) indicate that width is a fairly accurate indicator of degree of polyteny; it increases by a factor of $\sim\sqrt{2}$ with each round of replication. Three of the peaks in the histograms fit the prediction well (peaks centered at 1.5, 2.1, 3.1 μm), but the final peak in the salivary gland nuclei (3.5 μm) is at a lower width than expected. Chromosome width in the largest DNA class observed by Hartmann-Goldstein and Goldstein (1979) also fell below the predicted increase. From these data, it seems most likely that four rounds of replication separate the

smallest prothoracic gland nuclei from the largest salivary gland nuclei. A comparison of approximate chromosome volumes (Materials and Methods) presents a similar picture. There is an 18.5-fold range in volume between the smallest and largest chromosome complements; this is close to the 2^4=16 value expected for 4 doublings, assuming chromosome volume is proportional to chromosome dry mass and therefore, DNA content (Laird et al., 1980). While DNA content has not been directly measured, reference to the data from Laird et al. (1980) indicates the largest salivary gland nuclei should be in the 2048C class, i.e., 10 rounds of endoreduplication; this would put the lower prothoracic gland size class at 256C.

Chromosomes occupy a far greater fraction of the nuclear volume in salivary glands than in the other tissues (Table 4). The differences between all tissues are statistically significant. Interestingly, if nuclei from either prothoracic glands or midguts are divided into putative polyteny classes (Fig. 2), the volume fraction occupied by chromosomes in the higher polyteny nuclei is significantly higher than in the smaller ones (Table 4). Chromosomes in these tissues thus increase in volume more rapidly than do the nuclei in which they reside. However, nuclei in the two apparent polyteny classes in salivary glands have the same density of packing (nuclei were divided between those with an average band width greater than or equal to 3.3 μm and those below this). These relative trends are confirmed by an allometric analysis of nuclear versus chromosome volumes (Table 4, last column). Another measure also suggests that there is change in the properties of chromosome and nuclear growth at the highest levels of polyteny. In both prothoracic gland and midgut nuclei, chromosome width correlates with

chromosome length ($r=0.71$, $P<0.02$; $r=0.74$, $P<0.001$, respectively), whereas this is not true in the salivary gland ($r=0.22$, $P>0.2$). Nuclear volume in all tissues is correlated with both chromosome volume and chromosome width but increases at different relative rates in different tissues (Table 4). The possible significance of these morphometric measurements will be considered in the Discussion.

It is worth noting that the actual dimensions recorded in Tables 2-3 and Fig. 2 do not agree with measurements from any previous investigation except the length measurements of lax salivary gland chromosomes made by Bridges (1942). Most or all of the discrepancies are probably a consequence of the squashing and/or fixation steps required in these studies (Bridges, 1935; Beermann, 1962; Hartmann-Goldstein and Goldstein, 1979; Laird et al., 1980). Squashing will stretch the chromosomes to an unknown extent, while fixation will also generally alter chromosome and nuclear dimensions. For example, we find that fixing salivary glands in 3.7% formaldehyde can shrink chromosome lengths by over 30% (Hochstrasser, unpublished results; Mathog and Sedat, submitted). Similarly, previous measurements of nuclear volumes have also been done with fixed tissues, and lead to values much lower than those given in Table 3 (see Beermann, 1962).

Chromosome organizational motifs differ with cell type

The general packing of salivary gland chromosomes is characterized by a number of regular motifs which includes a generally polarized (Rabl) orientation of chromosomes, with centromeres and telomeres segregated to opposite sides of the nucleus; the invariant separation of chromosomes into nonintertwined intranuclear domains; and the close

packing of the arms of each autosome next to one another (Mathog et al., 1984; Hochstrasser et al., 1986). We argued that this is reminiscent of properties of chromosomes in mitotic telophase and as such may reflect what would be a remarkable degree of positional stability, considering that the last mitosis in this tissue is completed by the 8th hour of embryogenesis (Sonnenblick, 1950). One prediction of this argument is that it implies that nuclei with lower levels of polyteny (and diploid nuclei) will share these motifs.

Prothoracic gland nuclei, as many as four levels of polyteny below salivary gland nuclei, do indeed fulfill the prediction. The nucleus model in Fig. 3a is a representative example. In every nucleus chromosomes lie in distinct nonintertwined domains and in every nucleus, chromosome arms 2L and 2R and arms 3L and 3R are close intranuclear neighbors. As in salivary glands, no other pair of arms are regular neighbors. Finally, despite the fact that the chromocenter in prothoracic gland nuclei is generally in the interior of the nucleus (see below), it is still possible to define a polarization axis running from the chromocenter to the telomeres arrayed in the opposite hemisphere of the nucleus (telomeres are usually on the nuclear surface; see accompanying paper). This can be seen in Fig. 3a. Such a Rabl or pseudo-Rabl orientation is seen in ~73% of the chromosomes; this is comparable to the ~80% figure found for salivary glands (Hochstrasser et al., 1986).

A very different packing is seen in the nuclei of the great majority of middle midgut cells (Fig. 3b). All of the chromosome packing rules just described are regularly violated in this cell type. It is rarely possible to define a polarization axis: centromeres and telomeres are

found throughout the nucleus. The arms of each autosome are also in a wide range of relative positions. Most dramatic of all is the frequent intertwining of chromosomes. The nucleus model in Fig. 3b shows a clear example of intertwining between the X and 3R chromosomes; one of the optical sections that includes this region is shown in Fig. 1d and serves to illustrate that the chromosomes are actually in close contact with one another. In a graphic example of intertwining, displayed in Fig. 4, 2R is seen running through a coil in 3L; examination of the relevant optical sections shows that the coil is tightly wrapped around 2R. Not every nucleus has such tightly entangled chromosomes, but lesser encroachments are found in almost all of the nuclei (see Fig. 3b). In only one nucleus did the chromosomes show both no domain encroachments and a Rabl-like orientation, although each autosome's arms were only together near the chromocenter.

Hindgut nuclei appear intermediate in their preservation of these telophase-like motifs. The model in Fig. 3c comes closest to this description, although 3L and 3R do not follow the general centromere-telomere polarization. Several examples of chromosome intertwining, less pronounced than those in the midgut, from two of the remaining hindgut nuclei were found. In summary, nuclei in the hindgut and especially the midgut tend to deviate from the telophase-like properties seen in the non-gut tissues.

Chromosome coiling shows the same chirality in all tissues

An unexpected result from our analysis of salivary gland chromosomes was the discovery of a marked asymmetry in coiling direction: virtually all gyres are right-handed (Hochstrasser et al., 1986). Previous

reports had maintained that left- and right-handed coils were equally likely (Koller, 1935; Beermann, 1962; Ananiev and Barsky, 1985). The source of this chirality is unknown, although its occurrence in asynapsed homologs indicates it is not due to homologous pairing. These results do not reveal whether the asymmetry is a fundamental property of all polytene chromosomes or when and how polytene chromosomes coil. These questions can be addressed with the present data, in which a wide range of chromosome size and degree of coiling is seen.

Inspection of stereo-pairs (Fig. 3) demonstrate that all chromosomes in every tissue display the coiling asymmetry first seen in salivary glands. Even in the generally straight or meandering midgut chromosomes, the infrequent gyres are nevertheless almost invariably right-handed. Left-handed loops are found infrequently, e.g., in arm 3L in Fig. 3a. It is sometimes possible to directly verify the direction of coiling in the tightly coiled chromosomes of lower polyteny; this is illustrated in Fig. 5, which shows successive optical planes through an almost solenoidal region of a hindgut chromosome. Finally, the unpaired X chromosomes in the three male midgut nuclei reconstructed as well as a long asynapsed chromosome segment in another midgut nucleus could be roughly traced, and an apparent bias toward right-handed coiling was also seen, in agreement with our observations in salivary glands.

An objective way to demonstrate a bias in coiling direction is the triple product calculation (Braun, 1983; Mathog, 1985; Hochstrasser et al., 1986). This vector operation, $A \cdot (B \times C)$, where A, B, and C are successive vectors along a curve, will yield a positive scalar value if the vectors' relative orientations follow a right-handed screw, and vice-versa. Fig. 6 shows histograms of triple product values from each

cell type summed over all chromosome arms in all nuclei. As can be seen, all the histograms are skewed toward positive values (compare to Fig. 3 in Hochstrasser et al., 1986). Some differences between the plots, however, deserve comment. Firstly, the midgut histogram shows a very large peak around zero; this is precisely what is expected given the unusually straight path taken by much of each chromosome. In addition, the coils in this tissue tend to be flat, leading to triple product values near zero. Secondly, the ratio of positive to negative values is somewhat lower in the midgut nuclei. The reason for this is unclear since this is not seen by visual inspection of models; it may well reflect the predominance of straight chromosomal segments and flat gyres rather than a real difference in coiling chirality.

Different vector spacings were used for the calculations in different tissues because the chromosomes vary considerably in length (Tables 2,3) and in the characteristic dimensions of their coils. For instance, the tight coils in hindgut and prothoracic gland chromosomes will not be sampled adequately with the same vector spacing used for the much wider salivary gland chromosome gyres. Bending or coiling can be quantitated with an "unpacking ratio" parameter, which measures the ratio of the minimum distance between two points on the model path to the contour distance between these points; lower values indicate tighter coiling (Mathog, 1985). For example, using a 7 μm contour distance, prothoracic gland and hindgut chromosomes have average unpacking ratios of 0.592 (±0.012) and 0.643(±0.023), respectively, while for salivary gland chromosomes, it is 0.778 (±0.013). If prothoracic gland nuclei are divided into polyteny classes, the larger nuclei (0.605±0.004) are

less tightly coiled than the smaller ones (0.588±0.009; t=4.035, P‘0.005).

An unexpected variation to the "solenoidal" type of coiling described above has been found in a number of gut nuclei and one prothoracic gland nucleus. In these cases a segment of a chromosome arm folds back and twists about itself in a "plectonemic" or braid-like coil. If the forces leading to these interwound forms are related to those generating the right-handed solenoidal coils, one would predict that they will be left-handed. This is most easily understood using the node sign terminology introduced by Cozzarelli et al. (1984): in both plectonemic and solenoidal coils, the nodes or self-crossings will be positive. In fact, this is exactly what is observed: in 11 examples of interwound helices, every one is left-handed. Fig. 7 shows a series of optical sections through one of them. The midgut model in Fig. 3b has an interwound region in chromosome arm 3L, while the hindgut model (Fig. 3c) has an example in chromosome arm 3R. All of the 11 examples have two nodes; not all are as tightly wound as the one in Fig. 7. As will be outlined in the Discussion, these plectonemic coils may shed some light on the mechanism and timing of chiral chromosome coiling.

Tissue-specific aspects of nucleoli

Several intriguing tissue-specific differences in the large scale chromatin organization of particular portions of the genome have been found. One of these is the condensed DNA found within the nucleolus. The density and distribution of the DAPI-bright material within the nucleolus differ in a characteristic way between the cell types studied (Fig. 8). The prothoracic nucleolus generally has a relatively diffuse

DAPI fiber pattern (Fig. 8a), whereas the hindgut nucleolus contains a large number of small bright spots (Fig. 8b). In contrast to either the diffuse fiber or punctate pattern of DNA staining, midgut nucleolar chromatin is most frequently seen as a fibrous clot of material (Fig. 8c).

In addition to differences in chromatin morphology, nucleoli also vary in number between cell types. While the prothoracic gland nucleus almost always has only a single large nucleolus, representing from 4-8% of the nuclear volume (Table 3), midgut nuclei usually have multiple smaller nucleoli, frequently at the nuclear surface. The hindgut nucleus generally contains a single large nucleolus, although more than one has been observed. One or two nucleoli are typical of salivary gland nuclei (Semionov and Kirov, 1986). The fact that the different nucleoli in midgut nuclei are often far apart from both each other and from the nucleolar organizer at the base of the X chromosome may reflect an extrachromosomal state of the ribosomal DNA in this tissue.

Chromocenter structure and position is tissue-specific

The centromeric segments of each chromosome represent another region of the genome with a tissue-specific organization. Moreover, their location within the nucleus also varies between cell types. In salivary gland nuclei, the centromeric regions of each chromosome usually aggregate to form a single dense chromocenter; a small fraction of nuclei may contain two separate chromocenters (Hochstrasser et al., 1986). An invariant feature of salivary gland chromosome organization is the very close association of the chromocenter -even when there is more than one- with the nuclear surface (Mathog et al., 1984; Hochstrasser et

al., 1986). The causes of centromere aggregation and of nuclear surface apposition are not known.

In direct contrast to salivary gland nuclei, the prothoracic gland chromocenter is usually in the interior of the nucleus. This can be verified in the three-dimensional model in Fig. 3a. Since in telophase the centromeres are near one pole of the nucleus, at some point they must move toward the nuclear interior; it is interesting that something close to a Rabl orientation is nevertheless exhibited by these nuclei. Movement of centromeres away from the envelope has been documented in certain diploid cells (Moens and Church, 1977). Fig. 9a,b shows optical sections from different prothoracic gland nuclei that highlight the unusual morphology of the chromocenter; sections of DAPI-stained salivary gland chromocenters are shown in Fig. 9d,e for comparison. In contrast to the dense reticulum of chromatin seen in the latter examples, the prothoracic chromocenter forms a mat of thick, twisted fibers that is draped over a portion of the nucleolar surface.

Electron microscopic examination of chromocenters from each of these tissues (Fig. 9c,f) substantiates all of the above points. The prothoracic gland chromocenter is often in the nuclear interior, pressed against the large nucleolus; it consists of large, well separated fibers that join to the banded euchromatin and appears to have a coiled or zig-zag substructure. One can also see that it is embedded in a mass of small granules that are presumably RNP particles (compare to nucleolar substructure); this suggests that the β-heterochromatin is transcriptionally active in this tissue as well. The salivary gland chromocenter, on the other hand, shows the same sponge-like mass of beta heterochromatin fibers that is seen in the light microscope; the small

block of α-heterochromatin is also apparent (see Lakhotia and Jakob, 1974). Moreover, it is closely appressed to the nuclear envelope/lamina with multiple fibers extending to the bilayer. The close packing of the nuclear pores (Fig. 9f) makes it difficult to tell whether the fibers attach to pore edges or to the lamina; the latter seems more likely.

Chromocenter structure and intranuclear location are also distinctive in the two gut tissues. Hindgut β-heterochromatin exists as long fibers that usually connect to a dense mass; it is often not on the nuclear surface (Fig. 10d). Midgut chromocenter structure cannot be easily classified because it varies widely both within and between nuclei. Typically, it appears as shown in Fig. 10a-b with a loose network of short, criss-crossing fibers connecting denser clumps. Sometimes it forms an irregular ladder of widely spaced bands (Fig. 10c). Often, heterochromatic material that is not obviously connected to a chromosome is seen (arrowheads in Fig. 10b).

Also varying greatly is the extent to which the different centromeric regions associate. In 24 out of the 25 nuclei reconstructed, at least two chromocenters were found. A portion of each chromocenter is usually, but not always, attached to the nuclear envelope; this association appears much more tenuous than that observed in the salivary gland. It is noteworthy that differences in centric heterochromatin association and intranuclear position have been documented in diploid cells as well (Hsu et al., 1971; Comings and Okada, 1976).

Most remarkably, midgut and hindgut chromosomes actually appear to be broken in half in many nuclei: the proximal endpoints of the arms of an autosome are often far apart from one another, even on opposite sides

of the nucleus. Integrity of the centromeric region therefore appears not to be required in these tissues. In Fig. 3b, for example, the proximal endpoints of the left and right arms of chromosome 3 terminate on the envelope on opposite sides of the midgut nucleus, almost 50 μm apart. Similarly, in the hindgut nucleus in Fig. 3c, chromosome 3 is also severed, with proximal arm endpoints on opposite faces of the nucleus (the 3R proximal end can be seen in Fig. 8b to extend a short fiber to the nucleolus). It is sometimes difficult to tell whether a thin fiber runs between chromocentral regions (midgut fibers as long as 20 μm have been measured), but at least one autosome appears split in 20 of the 25 midgut nuclei; chromosome 3 is the most frequently broken. It is conceivable that a very fine DNA thread connects the widely separated centric endpoints, but these nuclei are extremely clear optically and very thin fibers are readily observed between ectopically paired loci or at centric endpoints that send a terminal fiber to the nuclear surface. We therefore think it is unlikely that such connections always exist.

Significantly, chromosomes never appear to break in the euchromatic portions. However, weak points, which contain late replicating, tandemly repeated DNA sequences (Zhimulev et al., 1982), are sometimes pulled out into thin fibers. Fig. 10c (asterisk) shows an example at locus 56F, which contains the tandemly repeated 5S RNA genes. Other loci that have been observed as long fibers include 11A, 12F, 35CD, 36CD, and 89E, all of which behave as weak points in salivary gland squashes.

Midgut nuclear shape is severely but reversibly deformed in vivo

Because of the many unusual characteristics of midgut nuclei, we became concerned about in vitro distortions. For example, it is

conceivable that the process of cutting the Ia/Ib segment free and isolating it in buffer A (Materials and Methods) leads to the collapse of an originally spherical nucleus that pulls the chromosomes out into long straight stretches and perhaps tears apart the chromocenter. The in vivo controls performed previously for salivary glands (Hochstrasser et al., 1986) could not be done with midgut nuclei as they are virtually invisible by bright field optics. As an alternative, we microinjected DAPI into the hemolymph of third instar larvae and examined the stained midgut within the living animal (see Materials and Methods). Video recordings were used for documentation.

The following observations were made. The Ia/Ib bend undergoes particularly pronounced muscular contractions with occasional quiescent phases (also see Strasburger, 1932). During these latter periods it is possible to examine nuclei closely. The generally straight or loosely coiled chromosomes and flat ellipsoidal nuclear shapes seen in the isolated guts are indeed seen in vivo (Fig. 11e,f). The "large cell" nuclei are subject to severe deformations as is illustrated by the video time series, taken at low magnification, in Fig. 11a-d. However, chromosomes are not simply floating freely and continuously rearranging; after a series of contractions, chromosomes appear to relax back to what appear to be identical configurations. This could be looked at more closely in guts isolated in buffer A without chelating agents (Materials and Methods); DAPI-stained guts will sometimes continue to contract under these conditions for 10-30 minutes. Here again, nuclei are strongly deformed by peristaltic contractions, and chromosomes, apparently shifting from these distortions, relax back to similar positions repeatedly, implying some kind of chromosome tethering (data

not shown). It is not known whether over a period of hours or days, chromosome positions can gradually change.

Other tissues also take up dye in DAPI-microinjected larvae. Prothoracic gland nuclei could be examined and appeared similar to the description given in previous sections for this tissue. The hindgut takes up the dye relatively slowly and is difficult to view within the larva, so a satisfactory in vivo description could not be obtained.

DISCUSSION

The three-dimensional organization of D. melanogaster polytene chromosomes in four wild-type tissues, three which have not been studied previously, has been characterized. Nuclei in these samples appear to span 3-4 levels of polyteny, and changes in chromosome packing could be studied not only as functions of cell type but also as functions of chromosome and nuclear size. While certain features of nuclear organization were found in common among all nuclei examined, pronounced tissue-specific but polyteny-independent differences were found in nuclear shape, chromosome arrangement, and local structure in specific chromosomal regions. Specifically, all chromosomes display a right-handed coiling chirality, independent of homolog pairing and despite large differences in size and degree of coiling. Conversely, in each cell type, the heterochromatic centromeric regions have a unique structure, tendency to associate, and intranuclear location. The morphology of the chromatin within nucleoli is also tissue-specific. Prothoracic and salivary gland nuclei share many of the same general chromosome packing motifs, whereas hindgut and especially midgut nuclei display striking departures from these regularities. Most surprisingly,

gut chromosomes are often broken apart in the heterochromatin around the centromere. In vivo observations reveal severe deformations of midgut nuclei which may account for some of their unusual properties; these observations also suggest that chromosomes are either anchored to multiple nuclear sites or are embedded in a gel phase which limits chromosome movement.

Polytene chromosome growth

The data in Fig. 2 suggest that the ~$\sqrt{2}$ dependence of chromosome band width on DNA content determined from chromosome squashes (Hartmann-Goldstein and Goldstein, 1979; Laird et al., 1980) is an an accurate reflection of the situation in vivo. This value indicates that when DNA content doubles, the new chromatids are packed laterally into chromomeres at a density similar to that of the previous polyteny level. That is, as a band grows, it probably does so not by changing modes of higher order chromatin packing but by reiterating a basic folding regime. However, chromosome length also increases as the level of ploidy is augmented (Table 3). The width and length changes would be compatible if length increases were limite to interbands (also see Beermann, 1962).

An interesting result is obtained by using the $\sqrt{2}$ value to extrapolate back to the 1C chromosome present before polytenization. If a 1.5 μm width (Fig. 2) represents a 256C DNA content, the width of the 1C fiber would be ~94 nm. Structures precisely in this size range (80-100 nm) have been observed by electron microscopy of Drosophila and human chromosomes (Belmont, A., J. Sedat, and D. Agard, submitted). Equivalently, the maximum cross-sectional area available to a single

chromatid in the average polytene band can be estimated (Laird et al., 1980). A 1.5 μm wide band containing 256 chromatids provides a maximumcross-sectional area per chromatid of 0.0069 μm^2, treating the chromosome as a cylinder. This area could accomodate a cylindrical fiber with a maximum diameter of ~94 nm, the same value calculated above.

These calculations raise the intriguing possibility that the banded structure of the polytene chromosome represents a direct geometric amplification of a chromomeric organization in diploid interphase chromatin. Study of polytene band/interband structure may thus provide direct insight in diploid chromatin organization. The correspondence also suggests that the full cross-section of the band is packed with chromatin, rather than having a toroidal organization (Mortin and Sedat, 1982). The size and arrangement of chromatid fibers within the band must also meet these boundary constraints. For example, a 50 nm fiber (Sedat and Manuelidis, 1978; Mortin and Sedat, 1982) could meet the ~94 nm limit by forming a flattened higher order coil or loop in which 3 stretches of the fiber are laterally packed across the band. On the other hand, 200 nm chromatid fibers (Sedat and Manuelidis, 1978) would be too large to pack in register laterally across a band; more complex staggered packings are imaginable but would be inconsistent with the implied correspondence between a polytene band and a chromomere in the diploid nucleus. To validate these conclusions it will be important to verify the DNA level assignments made here.

The increment in band width between the two polyteny levels in salivary glands is lower than expected (Fig. 2). Two alternate hypotheses could account for this. On the one hand, it may be due to only partial band replication; this would imply that either the

chromatids within a band replicate asynchronously or only a subset of the chromatids within a band will replicate at this stage. There is evidence for lateral asynchrony in salivary gland chromosome replication (Lakhotia and Sinha, 1983), and total replication time increases with polyteny (Rudkin, 1972). This might result if higher polyteny chromosomes must compete for limiting amounts of replication factors. On the other hand, a change in the mode of packing of chromatin within the bands might occur at this level of polyteny, e.g., a tighter lateral association of folded chromatids. Several other properties change concomitantly. The fraction of nuclear volume taken up by chromosomes no longer increases with polyteny although nuclear volume still increases. This would be consistent with a simultaneous shift to a more compact packing of chromatin within the chromosome as suggested in the second of the above hypotheses. Finally, band width does not correlate with chromosome length in salivary gland nuclei as it does in the smaller nuclei, perhaps also reflecting an adjustment of chromatid packing in bands and/or interbands. Analysis of smaller salivary gland chromosomes will be needed to determine to what extent tissue-specific factors are involved in these differences rather than the level of ploidy per se.

Chromosome coiling and chirality

That a predominance of right-handed coils typifies the chromosomes from all tissues studied, even in midgut nuclei which retain few of the properties found in the other nuclei, indicates that this chirality is a basic property of the polytene chromosome. As such, it will provide a useful boundary condition for models of polytene chromosome structure.

The data in this report allow the characteristics of the chirality to be defined more fully. First, it is present in chromosomes of low polyteny (as low as 256C). These short, thin chromosomes are also tightly coiled -more so than their much larger salivary gland counterparts. Prothoracic gland nuclei of higher polyteny have chromosomes with wider and apparently fewer gyres. Second, even in chromosomes that show much less of a tendency to coil, the gyres that are present are almost all right-handed. Third, the asymmetry appears to be retained in unpaired chromosome regions, as in the salivary gland (Hochstrasser et al., 1986). Finally, chromosomes can fold back on themselves into interwound coils that always twist in a left-handed direction, implying that this mode of coiling is mechanistically related to right-handed solenoidal coiling.

The relatively tight coiling of low polyteny chromosomes as well as the reduction of coiling as prothoracic gland chromosomes grow, implies that coiling generally decreases as polyteny increases, at least in later stages. This points to an early time in the life of the cell when the degree of coiling is maximal and suggests that as the chromosomal cable lengthens and thickens, the earlier gyres are eliminated (also see Beermann, 1962). Chromosome coiling may be a relic of mitotic chromosome spiralization (Darlington, 1965), or it may develop in the interphase nucleus. Data on mitotic chromosome coiling show no evidence of a preferred coiling direction (e.g., Manton and Smiles, 1943; Ohnuki, 1968). Because a chirality in mitotic coiling has implications for the mechanism of chromosome condensation, this issue deserves reinvestigation. If the chirality has an interphase origin, right-handed coils could result from a hierarchy of chiral molecular interactions

within and between chromatids, analogous to the left-handed collagen fibril. Alternatively, they may arise from the denaturation of the right-handed DNA duplex required for its templating functions; the positive torsion on either side of the denatured zone could lead to twisting or coiling of the chromosome. Such torsion is able to twist one DNA duplex around another during the replication of circular DNA molecules (Sundin and Varshavky, 1981).

The left-handed interwound loops described here provide some support for the idea of an interphase origin for chiral coiling. Chromosomal homologs in polytene nuclei are intimately synapsed along their entire length. Since they are not paired in late mitosis (Cooper, 1938), synapsis must occur during the ensuing interphase. Pairing is complete in the interwound polytene loops; thus, to generate them from mitotic coils requires refolding chromosomes that have only partially unfolded yet have the two homologs at least roughly synapsed. The simplest explanation is that an intrinsic torsional strain in the chromosome leads both to solenoidal coiling and occasionally to plectonemic coiling. The relic gyres seen in early prophase and then gradually eliminated would, in this view, be the remnants not of the previous mitotic spiralization (Darlington, 1965) but of interphase coiling. We are now attempting to reconstruct early prophase chromosomes to determine whether the predicted bias in coiling direction is present.

Chromosome positions and the physical properties of interphase nuclei

The prothoracic gland data are consistent with our earlier contention that features such as chromosome domain separation, Rabl orientation, and nearest-neighbor packing of autosome arms reflect the stable maintainance of chromosome positions since the last mitosis many

days before (Hochstrasser et al., 1986). Recently, Hilliker (1986) has provided support for this idea by induced chromosome interchanges in the salivary gland anlage of 10-14 hour embryos with gamma radiation; the resulting pattern of interchanges suggested that each chromosome arm occupies a restricted domain within the nucleus at this early stage.

The telophase condition may be regarded as the starting state for every interphase nucleus. Several polytene cell types appear to retain much of this condition despite large structural changes, homolog pairing, and the long time since telophase. What happens to hindgut and especially midgut nuclei that leads to chromosome entanglement, loss of the Rabl orientation, lack of nearest-neighbor packing of autosome arms, and apparently even chromosome breakage (but no loss of homolog pairing)? On the basis of in vivo and in vitro observations of midguts (Fig. 11), we suggest that these changes are traceable to the severe deformations of nuclei during peristaltic contractions.

An obvious time for such positional scrambling is at the end of the last embryonic mitosis, during the transition period when the mitotic spindle is depolymerizing and the interphase nucleus is being reestablished. If external forces were applied to the decondensing chromosomes during this transition, they may well be jostled into new positions, even intertwining with one another. It is known that the first gut contractions begin ~13-14 hours into embryogenesis (Ede and Counce, 1956), close to the time of the last gut mitoses. This hypothesis, while plausible, raises a paradox when applied to the breakage of centric heterochromatin since tearing apart diploid chromosomes that must later divide will surely lead to chromosome loss. An alternative explanation is that the nucleus responds to stresses in a

manner similar to certain pliant composite materials in which a three-dimensional system of high modulus fibers is embedded in a viscoelastic gel phase (Wainwright et al., 1982). Nucleoplasm has gel-like properties (D'Angelo, 1950), and the polytene chromosome, with its many aligned chromatids, might also be expected to behave as a high modulus crystalline polymer (Wainwright et al., 1982). As they grow, chromosomes may gradually move under the continual stresses, losing their Rabl orientations and sometimes entangling. As the number of aligned chromatids increases, the strength of the euchromatic chromosome segments will increase, but the unreplicated heterochromatin at their bases may simultaneously become susceptible to fracture under stress. This interpretation predicts that early midgut nuclei will be much more like nonstressed tissues, e.g., without chromosome intertwinings or breaks.

Chromatin organization of centric heterochromatin and nucleoli

The chromocenter is made up of two zones with distinct structural and functional properties (reviewed by Spear, 1977). The large segments of heterochromatin seen in mitotic chromosomes around each centromere are thought to be confined to the highly underreplicated and transcriptionally inactive α-heterochromatin in salivary gland cells. Within this region on the sex chromosomes is the nucleolar organizer, containing the ribosomal RNA cistrons, which are replicated to a higher level than the surrounding satellite-rich heterochromatin. The poorly banded β-heterochromatin, interposed between the αheterochromatin and the banded euchromatin, is replicated in synchrony with euchromatin and is highly active transcriptionally.

The structural variations seen between chromocenters in different tissues is primarily in the β-heterochromatin, which represents an unusual type of transition zone between a region of multiple chromatids and one with only a few. Such structural differences were unexpected since the banding pattern in different tissues is very similar (Holden and Ashburner, 1978; Richards, 1980). Since in some tissues the chromocenter can be in the nuclear interior, nuclear envelope interaction cannot be directly responsible for its heterochromatic properties. Laird (1973) has proposed a differential replication model in which a nested set of stalled replication forks mark the boundary between euchromatin and unreplicated heterochromatin and between the ribosomal cistrons and the surrounding heterochromatin. Such a structure has been directly demonstrated for amplified chorion genes (Osheim and Miller, 1983). The unusual DNA organization in beta heterochromatin may make its overall structure especially sensitive to tissue-specific differences in underlying orders of chromatin structure. Nucleosome linker length is known to vary widely between cell types. The structure of the "30 nm fiber" can change with linker length, particularly in the crossed linker model of Williams et al. (1986), and this change may translate into the altered chromocenter morphology that we observe.

Another possible facet of tissue-specific chromocenter structure is that the boundary between nonreplicating and replicating DNA might be located over different DNA sequences in different tissues. This could be one way of segregating particular gene sequences into either transcriptionally inert alpha heterochromatin or highly active beta-heterochromatin. Only certain genes may be able to function in

this environment. Several genes regarded as heterochromatic, e.g., the light gene, are near the euchromatin/heterochromatin junction (see Spofford, 1976), and their function may be modulated by the exact boundary of the replication domain. Indirect evidence for this idea comes from the differential replication of satellite sequences in various polytene or polyploid tissues of Drosophila adults (see Spear, 1977).

Position-effect variegation occurs when a gene that is normally in a euchromatic environment is placed next to a heterochromatic breakpoint (Spofford, 1976). Inactivation of the gene appears to occur by the propagation of a heterochromatic structure across the breakpoint into the gene. A translocated heat shock gene, for example, is heterochromatinized in a variegated fashion in salivary gland cells, and its reduced expression does not result from underreplication of the gene (Henikoff, 1981). Since in some tissues the chromocenter can be in the nuclear interior, nuclear envelope interaction cannot be directly responsible for its heterochromatic properties. From the varied structure of chromocentral heterochromatin, one may predict that the ability of a heterochromatic structure to propagate into a nearby gene that is active in several tissues would differ in each. Tissue differences in position effect variegation have in fact been documented (Spofford, 1976). Certain heterochromatin-specific nonhistone proteins may be involved in this phenomenon (James and Elgin, 1986), and it will interesting to learn whether these proteins differ in distribution or quantity between different cell types.

A tissue-specific organization of nucleolar chromatin is indicated by the different but characteristic appearance of DAPI-bright material

within the nucleolus of each tissue (Fig. 8). Nucleolar DNA consists primarily of pre-ribosomal RNA coding sequences separated by nontranscribed spacers (Pardue et al., 1970). It is conceivable that specific subsets of nucleolar sequences, e.g., the nontranscribed spacers, organize or associate differently in each tissue to yield distinctive chromatin morphologies. Alternatively, differential replication of intron^{+} and intron^{-} ribosomal genes (Endow, 1983) may be under tissue-specific control, resulting in different chromatin morphologies. Evidence that this occurs has been marshalled to explain the narrow range of pleiotropic effects seen with rDNA deletions (DeSalle and Templeton, 1986). These ideas can be tested by in situ hybridization with the appropriate DNA probes.

In summary, we have found that chromosomes and specialized regions within chromosomes have tissue-specific organizational features. Variations between cell types include potentially functionally significant differences in chromatin structure in the nucleolus and in centric heterochromatin and differences that probably reflect a mechanically active tissue environment. Chromosomes may have a regular means of packing DNA into bands and interbands that leads to an apparently constant packing density within bands and an increase in chromosome length as nuclei grow. Chromosome size measurements also place constraints on the way chromatin can fold into bands. A right-handed coiling chirality typifies chromosomes from all tissues; this has implications for the mechanism of mitotic chromosome condensation or for interphase chromosome substructure and DNA topology. Many of the issues raised by these data can be further examined by a comparative 3-D analysis of chromosome substructure, particularly of

chromocentral chromatin and band/interband regions. We are currently developing both high resolution optical and electron microscopic reconstruction techniques to allow this.

Figure 1. Sample optical sections from DAPI-stained polytene nuclei in three tissues. (a,b) Sections from prothoracic gland nuclei. a shows a nucleus from the low polyteny class, b a nucleus from the higher class. (c,d) Sections from the "large cells" of the middle midgut. (e,f) Sections from hindgut nuclei. The sections shown in this and all other figures are original, computationally unprocessed images. All bars, 5 µm.

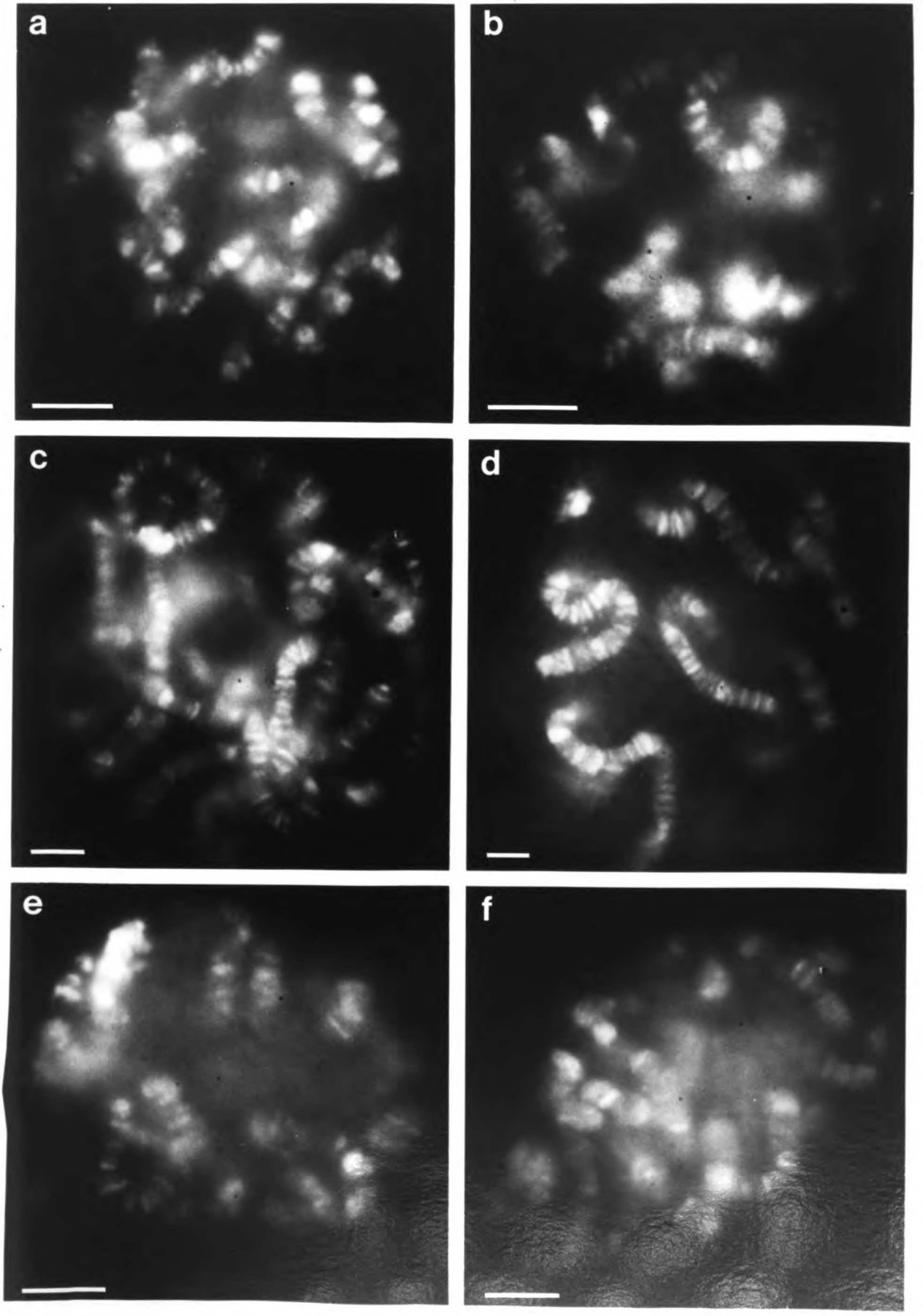
a
b
c
d
e
f

Figure 2. Average chromosome widths from four polytene tissues. Chromosome widths were measured at the same 10 prominent, unpuffed bands in 55 nuclei from 4 tissues (see Materials and Methods). Midgut (MG; 25 nuclei) and hindgut (4 nuclei) widths are shown above the central horizontal axis, prothoracic gland (PG; 11 nuclei) and salivary gland (SG; 15 nuclei) widths in inverted orientation below it. The hindgut chromosome diameters overlap the midgut widths in the 1.4 to 1.8 µm size interval (indicated by broken lines); an assignment to a particular polyteny class cannot be made from the limited hindgut data.

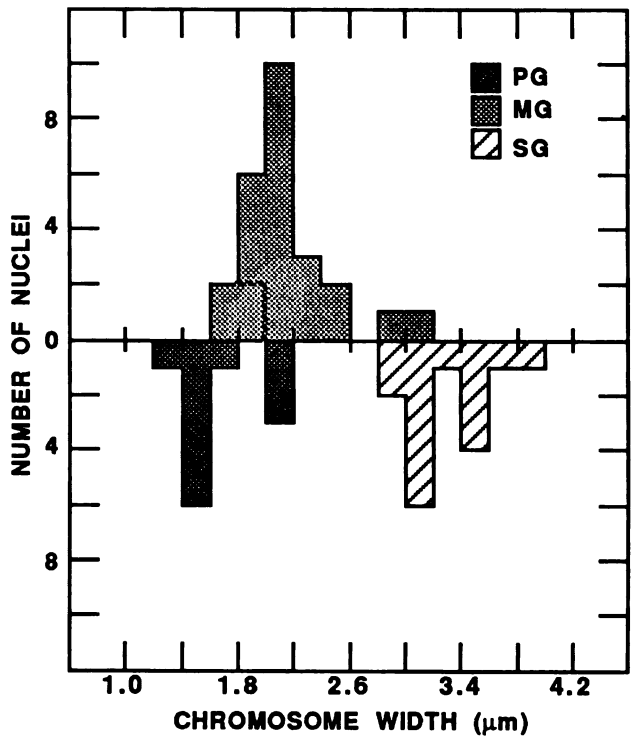
PG
MG
SG
8
4
0
4
8
NUMBER OF NUCLEI
1.0
1.8
2.6
3.4
4.2
CHROMOSOME WIDTH (μm)

Figure 3. Stereo-pairs of representative chromosome models from each tissue. (a) Prothoracic gland nucleus. Each chromosome arm is color coded as follows: X: green; 2L, red; 2R, blue: 3L, purple; 3R, light green; 4, yellow. The large pink ball represents the nucleolus. The crosses mark the telomeres of each chromosome arm and the squares their chromocentral endpoints. The X chromocentral endpoint is behind the nucleolus in this view. Because proximal heterochromatin is not modeled, the left and right arms of the major autosomes are not connected. (b) Middle midgut nucleus. The color code and markings are the same as in a. An optical section from this nucleus is shown in Fig. 1d, where the X and 3R telomeres can be seen as well as the intertwining of these two chromosome arms. (c) Hindgut nucleus. The color code and markings are as above (chromosome 4 is not modeled). Different optical sections from this nucleus can be seen in both Fig. 1e and Fig. 8b. Model diameters in vertical direction are approximately 21, 49, and 22 μm for a-c, respectively.

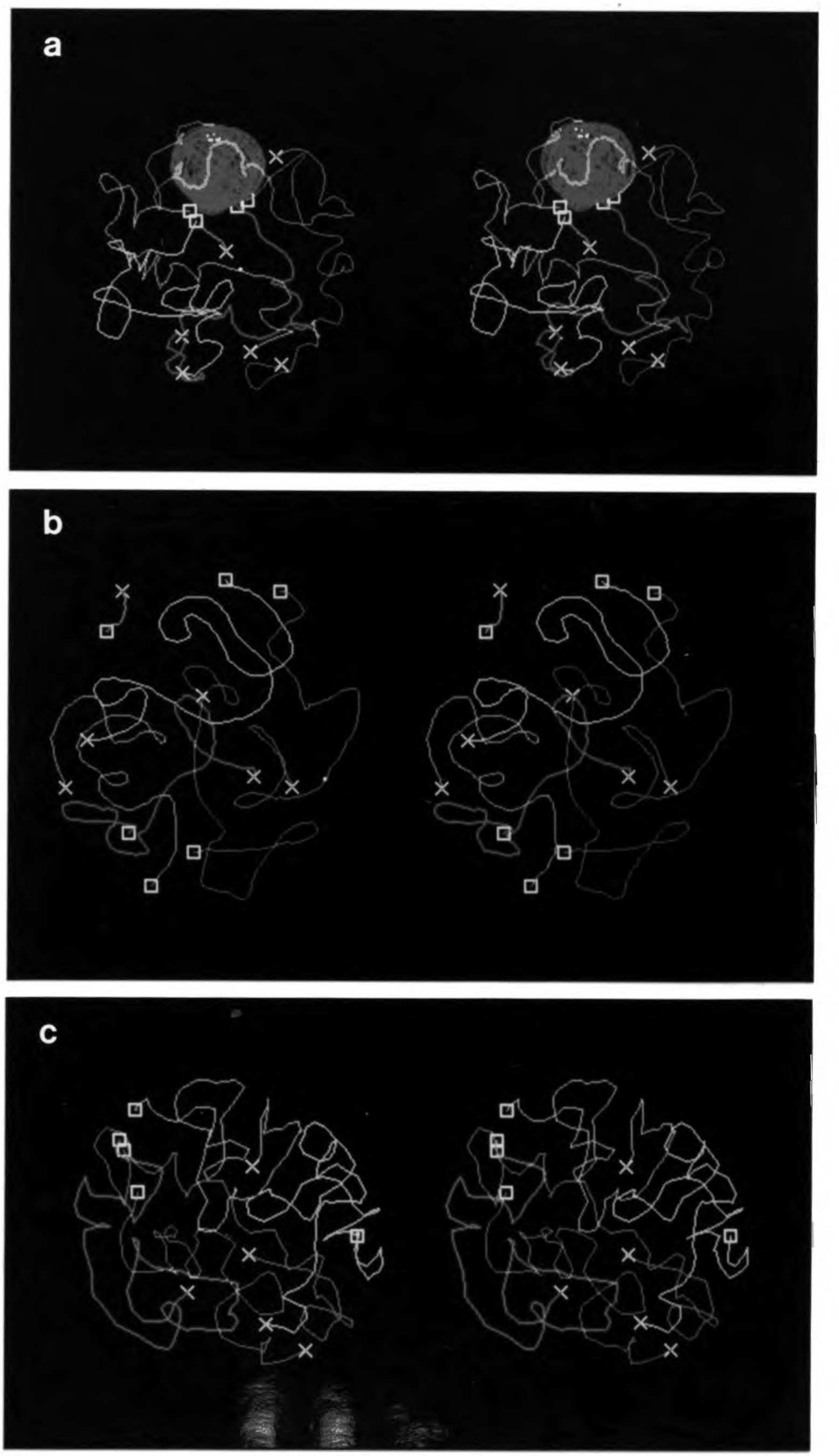
a
b
c

Figure 4. Middle midgut chromosome arm 2R intertwined with 3L. 2R runs through a right-handed coil in 3L. In the original section data, 3L is seen to be tightly wrapped around the other arm. Squares and crosses mark the chromocentral and telomeric endpoints, respectively, of each chromosome arm.

Figure 5. Right-handed solenoidal region of a hindgut chromosome. Successive optical planes, spaced at one notch intervals on the microscope focus knob, through a tightly coiled chromosome segment. The left photogragh (a) is the top section. Pictures were taken on a Zeiss Universal microscope of a sample prepared in the same way as the hindgut from which the nuclear reconstructions were made. Bar, 2 μm.

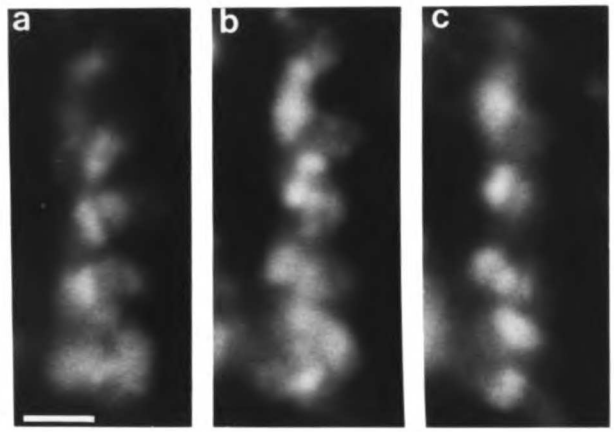
a
b
c

Figure 6. Triple product histograms for chromosomes in three tissues. Triple product values along each chromosome arm in every nucleus are histogrammed for each tissue. The triple product was calculated as described in the text. Positive values indicate right-handed coiling, negative values left-handed coiling. The vertical scale is arbitrary. Because of the different lengths of chromosomes in different tissues, different spacings between unit vectors were used to calculate the triple product; however, other spacings that are not extremely large or small yield the same qualitative results. Each individual chromosome arm shows the same skew toward positive values in each tissue. PG=Prothoracic gland: 55 chromosomes; 4 μm vector spacing. MG=Middle midgut: 110 chromosomes (the 3 male nuclei were omitted); 5 μm vector spacing. HG=Hindgut: 20 chromosomes; 4 μm vector spacing. The ratio of positive to negative values using the indicated vector spacings are: 1.9 (PG), 1.9 (HG), and 1.3 (MG).

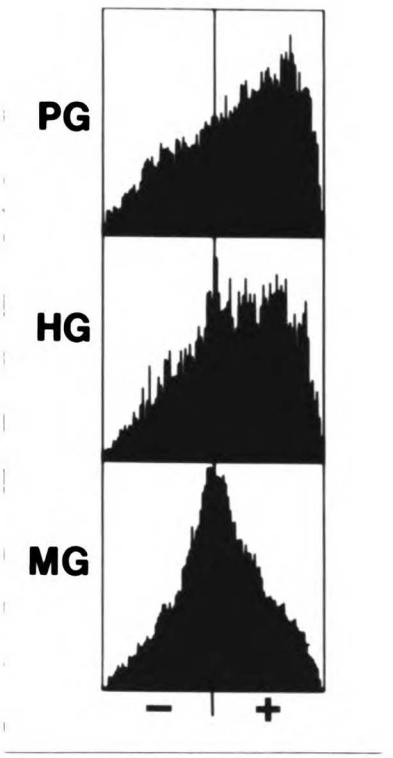
PG
HG
MG
−
+

Figure 7. Left-handed interwound loop in a chromosome arm from a middle midgut nucleus. Successive optical sections, spaced at 1.4 µm intervals, through a tightly interwound loop in the central region of 2R. The left photograph (a) is the topmost section. Bar, 3 µm.

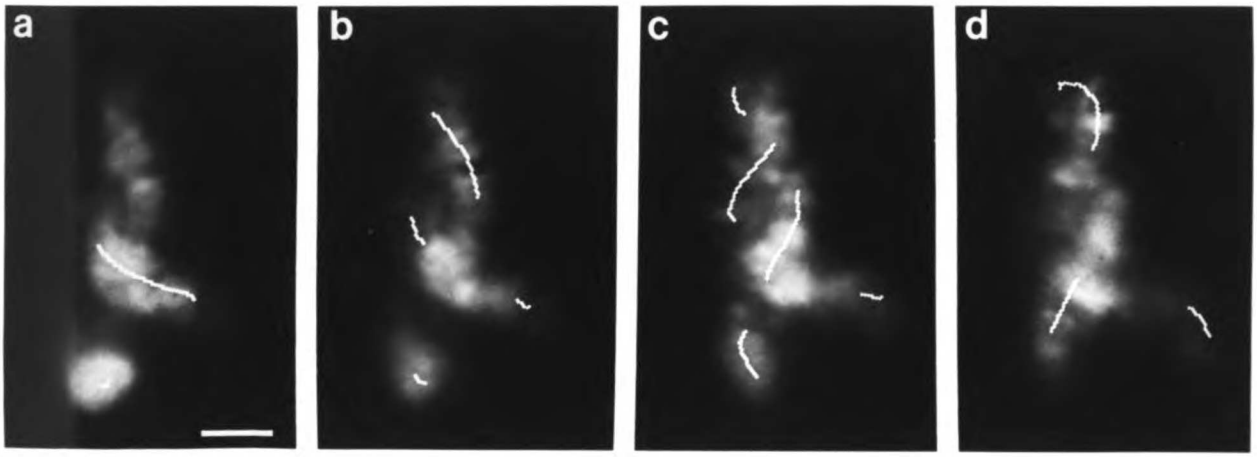
a
b
c
d

Figure 8. Structure of condensed nucleolar chromatin in 3 polytene tissues. (a) Prothoracic gland nucleolus showing the diffuse fibrillar pattern of DAPI staining typical of this tissue. (b) Hindgut nucleolus showing punctate pattern of DAPI-bright staining. The arrow points to a thin fiber running between the proximal end of 3R to the nucleolus. (c) Midgut nucleolus containing a dense mat of thick DAPI-bright fibers. All bars, 2 μm.

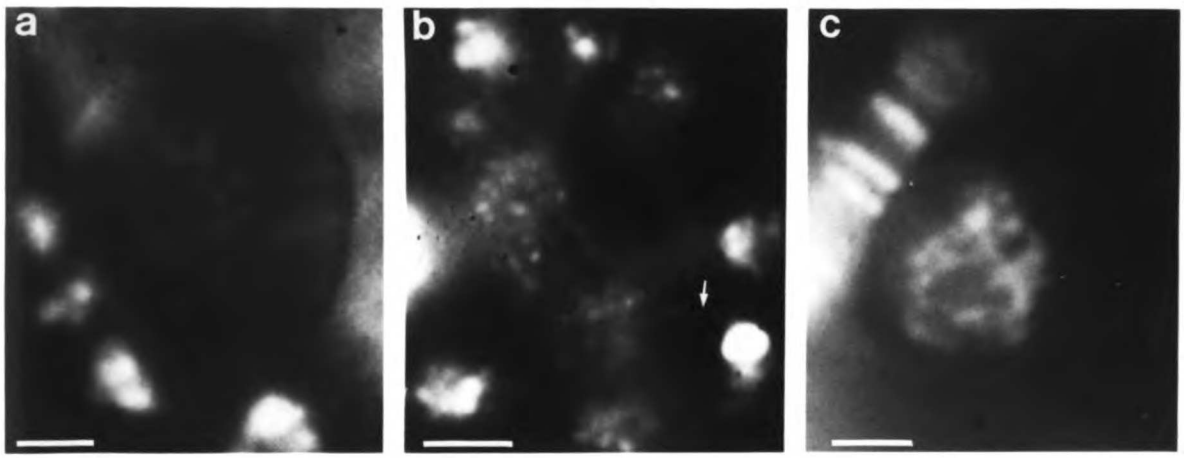
a
b
c

Figure 9. Chromocenter structure in prothoracic and salivary gland nuclei. (a,b) Optical sections of salivary gland chromocenters. In a only the centromeric region of chromosome 2 is seen; the other centromeres are located in another region of the nucleus, unconnected to this one. An irregular banding can be discerned. In b all the centromeric zones are aggregated, and the spongy chromatin structure is evident. Scale bar (for a,b), 3 μm. (c) Electron micrograph of a section through a salivary gland chromocenter. Arrowhead points to the zone of α-heterochromatin (see Lakhotia and Jakob, 1974). Some irregular bands in the β-heterochromatin can be made out in the right of the micrograph. Short fibers connect to the nuclear envelope between or to the edges of nuclear pores. (d,e) Optical sections of prothoracic gland chromocenters. The chromocenter is closely associated with the nucleolus in both nuclei. Scale bar (for d,e), 3 μm. (f) Electron micrograph of a prothoracic gland nucleus. The loose mat of twisted or zig-zagging fibers, which connect to the banded euchromatin at upper right, look very similar to the chromocentral structures seen in the optical images. A cloud of small particles similar in size to those seen in the nucleolus (N) surround the chromocenter. Bar (for c,f), 1 μm.

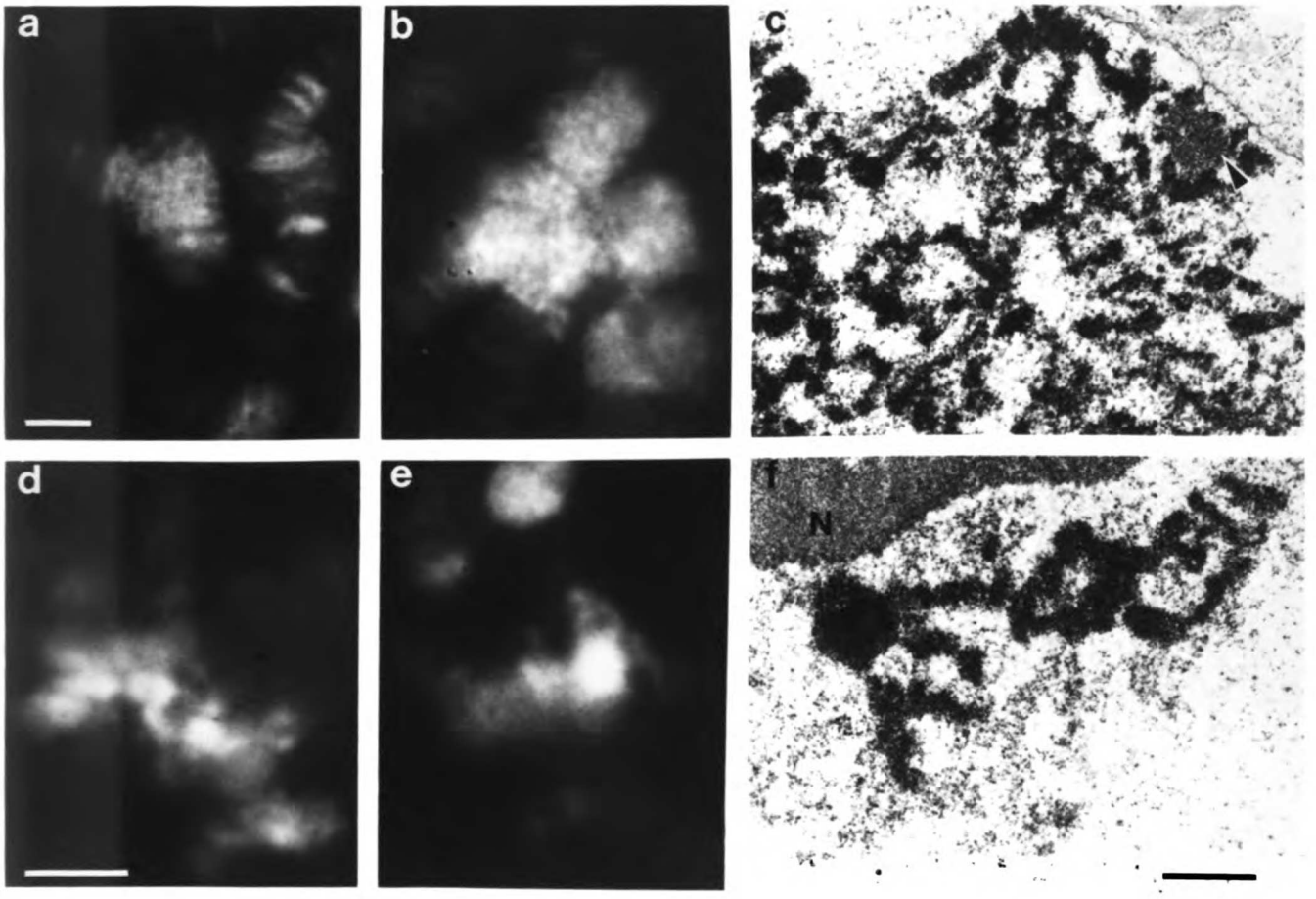
a
b
c
d
e
f
N

Figure 10. Chromocenter structure in middle midgut and hindgut nuclei. (a-c) Midgut chromocenters. a and a' are successive optical sections showing a network of heterochromatin fibers. In b the chromocentral endpoint of 3L (arrowhead) appears severed from that of 3R (stumpy arrow). Loose, heterochromatin is indicated by long arrows. The intercalary heterochromatin in 56F of 2R is pulled into a narrow fiber (asterisk). In c a portion of the X beta heterochromatin appears as a series of loosely linked bands and runs past a dense heterochromatic region of another chromosome. Scale bar (for a-c), 3 μm. (d) Hindgut chromocenter. Long fibers, only partly in focus, run to a denser mass of heterochromatin near the nucleolus. Bar, 3 μm.

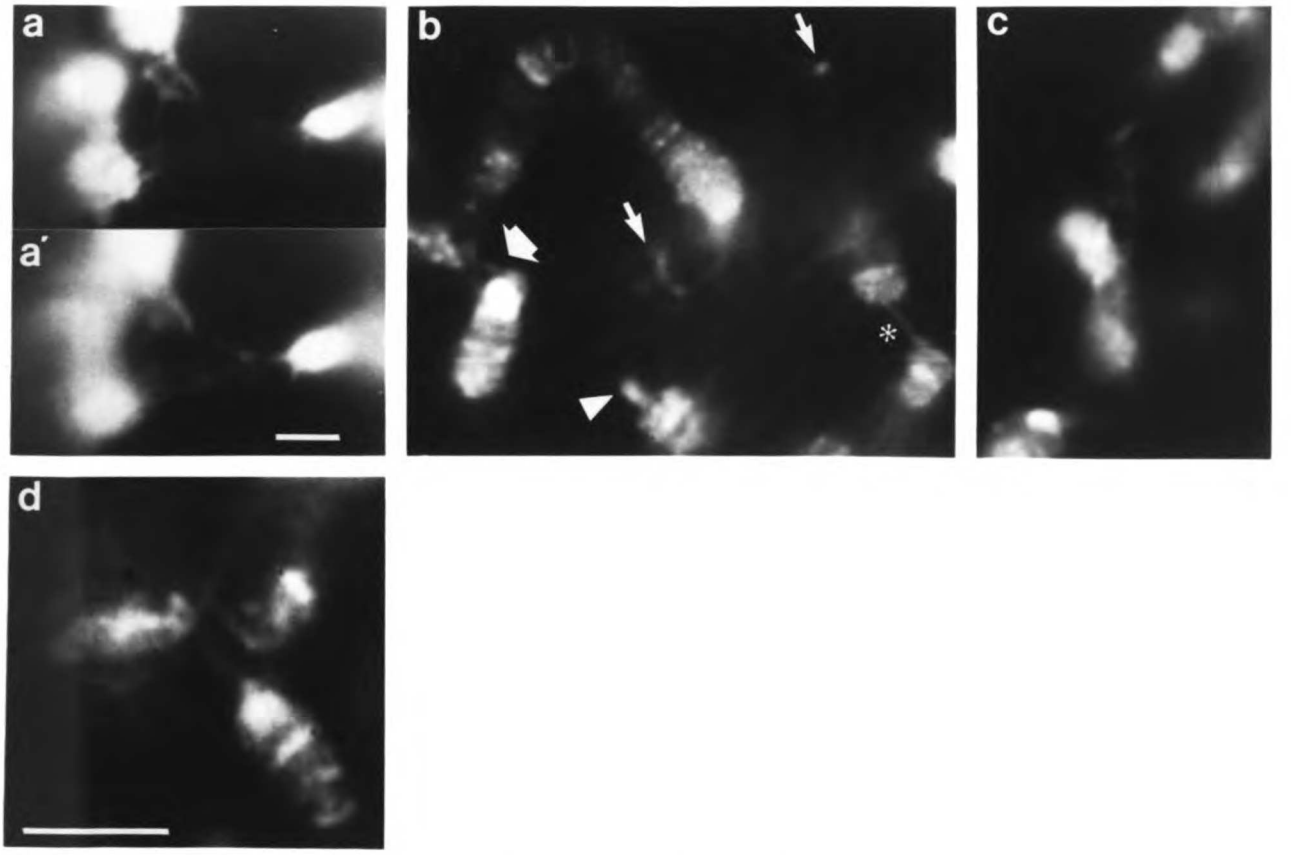
a
a'
b
c
d

Figure 11. Appearance of middle midgut nuclei in living larvae. (a-d) A series of video images of the same nucleus over an interval of ~10 seconds taken on a 3/4 inch Sony videocassette recorder. A low power (40X) objective lens was used for both increased depth of focus and ease of tracking nuclei. The series displays the dramatic changes in nuclear shape that occur during peristaltic contractions. (e,f) Different nuclei during phases with minimal local gut contraction taken with a 100X/1.3 numerical aperture Neofluar lens. Despite the low resolution of the recording medium, the ellipsoidal shape of the nuclei and the straight or meandering paths of the chromosomes that are also observed in isolated guts are apparent. Larvae were injected with a 200 µg/ml solution of DAPI; the dye is absorbed from the hemolymph by most tissues, particularly the midgut. Pictures of videoframe images were taken from a television monitor.

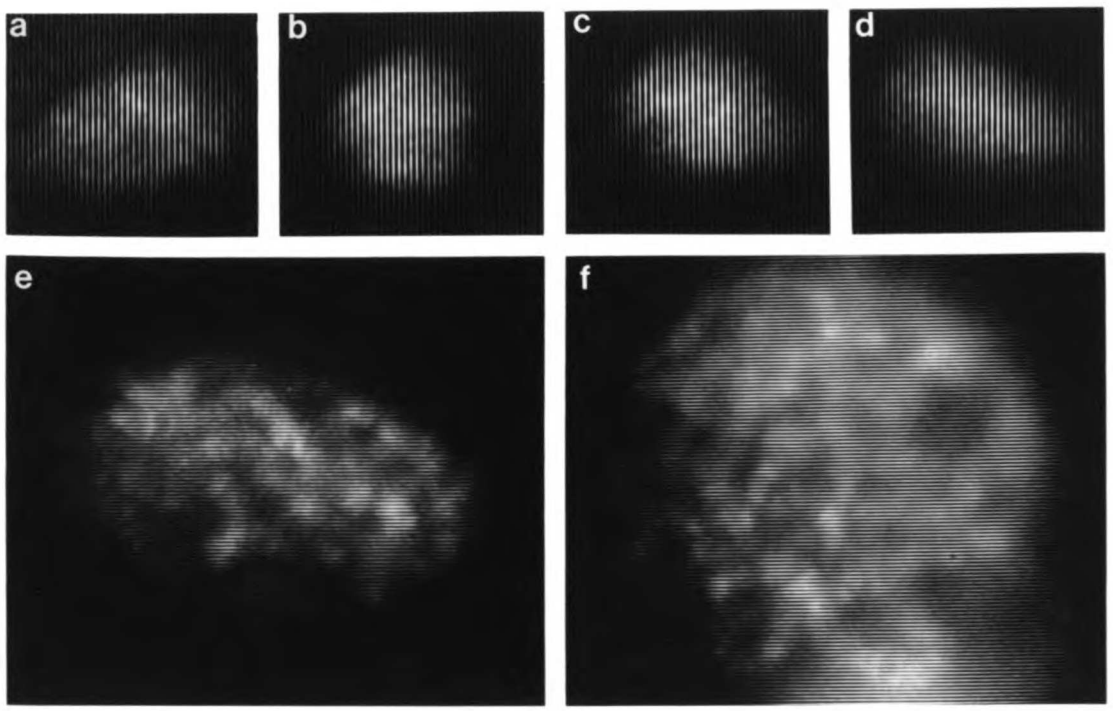
a
b
c
d
e
f

TABLES

Table 1: Average middle midgut nuclear diameters (±standard deviation).

Long axis length*	Short axis length*	Long axis/short axis
44±5 µm	20±4 µm	2.3±0.4

*Values from measurements of models to which the average chromosome diameter for each nucleus has been added (see Materials and Methods).

Table 2: Euchromatic chromosome arm lengths(mean±standard deviation, in µm).*

Chromosome arm	PG	HG	MG	SG
X	85.2±9.3	98.1±0.5	113.8±13.2**	139.8±4.7
2L	80.5±10.0	98.9±6.3	111.6±19.0	142.4±9.7
2R	73.6±7.4	96.2±5.5	111.9±15.2	144.3±7.8
3L	80.6±6.4	106.8±2.8	116.3±13.6	153.9±12.2
3R	103.1±11.3	127.0±8.2	142.0±18.2	184.5±11.5

*Chromosome arm endpoints given in Materials and Methods.

**Only the 22 female nuclei are included.

Table 3: Size characteristics of polytene nuclei.

Property	PG	HG	MG*	SG
Total euchromatic chromosome length (μm)				
Average(±S.D.)	423±41	527±19	604±73	765±35
Range	390-530	508-546	477-798	714-825
Nuclear volume (μm^3)				
Average(±S.D.)	5783±1297	6429±1134	19480±7618	18850±4443
Range	4543-7789	5687-8116	9150-35797	13253-31858
Nucleolar volume (μm^3)				
Average(±S.D.)	343±127	-	-	-
Range	201-586	-	-	-

*Only the 22 female nuclei are included.

Table 4: Comparison of Chromosome/Nucleus volume ratios.

Tissue	Presumptive Polyteny class	C/N(S.D.)	t	slope**
Prothoracic gland	256C	0.13(.02)		
			5.43*	0.44
	512C	0.20(.02)		
Middle midgut	512C	0.11(.03)		
			4.00*	0.73
	1024C	0.18(.02)		
Salivary gland	1024C	0.34(.03)		
			-	1.07
	2048C	0.34(.03)		

**Determined from log-log plot of nuclear (y) vs. chromosome (x) volume by linear regression (Materials & Methods).

*: $P < 0.001$

Chapter 4

Three-Dimensional Organization Of Drosophila Melanogaster Interphase Nuclei. II. Chromosome Spatial Organization and Gene Regulation

ABSTRACT

In the preceding article we compared the general organization of polytene chromosomes in four different Drosophila melanogaster cell types. Here we describe experiments aimed at both testing for a potential role of three-dimensional chromosome folding and positioning in modulating gene expression and examining specific chromosome interactions with different nuclear structures. By charting the configurations of salivary gland chromosomes as the cells undergo functional changes, it is shown that loci are not repositioned within the nucleus as the pattern of transcription changes. Heterologous loci also show no evidence of specific physical interactions with one another in any of the cell types. However, a specific subset of chromosomal loci is attached to the nuclear envelope, and this subset is extremely similar in at least two tissues. In contrast, no specific interactions between any locus and the nucleolus are found, but the base of the X chromosome, containing the nucleolar organizer, is closely linked to this organelle. These results are used to evaluate models of gene regulation that involve the specific intranuclear positioning of gene sequences. Finally, data is presented on an unusual class of nuclear envelope structures, filled with large, electron-dense particles, that are generally associated with chromosomes.

INTRODUCTION

Eukaryotic cells use a variety of mechanisms to ensure that genes are expressed in the cell types in which their products are required. The relative activity of a gene in different cell types can vary over at least eight orders of magnitude (Ivarie et al., 1983). It has

frequently been proposed that the specific positioning of genes within defined subnuclear compartments is a component of this remarkable range of control (Comings, 1968; Blobel, 1985; Hutchison and Weintraub, 1985; Jackson, 1986). In this paper we will focus on the potential role of the three-dimensional arrangement of chromosomal loci in the tissue-specific regulation of gene expression.

Continued interest in this question has been generated by studies of the so-called nuclear matrix, an insoluble residue left after treatment of nuclei with high or low salt concentrations, detergent, and DNAase. Many claims for specific association of certain DNA sequences with this structure, particularly of transcribed and/or replicating sequences, have been made. However, the data are not yet consistent enough to make strong conclusions (reviewed in Kaufmann et al., 1986). Most significantly, no relationship between this in vitro fraction and a structure existing in vivo has been demonstrated.

The idea that certain DNA sequences can be segregated into specific subnuclear compartments as a means of gene regulation has received support from a study of DNase hypersensitive sites in isolated nuclei. There is an apparent concentration of such sites -thought to mark active loci- in the periphery of the nucleus (Hutchison & Weintraub, 1985). On the other hand, [3H]uridine pulse-labeling experiments on intact cells indicate nascent transcripts are concentrated at euchromatin-heterochromatin boundaries, which are not necessarily at the nuclear surface (Fakan et al., 1976), so the issue remains open.

Indirect analysis of interphase chromosome positions, such as the elegant experiments of Cremer et al. (1982), has revealed that in many types of cells, chromosomes are maintained in relatively stable,

polarized configurations within limited subnuclear territories. Unfortunately, it has not yet been possible to describe the dispositions of chromosomes beyond this gross structural level. A review of experiments suggesting nonrandom elements in interphase chromosome spatial organization can be found in Comings (1980).

In the absence of direct data on the subject, a variety of hypotheses have been advanced that invoke a role for specific three-dimensional nuclear architectures in various aspects of gene regulation. In the present report, we test some of the predictions made by these models using a quantitative analysis of the three-dimensional folding of chromosomes in different polytene tissues of D. melanogaster and in salivary gland cells subjected to functional perturbations. We show that chromosomes do not fold into determinate configurations, that specific chromosome-envelope interactions occur but are unlikely to be necessary for tissue-specific gene expression, that specificity in chromosome-nucleolus contacts is restricted to the nucleolar organizer, and that chromosome configurations are remarkably stable even during drastic shifts in the pattern of transcription. We also provide data on an unusual class of nuclear envelope structures that may be involved in nuclear-cytoplasmic exchange. In the Discussion, the impact of these data on models of nuclear architecture will be considered.

MATERIALS AND METHODS

Sample preparation

Sample preparation for both light and electron microscopy are described in Hochstrasser and Sedat (preceding chapter).

Heat shock and ecdysone treatment of salivary glands

Either of two physiological media were employed for dissections and incubations: the buffer of Shield and Sang (1970) or Grace's insect medium (Gibco) as modified by Ashburner (1970). The latter lead to slight nuclear shape changes in the heat shock experiments but appeared otherwise satisfactory. Glands were mounted in buffer on a slide under a bridged coverslip, and the slide was sealed with paraffin oil. A Zeiss Neofluar 100X/1.3 numerical aperture objective lens was used with bright field optics. To achieve optimal contrast, the field diaphragm was closed down as far as possible, the condenser aperture was fully open, and the condenser lens was brought just short of the Kohler condition, i.e., slightly further away from the sample. Immersion oil was also put on the condenser lens. This technique was found to be superior to either phase contrast or Nomarski differential interference contrast methods.

In the first type of heat shock experiment, a temperature-controlled stage mount (ref) was modified to allow the use of a high resolution lens; supports constructed from pieces of glass coverslips and slides were affixed to the mount and made to be just slightly thicker than the slide/coverslip sandwich used to hold the glands. The mount was preheated to 37°C, and the slide was quickly taped onto it; the whole assembly was placed on the stage of a Zeiss Universal microscope with the slide side down and the objective lens extending into the hole in the metal mount. The glass supports were taped to the stage. 1-2 minutes is required between the taping of the slide and examination of the first nucleus. In some experiments nuclei were observed with a 40X/0.75 numerical aperture lens. Photographs were taken at one or a few

focal planes every 1-2 minutes for 20-35 minutes; in between, the full depth of the nucleus was monitored.

In the second kind of experiment, glands were placed on the microscope and two nuclei were selected for observation. Sets of bands visible in a selected focal plane in each were sketched. Photographs of 15-20 serial optical sections, spaced at one notch intervals on the focus knob, were then taken. The slide was subsequently placed on a 37°C hot plate for 20 or 30 minutes and immediately placed back on the microscope stage. The original focal plane from each nucleus was identified from its sketch, and a parallel series of optical planes was photographed. In several experiments, another 1.5-2 hours at room temperature were allowed to elapse and the same focal planes were rephotographed. After both types of experiment, glands were squashed in lactoacetoorcein to verify that the major heat shock loci were puffed. Other controls included treating glands identically except for the omission of the heat shock and testing glands for trypan blue exclusion after the experimental manipulations (a 0.4% dye solution was diffused into the space under the bridged coverslip; cells damaged by handling rapidly accumulated the dye and usually had pycnotic nuclei). Kodak 2415 film was always used and was developed in Kodak HC110 (Schedule F).

We checked the possibility that the heat shock loci were already clustered before the temperature shift. This was done be measuring the distances between all pairs of the 9 heat shock loci (or the 6 major ones) in 17 unfixed nuclei (Hochstrasser et al., 1986) and finding the average (overall average=13.9±3.2 μm). This value was then compared to the same measurement for a set of 9 (or 6) control loci. To match the relative locations of the heat shock loci in the genome, the control

loci were chosen by "projecting" the heat shock loci onto the other autosome (e.g., the 67B locus on 3L projects onto 27B on 2L). The control loci had a similar overall average separation (13.0±2.6 μm) to the heat shock loci.

For the ecdysone treatments, Grace's insect medium, modified according to Ashburner (1970), was used, and beta-ecdysteroid (Sigma) was added to a final concentration of 5 μM. Bright-field optical sections were collected in a manner analogous to the heat shock experiments except that in one experiment, optical sectioning was done on the computer-controlled Zeiss Axiomat microscope and images were stored on a magnetic disk. One lobe of the gland was squashed before each experiment to determine whether it had the PS1 (intermoult) puffing pattern (Ashburner, 1972). After collecting data at 1-2 hour intervals over an 8-12 hour span, the gland was squashed to ascertain the final puffing stage reached. The heat shock puffing pattern was not observed. As controls, we analyzed the puffing patterns of sets of PS1 glands that were subsequently mounted on slides and exposed to ecdysone as above. The estimated stages, based on a comparison with the tables in Ashburner (1972), were as follows: 4 hour incubation (~PS6), 6 hour (~PS8-9), 8 hour (~PS10-11), and 10 hour (~PS11-12). The kinetics appear similar to those described by Ashburner but a few differences were noted, e.g., 74EF/75B remained slightly puffed at later stages and 78D was unpuffed early but puffed at 6-8 hours. Finally, cells were shown to be alive by the trypan blue exclusion criterion at least 6.5 hours after mounting in 5 μM ecdysone.

Quantitative analysis of models

Chromosome-surface contact frequency plots are described in Hochstrasser et al. (1986); the maximum distance from the surface used as a cutoff to generate each of the plots is given in Figs. 4,5. The 2x2 contingency tests for the association of high frequency peaks in each tissue (selected as those frequencies with a random probability of less than 0.05 as determined by Monte Carlo calculations) with sites of intercalary heterochromatin and with the peaks in other tissues are described in the same reference. As before, the chromosome arms were divided into 3-letter subdivisions (e.g., 10A-10C) for the contingency tests. To test whether the overlap of contact peaks between tissues was truly due to specific local properties, we compared peak positions between nonhomologous arms in prothoracic and salivary gland, the two tissues showing a strong correlation of peak positions (prothoracic X vs. salivary gland 2L, etc.). The peak positions were found to be independent (chisq=0.897, P'0.3). Chromosome intradistance plots and the methods employed to analyze them are described in Mathog et al. (1984) and Hochstrasser et al. (1986). Chromosome distance to the nucleolar surface (see preceding chapter) was measured in a manner analogous to distance to the nuclear surface. A 2.0 or 2.25 μm cutoff was used to generate the contact frequency plots because this is close to the largest average chromosome diameter in any of the prothoracic gland nuclei.

RESULTS

Chromosome positions are not dynamically coupled to gene expression

The "nuclear address" hypothesis posits that the expression of a gene will depend on its placement in a specific compartment or position within the nucleus (e.g., Bingham and Zachar, 1985). One feature of the hypothesis that has not yet been tested is the possibility that gene spatial arrangements are dynamic and undergo specific changes as the pattern of transcription changes, either as a function of development or in response to exogenous signals. For example, specific loci may translocate to the nuclear envelope for efficient expression (Hutchison and Weintraub, 1985). Such changes, if they occur asynchronously within a tissue, may also account for the finding that chromosome configurations have only limited similarities between cells of the salivary gland (Hochstrasser et al., 1986). Different cells within the same salivary gland, for example, are known to differ in the timing of glue granule formation (Berendes and Ashburner, 1978) and in the general steady state levels of RNA transcripts (Probeck and Rensing, 1974).

The hypothesis of dynamic gene positioning was tested by examining salivary gland chromosome dispositions before, during, and after heat shock. Raising the temperature of salivary glands from 25°C to 37°C, in vivo or in vitro, leads to a dramatic change in the pattern of transcription; most genes previously active cease being transcribed while a specific new set of genes is activated (Ashburner, 1970). Rather than attempt to construct an entire new set of chromosome models from heat shocked glands and compare them to our previous data, we examined the same nuclei in both states. This could be done with bright field optical microscopy (Materials and Methods).

The experiment was performed in two ways. In the first, third instar salivary glands were mounted in physiological medium on a

temperature controlled stage heated to 37°C. This allowed nuclei to be monitored continuously for changes in chromosome positions. In the second, optical sections were first collected from several nuclei in a gland, the gland was then subjected to a 20-30 minute heat shock, and a new set of optical sections were collected from the same nuclei. A total of 10 nuclei from 5 glands were studied in the latter set of experiments, about two dozen in the former. Fig. 1 shows corresponding optical sections from nuclei before and after heat shock. In Fig. 1g an optical plane similar to those in Fig. 1c,f has also been photographed 1.5 hours (at room temperature) after heat shock. The question of direct interest can be readily answered: there are no prominent movements of chromosome segments in any of the nuclei from any of the experiments. Very small movements of ~1 μm or less may occur and are in fact observed on rare occasions. It should be noted that before heat shock, the heat shock loci are neither preferentially localized in the nuclear periphery (Hochstrasser et al., 1986) nor closely clustered within any subnuclear domain (see Materials and Methods).

Two other observations from these experiments should be pointed out. First, there is a rather dramatic change in nucleolar shape and/or position after heat shock (Fig. 1). It tends to go from an irregular, asymmetric structure to one that is simpler in shape and smoother in outline. Changes in nucleolar morphology during heat shock have previously been noted in diploid cells (e.g., Pelham, 1984), and may be related to the block in ribosome processing and assembly during such a stress (Pelham, 1984). The effect is at least partially reversible: 1.5-2 hours after returning to room temperature, the nucleolus is again more irregularly shaped. Second, the optical properties of the cell are

altered by heat shock. Immediately after treatment, the nucleus is optically much clearer and the nuclear boundary much more distinct. This may be due to the known cytoskeletal rearrangements that accompany heat shock, e.g., collapse of the intermediate filament network around the nucleus (Biessmann and Walters ref). This optical effect is also reversible (Fig. 1). It is interesting that despite these cytological changes around and amidst the chromosomes, their configurations remain unperturbed.

The analogous experiment has been done by incubating salivary glands with moulting hormone, beta-ecdysone, and charting chromosome dispositions. This treatment is known to simulate very closely the sequence of puffing changes seen in vivo (Ashburner, 1970b). 6 nuclei from 2 glands have been examined over 8-12 hour periods at 1 or 2 hour intervals. These experiments are complicated by various cytological changes that occur over these long times, including changes in nuclear shape and/or orientation, changes in nucleolar shape, swelling of the lumen of the gland, and pronounced changes in optical clarity presumably due to accumulation of cytoplasmic glue granules. Hence, only a half dozen or so chromosome segments could be reliably identified at most or all the time points. All of these appeared unchanged in position or orientation (data not shown). So to a first approximation, this result agrees with the heat shock experiments and with in vivo controls done over a more limited timespan (Hochstrasser et al., 1986).

Nonspecific chromosome configurations in all cell types

The manner in which the genome is packaged in the interphase nucleus clearly has many tissue-specific aspects in both diploid (e.g., Hsu et

al., 1971; Comings, 1980) and polytene cells (preceding chapter). For example, tissue-specific intranuclear locations and associations of centric heterochromatin typify nuclei in many cell types. To what extent this tissue-specificity involves the precise relative positioning of genes has been a matter of intense speculation (Comings, 1968; Lewin, 1981; Bennett, 1983; Blobel, 1985). Chromosome configurations may be established early in development, e.g., after the final mitoses of particular cell lineages, to specifically position loci that must at some point be activated in the differentiated cell. With chromosome models from a large set of nuclei in a different tissues, these speculations can now be experimentally tested.

Specific gene-gene structural interactions were not found in salivary glands (Hochstrasser et al., 1986). However, we do not know if this is generally true of interphase nuclei. In addition, several technical limitations are encountered in this tissue. First, the chromosomes are exceptionally thick; because the model is made by tracing a set of lines roughly through the center of the chromosomes, wider ones allow a greater range of point placement during the tracing which may partially obscure local folding similarities between nuclei. In prothoracic glands, with chromosomes 1/3-1/2 the width of those in the salivary gland, this difficulty is correspondingly reduced. Second, heterogeneity of salivary gland cell type could not be rigorously ruled out. This should not be a problem with the "large cells" (Poulson and Waterhouse, 1960) of the middle midgut. Almost all the cells examined were right at the Ia/Ib midgut bend (see preceding chapter). Morphologically, these cells are obviously distinct from the cells around them; moreover, histochemical and ultrastructural studies, among

others, clearly indicate that this cell type is segregated from neighboring midgut cell types (Poulson and Waterhouse, 1960).

Chromosome configurations have been analyzed in three new tissues: the prothoracic gland, the "large cells" of the middle midgut, and the hindgut. Prothoracic gland nuclei are very similar in general chromosome organization to salivary gland nuclei; nuclei from the other tissues are not (preceding chapter). As in our earlier work, we have emphasized the use of intradistance plots to compare chromosome folding in different nuclei (Mathog et al., 1984; Hochstrasser et al., 1986). In these plots, the absolute distance between every pair of loci on a chromosome model is measured and then plotted as an intensity value on a two-dimensional grid in which each axis represents cytological position along the chromosome. The pattern of intensities will be a mapped representation of the three-dimensional folding of the chromosome. Plots generated for a particular chromosome arm from every nucleus can be compared in several ways to look for similarities in chromosome folding.

Fig. 2 displays "rank order" intradistance plots for chromosome arm 2L from both prothoracic gland and midgut nuclei. What are ranked in ascending order in such plots are the intensity values (intradistances) at each point in the original set of plots (see above references). To illustrate how one reads such a plot, consider the point in Fig. 2a marked by an arrowhead. This point represents the pair of cytological loci 25C and 27C. Its intensity value (shade of gray) in this rank=5 plot represents a 3 μm distance. Thus, 25C and 27C are within 3 μm of each other (in the model) in at least 5 of the 11 nuclei examined.

From Fig. 2a it is evident that very few loci show a common set of close physical interactions even in a small subset (less than half) of the prothoracic gland nuclei, and these common contacts are confined to the region along the diagonal of the plot, i.e., to loci that are necessarily close together by virtue of their chromosome position. Prothoracic gland chromosomes in these nuclei have an average diameter of 1.6 μm, and the average length between each cytological division (e.g., 21A to 22A) is ~4 μm (see preceding chapter). Thus, to continue with the example above, the 25C and 27C loci would be ~8 μm apart if the chromosome ran perfectly straight through this region; to find that in a limited number of nuclei, these two sites are within 3 μm of each other is not surprising. Much of the chromosome in this tissue is tightly coiled; the off-diagonal features in Fig. 2a could simply indicate that the bending of the chromosome needed to achieve this coiling sometimes occurs in similar segments in several nuclei. That the plot is primarily an indication of relatively nonspecific chromosome bending rather than specific locus-locus interactions is supported by the control shown in Fig. 2b. To make this plot, the 11 original plots have had their intensity values shifted by different random distances along the diagonal; the resulting rank=5 plot shown in the figure therefore reflects only the random overlap of intensity values in the original plots (see Hochstrasser et al. (1986) for a detailed explanation). As can be seen, the randomized plot looks very similar to the original rank order plot, having features as far off the diagonal as in the latter case.

The midgut rank order plot in Fig. 2c reveals the same lack of folding specificity. Because chromosomes are much straighter in this

tissue, the intensity overlaps in the rank order plots due to nonspecific bending drop off even more rapidly as one goes up in rank; lower intensity values (closer appositions) rapidly shrink toward the diagonal. Fig 2c indicates that no two loci separated by more than ~2 cytological divisions on the chromosome are within 5 μm of each other in even 20% (5/25) of the nuclei. The similarity of the randomized midgut plot (Fig. 2d) to Fig. 2c further suggests a lack of folding specificity. The absence of regularities in midgut chromosome configurations can be directly verified by examining chromosome models. Fig. 3 shows stereo-pair models of 2L from 4 different nuclei. Chromosome configurations range from an uncoiled horseshoe shape to a tight ball of loops; local similarities are also wanting. Hence, we are not missing examples of specific three-dimensional configurations in the process of abstracting the information into intradistance plots.

Hindgut chromosome models were also directly compared and found to lack consistent similarities. Other ways of comparing plots, e.g., by direct examination of individual intradistance plots from all the nuclei, confirm these conclusions. We have also failed to find specific interactions between loci on different chromosome arms using interdistance plots, although the general relative arrangement of chromosome arms can be determined this way. Finally, while we have focussed on close contacts between loci, a specific tendency for loci to be positioned far from each other, beyond the general effect of Rabl orientations found in some of the cell types, is not evident either. In summary, in no tissue have we found evidence for specific chromosome folding or specific interactions between a particular pair or small groups of loci.

Specific chromosome-nuclear envelope contacts in different tissues

While chromosomes do not have determinate three-dimensional configurations, they may nevertheless form specific contacts with the nuclear envelope. This was shown to be the case in salivary glands (Hochstrasser et al., 1986). It is not known, however, what functional significance these specific surface contacts may have. One possibility often raised is that specific genetic loci are situated on the envelope in different cell types as a means of modulating tissue-specific gene expression (Hutchison and Weintraub, 1985; Blobel, 1985). A comparison of high frequency surface contacts in the different tissues studied here allows such an hypothesis to be experimentally tested.

Surface contact frequencies for the 5 major arms in both midgut and prothoracic gland nuclei are shown in Fig. 4. Peaks in these plots represent chromosomal loci that frequently appose the nuclear envelope. Because peaks and valleys are expected even with random juxtapositions, a selection criterion must be used to choose those peaks that are high enough to make it relatively unlikely that they are due to random contacts. The Monte Carlo method for determining random probabilities was described previously (Hochstrasser et al., 1986). As before, we have chosen a cutoff of $P < 0.05$ (random probability of occurring this many or more times) for selecting frequency peaks that are likely to represent specific contacts; as a comparison with a large new set of models from salivary gland nuclei has shown, this cutoff provides a relatively conservative estimate of the number of specific surface contacting loci (Mathog and Sedat, submitted).

As in salivary glands, different loci on prothoracic gland chromosomes vary markedly in the frequency with which they are found in

the nuclear periphery (Fig. 4a). At least 23 loci (arrows) are on the envelope at frequencies that are unlikely, by the above criterion, if contacts were only made randomly. Significantly, a very strong concordance between this set of loci and the high frequency contacts in salivary glands has been found (Fig. 5). The relation was assayed with a 2x2 contingency test (Hochstrasser et al., 1986) and found to be highly significant (chisq=35.6, P''0.001). These sites are also closely associated with intercalary heterochromatin containing loci (Zhimulev et al., 1982) by the same test (chisq=23.3, P''0.001).

The similarity between the two tissues extends further. First, in both tissues the average frequency of surface contacts is lowest in chromosome arm 2R. Second, of the 15 high frequency contacts identified in the salivary gland, 12 overlap sites found in the prothoracic gland. The exceptions are instructive. One of them is the single salivary gland peak that was not at an intercalary heterochromatin position (72B). The other two peaks not found in prothoracic glands are centered at 64C and 67D; in both cases, these loci fall just below the P'0.05 cutoff and may thus represent sampling effects rather than real differences. Another possibility, for 64C at least, is that a neighboring intercalary heterochromatin site interferes with its ability to reach the surface: 65C has a strong peak in the prothoracic gland data. The 19CE peak is actually found in salivary glands as well, although we chose not to discuss it because of its proximity to the surface contacting chromocenter. The chromocenter in usually not on the surface in prothoracic gland nuclei (preceding chapter). Finally, of the 10 prothoracic gland high frequency contacts not found in the original salivary gland data set, 7 actually do form peaks in another collection

of salivary gland nuclei (Mathog and Sedat, submitted), and 8 (including all 7 of the above) overlap intercalary heterochromatin-containing loci (4D, 59C, 60F, 61A, 65C, 75C, 86D and 89E). Thus, 20 of the 23 high frequency contacts in prothoracic gland nuclei have corresponding frequency peaks in salivary gland nuclei and 21/23 overlap intercalary heterochromatin loci. The extent of variation between the different tissues is comparable to the variation seen between different samples of salivary gland nuclei. In conclusion, the specificity of peripheral localization of chromosomal loci appears to be indistinguishable between the two tissues and in both is associated with sites containing intercalary heterochromatin.

A very different picture emerges when chromosome-nuclear surface appositions are analyzed in middle midgut nuclei (Figs. 4b,5). The characteristic pattern of surface contacts seen in the previous tissues is no longer present. In fact, an apparent loss of specificity is seen. Only 12 loci show contact frequencies at or above the $P<0.05$ cutoff, and 5 of these are at telomeres. The patterns of peaks are also flatter; this is reflected in a lower variance in peak height across each plot as compared to salivary and prothoracic gland plots. The very high frequency peaks that characterize the latter tissues, e.g., at 12EF and 35AC, are absent. Nonetheless, there remains a small (but inconsistent) overlap in the patterns between tissues. Midgut contacts are associated with both prothoracic (chisq=7.95, $P<0.01$) and salivary gland (chisq=8.97, $P<0.01$) frequency peaks, but if the telomeric divisions are omitted from the comparison, the former association no longer achieves significance (chisq=1.60, $P>0.2$). A correlation with intercalary heterochromatin, largely due to the telomeric contacts, is also observed

(chisq=12.1, P‘0.001). Possible reasons for the dichotomy between midgut nuclear surface contacts and those in the other tissues will be considered in the Discussion.

With only four hindgut nuclei reconstructed, a complete analysis of surface apposition frequencies cannot be done, but a preliminary survey is suggestive. In Fig. 5, the surface contact frequency plot for chromosome arm 2L is compared to the corresponding plots in the other three tissues. There is already some indication of the pattern of contacts seen in the prothoracic and salivary glands, especially in the 33-36 interval. Contingency tests, using only regions that are on the surface in all four hindgut nuclei, show a significant association with the peaks in all the other tissues as well as with intercalary heterochromatin (data not shown).

That certain chromosomal loci localize to the nuclear periphery was assumed to be due to their specific attachment to the nuclear envelope (Hochstrasser et al., 1986), but since we never actually saw this structure in our light microscope images, this assumption was unproven. To study these presumptive envelope-chromosome interactions, an electron microscopic analysis of thin-sectioned polytene cells was undertaken. While it is easy to find chromosome segments abutting the envelope in such sections, this is not sufficient evidence for an actual attachment. However, we have found a number of examples of regions of the envelope that are pulled inward toward a chromosome (Fig. 6). These are either attached to long chromatin fibers (Fig. 6b,c) or to a stretch of densely staining chromatin with many short fibers (Fig. 6a). As with chromocentral attachment to the envelope (preceding chapter), it is not possible to ascertain whether the fibers (Fig. 6b) attach to the edges

of nuclear pores or to the lamina around them, although our prejudice is again in favor of the latter. In addition, it may be noted from Fig. 6b that there is no concentration of nuclear pores near the sites of chromosome attachment, pores appearing essentially close packed throughout the envelope.

Only the chromocenter is specifically associated with the nucleolus

Several reports claim specific interactions between certain chromosomal loci and the nucleolus in Drosophila salivary glands (Ananiev et al., 1981; Steffenson, 1977). One locus in particular, 56EF, may be expected to associate with the nucleolus since it contains the genes coding for 5S ribosomal RNA. Because of the clarity of the single large nucleolus in prothoracic glands, it was possible to model its surface (see preceding chapter). Plots of the frequency of appositions between loci on chromosome X or 2R and the nucleolus are shown in Fig. 7. The number of close contacts between any particular locus (on any arm) and the nucleolar surface is low. 56EF is never within the 2.25 μm cutoff used to generate the plot; in 10/11 nuclei it is at least 5 μm away and in 3 nuclei it is over 10 μm away. The only euchromatic locus that appears with high frequency on the nucleolus is 19F/20A, at the proximal end of X (arrow). However, the nucleolar organizer is located in the heterochromatin at the base of X, and since the chromocenter is generally draped over the nucleolus (see preceding chapter), the 19F/20A peak may simply reflect this proximity. Small peaks at the base of several other chromosome arms support this contention.

That the base of the X chromosome is regularly associated with the nucleolus is not necessarily a trivial point. There are both cytological and biochemical data that suggest that ribosomal DNA, which is largely located within the nucleolus (Pardue et al., 1970), can actually be extrachromosomal in polytene cells (Semionov and Kirov, 1986; Zuchowski and H ref). In this state, it need not remain closely linked to the X chromosome. Interestingly, the euchromatic proximal end of X (around 20A) is often on the opposite side of the nucleolus from the rest of the chromocenter (see the model in Fig. 3a of the preceding chapter), and DNA extending in toward the centrally located chromatin within the nucleolus is sometimes seen. It is as if the nucleolus, expanding from the nucleolar organizer, pushed the distal region of the X chromosome away from the rest of the chromocenter as it grew. While not definitive, these observations suggest that in this tissue at least, nucleolar DNA is still continuous with the X chromosome. Finally, while no single locus associates with the nucleolus very often, it was noted that almost 3/4 of the X chromosome, on average, lies within a 5 μm shell around this organelle, whereas for the autosome arms, this average ranges from only 34% to 56%.

DISCUSSION

The experiments described here were directed toward both testing for a possible role of three-dimensional chromosome folding in modulating gene expression and examining specific chromosomal interactions with different nuclear structures. Chromosomal loci are not repositioned within the nucleus when the pattern of transcription changes during heat shock or ecdysone treatment, and they are not specifically configured in any of the differentiated cell types studied. On the other hand, a specific subset of chromosomal loci is attached to the nuclear envelope, and this subset is very similar in two of the tissues and possibly a third. No high frequency interactions between any euchromatic locus and the nucleolus were found except near the base of the X chromosome, which contains the nucleolar organizer.

These data will help to evaluate some of the models invoking a role for the three-dimensional folding of the interphase genome in regulating gene expression. In what follows, we implicitly regard a polytene interphase cell as equivalent to a differentiated diploid cell. This is a reasonable assumption. Polytene tissues are metabolically active and must synthesize many of the enzymes and molecules present in diploid cells. They are characterized by tissue and developmentally-specific patterns of gene expression (Ashburner, 1972). The same transcriptional machinery and DNA regulatory elements used in diploid cells are found in polytene cells as well (e.g., McGinnis et al., 1983). DNA in both classes of cells is organized into nucleosomes (Hill et al., 1982) and into chromatin structures with specific patterns of DNAase hypersensitive sites (McGinnis et al., 1983). The occurrence of transitions between polyteny and endopolyploidy and even from polyploidy

back down to a diploid state (Ashburner, 1976) also argues against a fundamental difference in genome architecture between these kinds of cells. Finally, we have found many aspects of polytene chromosome packing that are seen in diploid cells as well (preceding chapter; Hochstrasser et al., 1986). Possible exceptions to this general similarity will be evaluated below.

Gene regulation by relative gene positioning

Some authors have proposed that particular gene sequences may be able to actively manuever into different functional compartments within the nucleus. Hutchison and Weintraub (1985), for example, suggest that one step in activating a gene may be to tag it in a way that allows the gene to move into an active compartment. The experiments described here, using heat shock or ecdysone treatment to reset the pattern of transcription in salivary glands while the dispositions of chromosomes were followed, argue against repositioning of genes playing a part in gene regulation in a terminally differentiated cell . Chromosome positions are remarkably stable, even in the face of cytoskeletal rearrangements and changes in nucleolar shape and position (Fig. 1). These results also render highly improbable the idea that the wide range in chromosome configurations seen in salivary glands (Hochstrasser et al., 1986) was due to asynchronous functional states in the collection of cells examined.

A number of theories propose that genes are positioned within the interphase nucleus in a tissue-specific manner (see Comings 1968, 1980). The most extreme models posit a specific genomic three-dimensional structure in each differentiated cell type (Steffensen, 1977; Blobel,

1985). This view is succinctly stated by Steffensen: "Simply, gene placement is nuclear determination." Other models are described in vaguer terms, but also invoke higher order gene-gene interactions or superdomains (Bennett, 1983; Feldman and Avivi, 1984; Sved, 1976) that are thought to "reflect strong selection for their economic and efficient action" (Bennett, 1983).

We have now examined the spatial organization of nuclei in four different tissues spanning 3-4 levels of ploidy. In none of them have we found any indication of specific chromosome configurations. This is especially clear in midgut nuclei, where a chromosome can range from a tight ball of coils to a horseshoe shape with no coils at all (Fig. 3). Additional, indirect evidence includes the variable association of midgut centromeric regions, including apparent chromosome breakage and occasional interwound foldback loops forming in nonsimilar chromosome segments (preceding chapter). There are also no obvious subpopulations of cells within a tissue that show specific longer range interactions (Fig. 2), although complex combinatorial schemes involving large numbers of loci in different but specific interactions with one another cannot be ruled out. It must be emphasized that the nuclei in this study have been subjected to a minimum of manipulation and were examined under conditions as close to in vivo as possible. Moreover, the ability to superimpose the cytogenetic sequence of bands onto the chromosome models has made possible an unprecedented level of precision in making comparisons between nuclei. It therefore may be stated that a tissue-specific genomic three-dimensional structure is not a general feature of interphase nuclei.

In addition to the many similarities between diploid and polytene cells (see above), the fact that low polyteny chromosomes, as well as those in salivary glands, do not have specific configurations lends credence to an extrapolation of our conclusions to diploid cells. Strictly speaking, however, specific locus-locus interactions in diploid chromosomes cannot be unequivocally dismissed even though it is unclear why such interactions would be necessary in diploid cells and not polytene ones, since if anywhere, it is in very large nuclei that one might expect diffusion times of factors going between loci to become a significant limitation. It also is possible, in principle, that specific interactions are important early in development, but "relax" in terminally differentiated cells. Finally, the data in Figs. 2-3 do not address the organization of DNA at the level of bands or small stretches of bands. For example, euchromatin position effects are now well known (Spradling and Rubin, 1983); our results indicate they are not the result of long range locus-locus interactions.

Gene regulation by gene positioning in subnuclear compartments

Direct gene-gene interaction represents only one possible type of higher order functional compartmentalization. Another potential compartment is the nuclear periphery (Heslop-Harrison and Bennett, 1984; Hutchison and Weintraub, 1985), where specific genes in each differentiated cell type may be "gated" via nuclear pores to the cytoplasm (Blobel, 1985; see also Kaufmann and Gay, 1958). The localization of specific chromosomal loci to the nuclear periphery in salivary glands (Hochstrasser et al., 1986) could be taken as support for this hypothesis. However, the specificity of peripheral

localization is almost identical to that found in the prothoracic gland (Figs. 4,5). Thus, the genes that are usually located on or very near the nuclear surface are essentially the same in the two cell types. Yet prothoracic and salivary glands have very different patterns of gene activity (Holden and Ashburner, 1978; Hochstrasser, in prep.). For example, of the 24 prominent puffs found on 3L, a minimum of 14 or 58% are active in only one of the two tissues (Holden and Ashburner, 1978). The fact that few of the contact loci are on the surface in 100% of the nuclei also suggests that a gene need not be on the surface to function properly (although the method of measurement may miss occasional contacts and attachments to envelope infoldings could be missed).

One could argue that the similar positions of high frequency contacts in the two tissues (and possibly the hindgut as well) reflect the presence at these loci of "housekeeping genes" that are expressed in all tissues and must be localized at the envelope. It is unlikely that surface localization is essential for the correct regulation of such genes, however, given the reduced and/or altered specificity of envelope contacts in the middle midgut (Fig. 4). Many of the high frequency contacts in the other tissues are only occasionally on the surface in this tissue, and considerably fewer loci regularly make contacts. The different contact pattern found in midgut cells may be related to the fact that these nuclei are subject to strong deformations that probably contribute to chromosome tangling and possibly breakage (preceding chapter). These deformations may sometimes shear away envelope attachments as well, thus partially washing out the specificity of contacts. Alternatively, the relative timing of envelope attachment and chromosome decondensation during early interphase may be different in

these cells, presenting, for example, fewer potential binding sites to the surface, or the very straight midgut chromosomes may not bend frequently enough to allow the dispersed set of intercalary heterochromatin sites to regularly appose the surface.

It is interesting that the similarity between the high frequency surface contacts in prothoracic and salivary glands does not extend to the chromocenter (preceding chapter). As with the salivary gland chromocenter, the electron microscopic data (Fig. 6) implicate direct attachment to the envelope of loci with characteristics of intercalary heterochromatin as the cause of specific peripheral localization. This is supported by the strong correlation of high frequency envelope contacts with such loci. Thus, intercalary heterochromatin may not simply be a very small amount of the same sort of chromatin that makes up the chromocenter, but may well have distinct structural and functional properties. It probably also has a similar structure in different tissues -even though it is difficult to discern directly- that invests it with a high envelope affinity.

The common feature of intercalary heterochromatin that is thought to lead to properties such as constriction in squashes and ectopic fibers is the presence of underreplicated, tandemly repeated DNA sequences (Zhimulev et al., 1982). Perhaps this also accounts for its avid envelope binding, e.g., by pairing to repeated structural motifs in the polymeric lamina or by allowing the cooperative assembly of a chromatin structure with high envelope affinity. One perplexing aspect of the general association between intercalary heterochromatin loci and envelope binding is that a number of such loci (e.g., 3C, 11A) are in fact not in frequent contact with the surface. It will be interesting

to learn what molecular properties might distinguish these exceptional cases. For example, certain nonhistone proteins are known to bind to a subset of intercalary heterochromatin loci (James and Elgin, 1986), and such proteins may mediate envelope attachment. This can be tested by antibody staining of intact polytene or diploid nuclei.

Another potential functional compartment within the nucleus is the perinucleolar zone. Certain genes involved in nucleolar function, e.g., the 5S RNA genes, may localize to the nucleolus (Steffenson, 1977; Pardue et al., 1973). However, we find no specific associations in prothoracic gland nuclei except in the vicinity of the nucleolar organizer (Fig. 7). This is actually consistent with in situ hybridizations done in Xenopus which show the same distribution of 5S DNA in both wild type and anucleolate somatic cells (Pardue et al., 1973). As mentioned in the Results, the close link between the nucleolar organizer and the nucleolus may well indicate that nucleolar DNA is not extrachromosomal in this tissue as it has been suggested to be in salivary glands (Semionov and Kirov, 1986 and references therein).

A final nuclear compartment to consider is the hypothesized nuclear matrix (Kaufman et al., 1986). We have no evidence for or against such a structure and so cannot test whether genes are specifically positioned with respect to it except insofar as the nuclear lamina is considered a matrix component. A major protein in the matrix fraction is topoisomerase II; it was shown to localize along chromosomes in Drosophila salivary glands (Berrios et al., 1985). Topoisomerase II is also known to bind to specific DNA sequences and to be associated with replicating DNA (Nelson et al., 1986). These findings highlight a major point of contention about the internal matrix, namely, whether it is a

coherent structural entity that does not simply represent a set of chromosomal components of low solubility. These alternatives cannot be distinguished by the available data.

The transvection effect and nuclear structure

One unexplained genetic phenomenon often interpreted in terms of a specific three-dimensional genome architecture is the transvection effect. In this effect, the phenotype associated with a pair of alleles appears to depend on whether they are homologously paired to each other. It has been documented in both diploid and polytene tissues (Kornher and Brutlag, 1986 and references therein). The best studied case involves the effect of the zeste gene on transvection at the white locus. With the z(1) allele, the color of the fly's eyes are yellow when two copies of the white gene are paired and wild-type when they are not (Jack and Judd, 1979). A certain mutant allele of white, w(DZL), when combined with a wild type copy also yields yellow-eyed flies only if the two alleles are synapsed (see Bingham and Zachar, 1985).

Bingham and Zachar (1985) favor an explanation of transvection in which the synapsed pair of alleles are positioned as a unit in a specific compartment within the nucleus. The w(DZL) allele, when synapsed with the wild type copy, is thought to cause the latter to be placed in a nuclear position inappropriate for its expression. The z(1) product must somehow antagonize the correct positioning of the white genes as well, although only if they are paired. The evidence from our analysis weighs against this model, unless the hypothetical compartment to which tranvection-sensitive genes are supposed to segregate is some as yet undefined structure(s) diffusely distributed within the nucleus.

Transvection-sensitive genes, including Sgs-4, which is active in the salivary gland (Kornher and Brutlag, 1986), are not specifically localized near the nuclear surface, the nucleolus, or one or a few other chromosomal loci.

While our results argue against many of the exotic models outlined above, the finding of indeterminate chromosome configurations, coupled to their relatively static positions over both short and long developmental periods, is not without potential genetic consequences. These conditions could place important constraints on DNA transactions that depend on the juxtaposition of particular DNA sequences, e.g., recombination, DNA repair, and some types of transcriptional control. A possibile example of the latter is suggested by in vitro evidence that transcription factors can move between DNA molecules by a rapid direct transfer mechanism (Fried and Crothers, 1984; Kmiec et al., 1986). The assembly of a transcriptionally competent 5S RNA gene complex has been proposed to occur via a metastable intermediate that must exist for a certain minimum time; if there is a limiting amount of trancription factor, rapid DNA-mediated transfer of factors between sites could prevent this minimum time from being reached (Kmiec et al., 1986). Our data suggest that this mechanism could not operate effectively in vivo unless the multiple binding sites were clustered because transfer is unlikely to be sufficiently rapid over very long, statically arrayed chromosomes (Fried and Crothers, 1984).

Clustering in cis may be selectively maintained for multicopy or otherwise related genes that are subject to this mode of regulation. At least two other situations where factor transfer between closely positioned DNA molecules may be important can be suggested. The

zeste-white interaction could be explained by supposing that in a z(1) background, a limiting amount of a positive transcription factor(s) for white is available and can transfer rapidly between synapsed gene copies, preventing a metastable transcription complex from existing on either copy long enough to be actively assembled. The paired chromatids in polytene nuclei may provide another example, with DNA-mediated transfer allowing the hundreds or thousands of gene copies to function as a tightly regulated unit even through many rounds of replication.

APPENDIX

The unusual pod-like structures seen near chromosome attachments (Fig. 6a,c) were found in many regions of the envelope, usually filled with large electron-dense particles. Fig. 8 provides further examples. The "pods" appear to involve infoldings of the inner nuclear membrane only. The electron density and appearance of the material inside them is distinct from both nucleoplasm and cytoplasm. They are surrounded by an electron dense layer similar to the nuclear lamina which is continuous with it. Several examples of circular structures, tentatively identified as pore annuli, have been seen in grazing sections (Fig. 8f). The pods often (always?) occur together with double membrane blebs (Gay, 1956) into the cytoplasm. Occasionally, they are also associated with double membrane invaginations.

The particles in the pods are exceptionally large, ranging in size from ~100 to at least 200 nm. Over 30 can sometimes be counted in a single gold section, implying that hundreds may fill a large pod. The substructure of the particles indicates they involve aggregates of smaller particles (e.g., Fig. 8g). Perinuclear pods have also been

observed in the midgut (Fig. 8d). In reexamining the micrograghs of envelope blebs made by Gay (1955, 1956), we could sometimes discern material similar to what has been described here; however, pod structure was not well preserved, and they were regarded as dense chromosomal fibers (Gay, 1956). Looking at salivary glands from timed developmental stages, Gay found that blebs only appeared when the cytoplasm was filling with glue granules. In fact, the glands in which we observed pods were packed with large glue granules.

Perinuclear pods may provide insight into several aspects of envelope structure and chromosome interaction. We wish to learn whether the chromosome association is linked to pod formation, e.g., if attachments create tension on the inner envelope that can help pull apart the two membranes at these points. Obvious questions about the structural changes in envelope components are also raised. The nature of the large particles is unclear, although their morphology suggests they may be RNP particles. We are currently testing this proposition with immunogold labeling of RNP proteins. It is worth pointing out a potential parallel with the large RNP particles found at the 93D locus (Dangli et al., 198?). The size of these particles is similar to those in perinuclear pods, and they also appear to be aggregates of smaller (RNP) particles. The 93D particles accumulate to high levels under heat shock conditions. Conceivably, the accumulation of giant particles in both 93D and perinuclear pods is due to a block or backup in RNP processing or transport. Finally, it is unlikely that these chromosome-envelope interfaces represent the transport of gene products synthesized only from the chromosomal locus directly attached since our

data argue against the tissue or stage-specific attachments of loci that are implied in such a model.

Figure 1. Effect of heat shock on chromosome positions. (a-c) Optical planes of nuclei in living salivary glands photographed before heat shock. a and b are different planes within the same nucleus. (d-f) Corresponding optical sections from the same nuclei shown in the first row but after a 30 minute (d,e) or 20 minute (f) heat shock at 37 C. The similarity of chromosome positions is evident as is the change in nucleolar shape. (g) A section of the ~same optical plane shown in c,f after the gland has been at room temperature for 1.5 hours following the heat shock. A reversible change in optical clarity can be discerned. The arrowhead points to the "ballet skirt" in division 68 of 3L; the 67B heat shock locus is nearby (not visible in section). Bar, 10 μm.

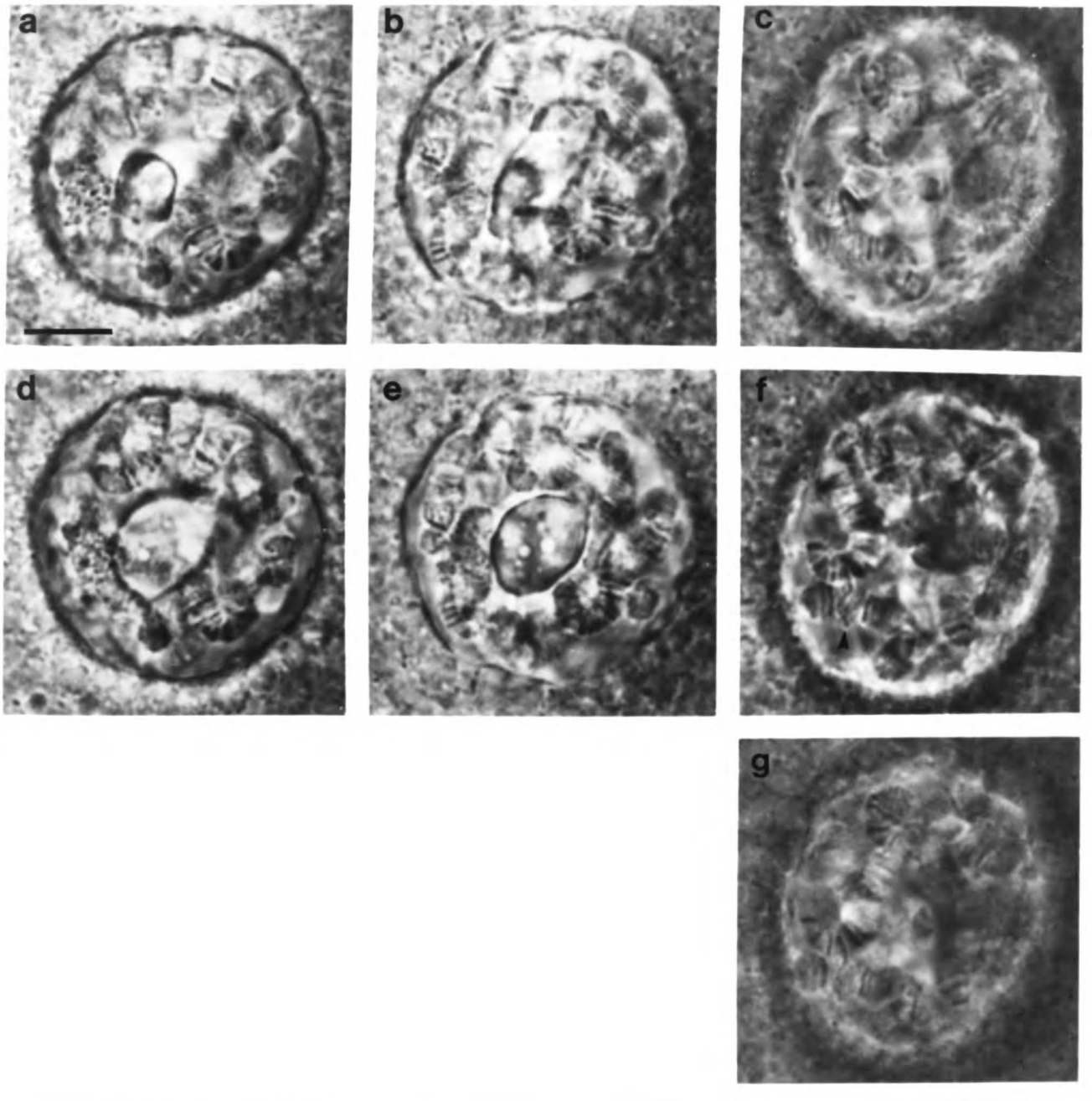
a
b
c
d
e
f
g

Figure 2. 3-D folding of prothoracic gland and midgut chromosomes. (a) A rank=5 rank order intradistance plot for prothoracic gland chromosome 2L. The plot was generated from the original set of 11 2L intradistance plots. Distances between loci are represented by contoured intensity values; the darkest regions mark pairs of loci closest together in space. Distances are rank ordered at each pixel from the smallest (rank=1) to the largest (rank=11). Contour steps are separated by 1 μm, and distances greater than 5 μm are set to white. Cytological position is plotted along both axes with grid lines separated by two cytological divisions. T=telomere (21A). CC=chromocentral endpoint (40F, but cytology only followed to 40A). For further explanation, see text. The arrowhead marks an area representing the interaction of 25C and 27C, which are within 3 μm of each other in at least 5 out of 11 nuclei. (b) A rank=5 rank order intradistance plot generated from the same set of 11 prothoracic gland 2L intradistance plots except that the intradistance values were randomly displaced with respect to the cytogenetic sequence by a different amount in each (see text). Values are plotted as in a. (c) A rank=5 rank order intradistance plot for middle midgut chromosome 2L. The plot was made from the original set of 25 2L intradistance plots. (d) The analogous rank=5 plot generated from the set of 25 midgut 2L intradistance plots that had been randomly displaced relative to one another.

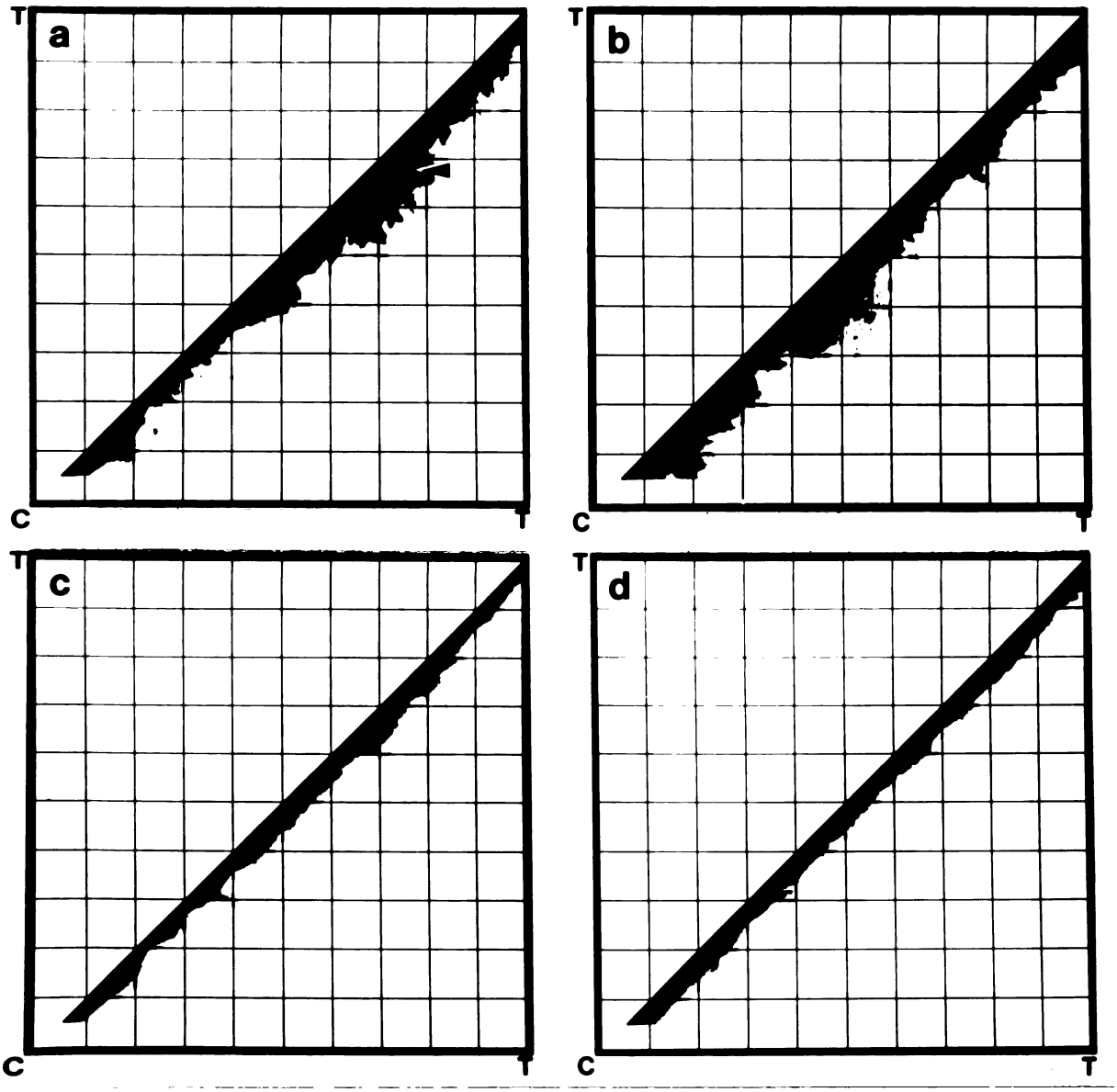
a
T
C
T
b
T
C
T
c
T
C
T
d
T
C
T

Figure 3. Chromosome arm 2L in four different middle midgut nuclei. The wide range of configurations is evident.

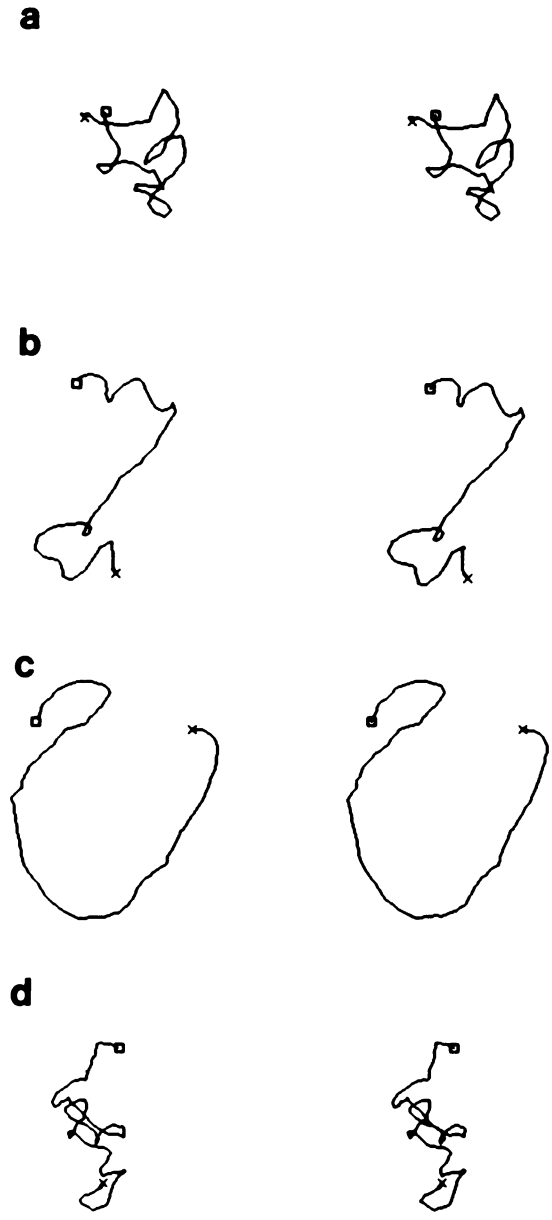
a
b
c
d

Figure 4. Nuclear surface contact frequencies for the 5 major chromosome arms. a) Surface contact frequencies for chromosomes in 11 prothoracic gland cells. A locus was considered to contact the surface if it fell within 0.75 µm of the convex polygon in which the model was inscribed (Mathog et al., 1984). This cutoff is slightly smaller than that used for midgut chromosomes (b) because these chromosomes are thinner and with the smaller number of nuclei, the plots are more sensitive to random contacts. The abscissa represents cytological position, with each vertical division representing one cytological division (e.g., 1A-1F) in the respective arms (Bridges, 1935). The ordinate scale runs from 0 to 11 (out of 11). T=telomere. C=chromocenter. The values in the left-most division in each plot have been set to zero because the cytology is not followed into these areas. Cytology was noted on the models at 20 loci on each chromosome (telomeres and all A1 bands, e.g., 15A1); cytological points in between were place by linear interpolation between the identified loci (Mathog et al., 1984). The telomeres in the 2R and 3R plots fall one letter subdivision short of the right end. The arrowheads highlight regions where the contact frequency is at or above the $P<0.05$ cutoff (indicated by the dashed lines). Note that broad bands could represent the overlap of two or more attachments, e.g., there are 3 strong intercalary heterochromatin sites between 83D and 84D. (b) Surface contact frequencies for chromosomes in 25 middle midgut cells. All aspects of the plot are exactly as in a except that the ordinate scale is 0-25 (out of 25) and the plots were generated with a 1.0 µm cutoff distance. Cytology on the X chromosome in 2 of the 3 male nuclei could not be identified along the entire arm, so the plot of X

chromosome contacts includes 23 chromosomes rather than 25 (ordinate scale is therefore 0-23).

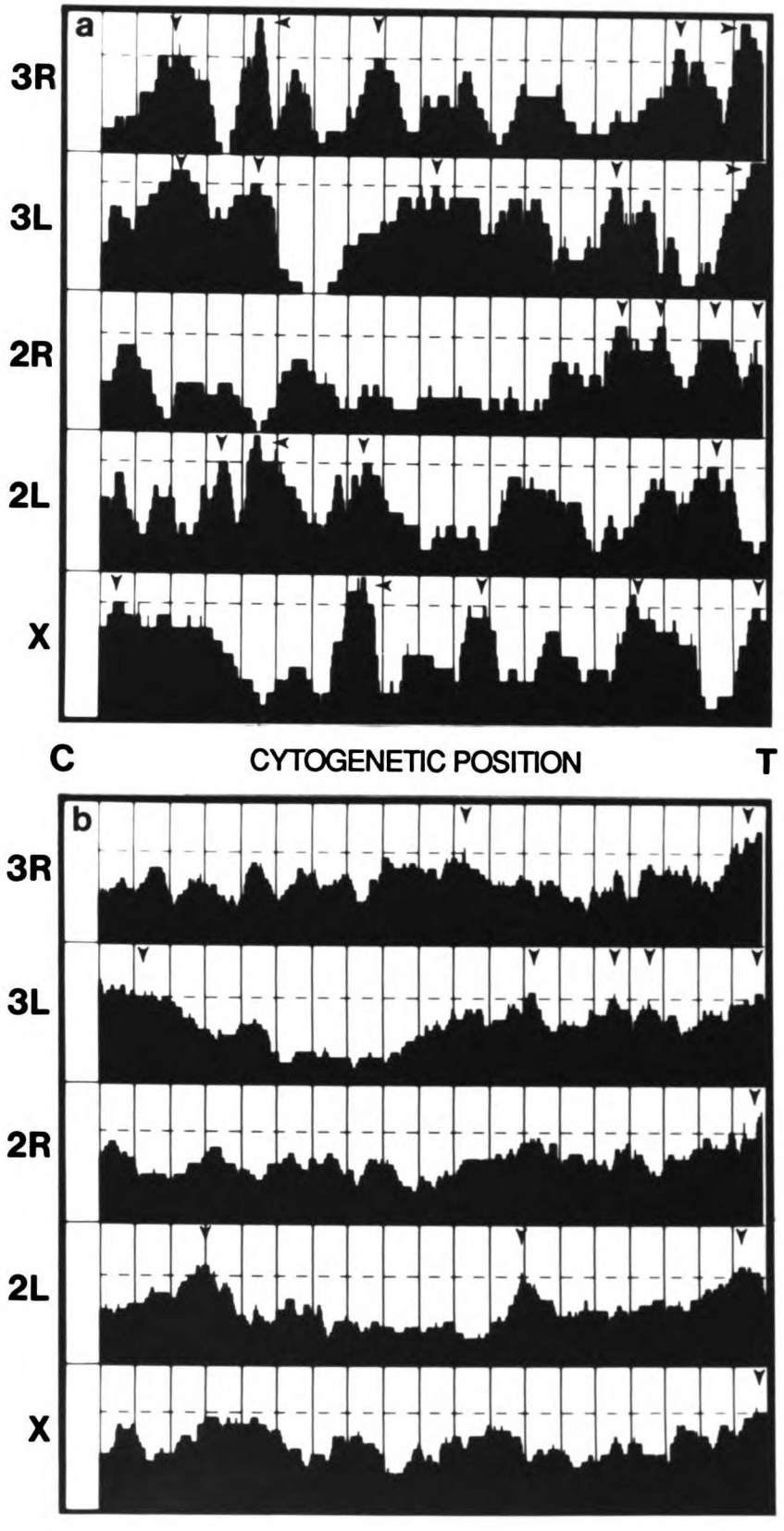
a
3R
3L
2R
2L
X
C
CYTOGENETIC POSITION
T
b
3R
3L
2R
2L
X

Figure 5. A comparison of nuclear surface contact frequencies for 2L in four tissues. Plots are made as in Fig. 4, and include 2 plots from that figure. (a) Midgut (25 nuclei; cutoff distance of 1 μm). (b) Salivary gland (24 nuclei; cutoff distance of 1 μm). Reprinted from Hochstrasser et al. (1986). (c) Prothoracic gland (11 nuclei; cutoff distance of 0.75 μm). (d) Hindgut (4 nuclei; cutoff distance of 0.5 μm).

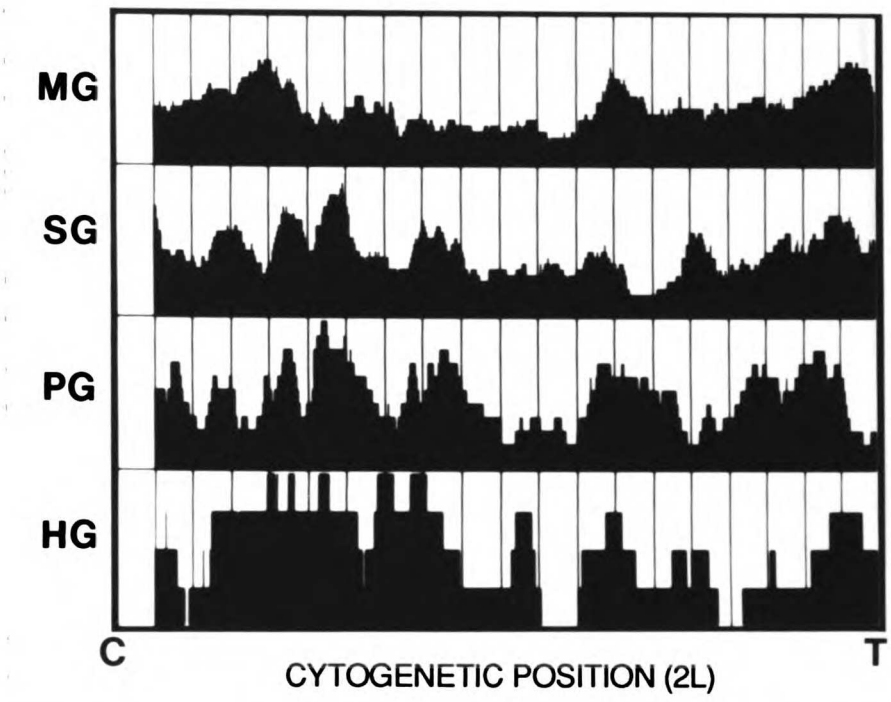
MG
SG
PG
HG
C
T
CYTOGENETIC POSITION (2L)

Figure 6. Salivary gland chromosome connections to the inner nuclear envelope. a) Dense banded region of a chromosome sending many short fibers to the envelope; the envelope appears to be drawn up against the chromosome. The unusual structure next to the chromosome is described in the text. b) A pair of salivary gland chromosome fibers (arrowheads) run to the envelope and appear to pull the attached regions inward. Nuclear pores do not concentrate around these attachments. c) A prominent ectopic fiber (arrowhead) attached to an infolded region of the inner envelope. Bar, 1 μm.

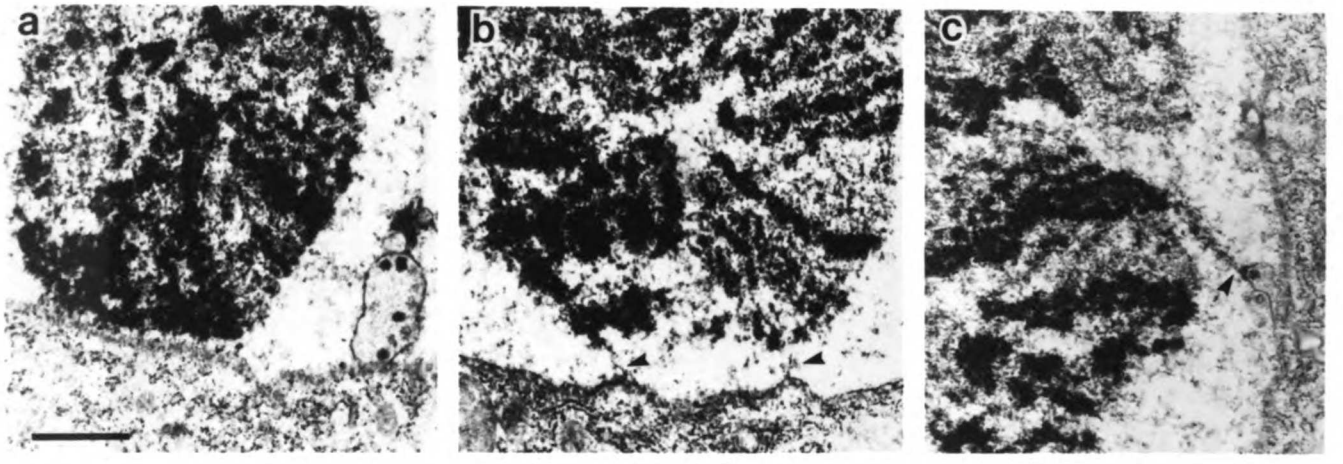
a
b
c

Figure 7. Nucleolar contact frequencies for X and 2R in prothoracic gland nuclei. Plots are generated and represented in the same way as nuclear surface contact frequency plots, e.g., Figure 4. The cutoff distance (between the chromosome model and the nucleolar surface) used to make the plot was 2.25 μm. The black arrow points to 19F/20A, which is on the nucleolar surface in 8/11 nuclei. The open arrow points to 56EF, the locus containing the 5S RNA genes, which is never within the 2.25 μm cutoff.

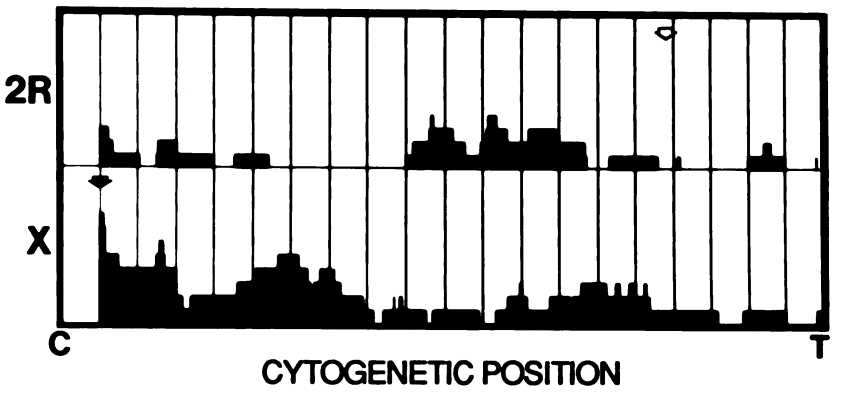
2R
X
C
T
CYTOGENETIC POSITION

Figure 8. Podlike infoldings of the nuclear envelope. (a-c) Different multichambered pods in salivary gland nuclei, often extending a laminate arm to a chromosome. The large particles with variable electron densities are usually roughly circular in cross section but other forms, including a horseshoe shape, are also seen. (d) Pod associated with a double membrane bleb into the cytoplasm of a middle midgut cell. (e) A complex envelope structure including a double membrane invagination containing ribosomes and glue granules, a bleb, and granule-containing pods. The arrowhead points to a region where the outer envelope is separating from the inner one within the invagination. (f) A grazing section of a pod forming from a double membrane invagination. An area with structures suggestive of pore annuli is indicated by an arrowhead. e and f are from serial sections of salivary gland nuclei. (g) A higher magnification view of a salivary gland pod structure. Close examination of the dense particles suggests they are made up of smaller particles. All bars, 0.5 μm (a-b; c-f; g).

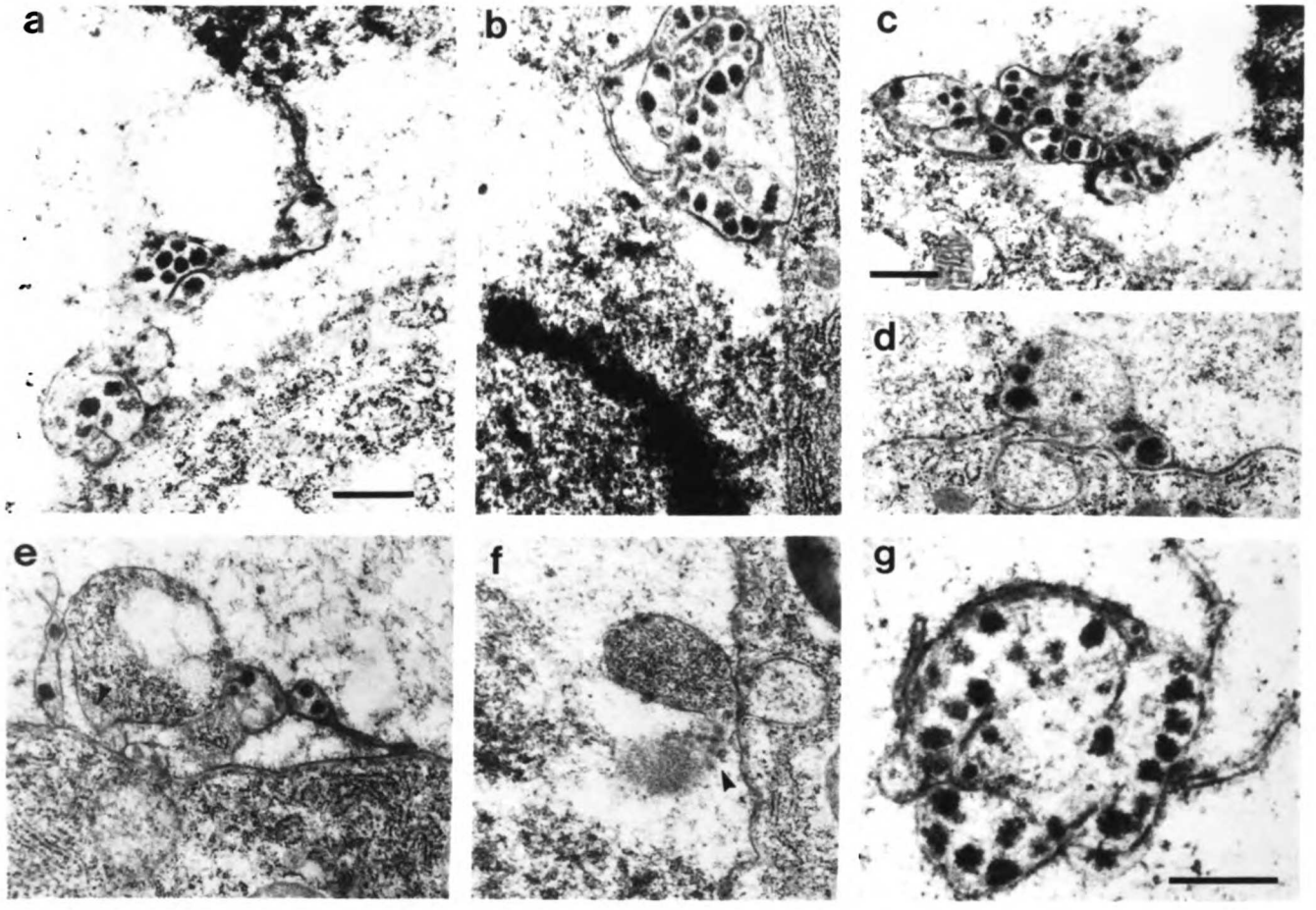
a
b
c
d
e
f
g

Chapter 5

Chromosome Structure In 4 Wild-Type Polytene Tissues Of *Drosophila Melanogaster*. HSP70 Heat Shock Loci Are Expressed Unequally In The Midgut In A Manner Dependent On Growth Temperature

ABSTRACT

A systematic screen of wild-type D. melanogaster larval organs has revealed 3 additional tissues with suitable polyteny for detailed cytogenetic analysis: the prothoracic gland, hindgut, and middle midgut. Chromosome banding patterns are very similar between tissues, but puffing patterns show considerable differences. In intact nuclei, oblique substructural elements can sometimes be detected in bands from some of the tissues. As a way of exploiting these newly characterized chromosomes, the heat shock puff response in midgut cells has been studied in detail. The puffing pattern is very similar to that in salivary glands, but an unexpected difference was found in the relative activity of the two hsp70 loci, 87A7 and 87C1. When larvae are raised at 16°C, heat shocks ranging from 10 to 60 min induce only a weak midgut puff at 87A7 that is much smaller than that at 87C1, in contrast to other tissues where both are strongly induced. In pulse-labeled nuclei, a ~5-fold difference in transcriptional activity at the two loci is observed. However, when larvae are raised at 25°C, the converse is found: the 87A7 puff is larger, and little or no puffing is detectable at 87C1. The unusual modulation of these loci suggests a possible explanation for the evolutionary conservation in Drosophila of two separate sites for almost identical hsp70 genes: under different conditions, only one of them can be fully activated in some cell types.

INTRODUCTION

The giant polytene chromosomes in the larval salivary glands of Drosophila melanogaster have been used extensively for investigations of chromosome structure and organization. Detailed banding maps have been

made (Bridges, 1935), and a large collection of chromosome aberrations is available (Lindsley and Grell, 1968). The facile genetic and molecular analyses that can be performed in this organism also make it ideal for the study of chromosome structure-function relations.

Some thirty-five years ago, an issue of great controversy was whether the pattern of chromosome bands was a tissue-specific property. For example, if the pattern of condensed and decondensed regions represents the pattern of (potentially) active and inactive loci, then banding differences between functionally distinct tissues would be expected. The classical studies of Beermann (1952) and Pavan and Breuer (1952) in Chironomus and Ryncosciara, respectively, demonstrated that the number and sequence of bands were very similar in all somatic cell types examined. The main differences were attributable to variable puffing activity, although minor differences, such as altered band spacings, were noted. More recently, however, Zhimulev and colleagues (1981) have put forward the view that the general similarity of banding between tissues is due to the predominance of "housekeeping genes" in the repertoire of active genes and that minor banding differences in fact reflect loci with tissue-specific function. The further investigation of this issue will therefore require high resolution studies of chromosome banding in alternate tissues.

Berendes (1965, 1966) compared the puffing activities in three tissues of D. hydei and reported a surprising paucity of tissue-specific puffs -only 3 to 7 per tissue. On the other hand, in the DTS-3 mutant of D. melanogaster, which shows hypertrophy of the prothoracic gland, Holden and Ashburner (1978) noted many puffing differences between this tissue and the salivary gland; however, the normal pattern of salivary

gland chromosome puffing is also altered in this mutant. In the only study of a wild-type D. melanogaster tissue, Richards (1982) reported that fat body chromosomes showed a number of puffing differences from those in salivary glands.

The present work was stimulated by a search for wild-type larval organs with suitable polyteny and optical clarity to study the three-dimensional arrangement of chromosomes in intact, unfixed tissues (Hochstrasser and Sedat, submitted). Because fat body cells are opaque and their chromosomes are very small, they are unsuitable for such studies. From a systematic screen of DAPI-stained whole mounts of larval organs, I have now found three tissues with the desired characteristics: the prothoracic gland, the hindgut, and the "large cells" of the middle midgut (Poulson and Waterhouse, 1960). Difficulties in tracing the banding pattern in situ, as in our earlier analysis of salivary glands (Mathog et al., 1984; Hochstrasser et al., 1986), necessitated the assembly of picture montages of squashed chromosomes from each tissue to serve as guide maps. In the course of this work, banding and, to a more limited extent, puffing patterns could be characterized.

The possibility of exploiting these new tissues for detailed cytogenetic comparisons of puffing was explored in a study of the heat shock puff response. High temperature and other stresses induce a specific set of chromosome puffs and cause the regression of previously active puffs (Ritossa, 1962; Ashburner, 1970). While the general similarity in the response in different tissues is well documented (Ritossa, 1964; Bonner and Pardue, 1976), some cell type-specific modifications to the pattern have been detected (see Ashburner and

Bonner, 1979). The data in the present report on the two hsp70 coding loci provide an unexpected twist to the finding of tissue-specific heterogeneity.

The 70,000 dalton heat shock protein, hsp70, is one of the most highly conserved proteins known, having ~50% amino acid homology between Drosophila and E. coli (Craig, 1984). In D. melanogaster, 2 copies of the gene reside at the 87A7 locus and usually 3 at 87C1. Between loci, a 4.2% sequence divergence within the coding region is found (2.7% at the amino acid level). In the 5' non-coding region of the sequence unit conserved between all hsp70 genes, there is a 15% sequence divergence between the 87A7 and 87C1 copies. Limited sequence data shows even less divergence between genes within the same locus. In the region between oppositely oriented copies of the 87C1 hsp70 genes, there also exist tandemly repeated coding sequences for the αβ heat-induced transcripts (reviewed by Craig, 1984).

In the salivary gland, expression from the two hsp70 loci is normally roughly equal as judged by puff size and ^{3}H-uridine pulse-labeling (Ashburner, 1970; Bonner and Pardue, 1976). I show here that the situation in the middle midgut "large cells" is quite different. When larvae are raised at 16°C, the 87C1 locus is much more strongly expressed during a heat shock than is the 87A7 site as judged by puff size and ^{3}H-uridine incorporation. However, when larvae are grown at 25°C, the exact converse is found: 87A7 puffs more strongly, and 87C1 is at most only weakly expressed. This unusual modulation of the expression of different copies of a gene that are essentially identical in amino acid sequence could account for the evolutionary conservation of two separate coding loci.

MATERIALS AND METHODS

Fly stocks and growth conditions

Three different wild-type stocks were used. Two, a Canton-S stock and an Oregon-R stock, were obtained from T. Kornberg. The third was an Oregon-R stock from S. Beckendorf that had been made isogenic for the X chromosome (referred to as OR-isoX in Hochstrasser et al., 1986). No clear differences in puffing between stocks were noted, and further reference to stock identity will not be given except where appropriate. Flies were raised on standard cornmeal food supplemented with yeast in uncrowded half-pint bottles. For the 16°C condition, flies were either allowed to lay eggs for 1-2 d at 25°C with the bottles then being transfered to 16°C, or the entire growth period occurred at 16°C. No differences in the heat shock puffing patterns were found between these two regimes. Leaving 16°C-reared larvae at room temperature for several h before heat shock also did not affect the subsequent puffing response. All the studies of chromosome banding and non-heat shock puffing were done with Oregon-R larvae raised at 16°C. Late third-instar larvae were dissected that were crawling along the bottle sides, usually near the edge of the food.

Tissue preparation and squashing methods

The buffer used for all dissections and for staining of intact tissues with the DNA-specific fluorescent dye DAPI (4',6-diamidino-2-phenylindole) was the following: 15 mM HEPES, 0.15 mM spermine, 0.5 mM spermidine, 80 mM KCl, 15 mM NaCl, 0.1 mM EGTA, 0.5 mM EDTA, 15 mM 2-mercaptoethanol, pH 6.8 (Buffer A; Burgoyne et al., 1971).

The search for high polyteny tissues was done by spreading out the visceral organs and splaying open the body wall of late third instar larvae on a slide and staining them with DAPI. Specimens were examined with epifluoresence optics on a Zeiss Universal microscope.

Several techniques for squashing the different tissues were tried. For prothoracic gland squashes, the following procedure was found to give good results. The ring gland, which includes the prothoracic gland, was removed from the larva but was not dissected free of the brain and ventral ganglion tissue with which it was associated. The tissue was placed in a drop of Buffer A containing 1% Triton X-100 for 1 min. The buffer was replaced with a drop of 1N HCl. After 3 min of hydrolysis, the tissue was stained for ~3 min in a solution of 22:39:2 lactoacetoorcein and squashed by tapping the coverslip with a needle. For the heat shock experiments, this procedure was replaced by the method used with heat shocked midgut tissues to eliminate possible differences due to squashing conditions. The midgut was generally squashed as follows. The middle midgut "large cells," which are between the copper-accumulating calycocytes and the "iron cells" (Poulson and Waterhouse, 1960), was dissected out by cutting the intestine near either side of the Ia/Ib bend (Strasburger, 1932). After incubating for 1-2 min in 1% Triton X-100, the midgut was placed in a drop of 45% acetic acid for several min. This was replaced with the staining solution and squashed after 2-3 min. Sometimes the 45% acetic acid step was omitted as was the detergent pretreatment. Neither had a noticeable effect on the heat shock puffing pattern. Care must be taken in using a 1N HCl hydrolysis step at least in this tissue because chromosomes are easily overstained and puffs often appear to be reduced in size. Hindgut

and salivary gland squashes were done after a 45% acetic acid fixation and staining in lactoacetoorcein.

Photographs of squashes were taken with a 100X/1.3 numerical aperture Zeiss Planapo phase objective lens. Puff sizes were measured from negatives with a Leitz dissecting microscope fitted with a Nikon ocular micrometer. Details of the conditions and techniques used for electron and 3-D fluoresence optical sectioning microscopy are given in Hochstrasser and Sedat (submitted).

Pulse labeling and autoradiography

Immediately after the heat shock treatment of female larvae, midguts or salivary glands were dissected into the physiological medium of Shield and Sang (1970). The tissues were then transferred to a drop of this medium containing 500 µCi/ml 5-^{3}H-uridine (specific activity, 27.8 Ci/mmole, Amersham) and incubated for 5 min. After a 1 min wash in medium containing 2 µM unlabeled uridine, the tissues were fixed in fresh 45% acetic acid for 1.5 min and then squashed under a siliconized coverslip. Following removal of the coverslips, slides were dehydrated in cold 95% ethanol and allowed to dry. Slides were coated with Kodak NTB-2 emulsion and were developed with D19 (Kodak) after 4 d at 4°C. The preparations were stained with Giemsa (Baker) and mounted in distilled water. Because of the very different labeling intensities of 87A and 87C, it was difficult to obtain quantitative grain counts from both loci in the same squash. Approximate counts at the 87A and 87C loci were made from 8 midgut nuclei from larvae raised at 16°C; a labeling ratio for 87C/87A of 5.4±1.8 was derived; this number is intended only as an estimate of the relative activities of the two loci.

RESULTS

A careful screening of whole mounts of DAPI-stained larval organs revealed three tissues besides salivary glands with levels of polyteny suitable for detailed cytogenetic analysis: the prothoracic gland, hindgut, and the "large cells" of the middle midgut. Certain other tissues sometimes had relatively high polyteny nuclei (probably about 256C), including the Malpighian tubules, hypoderm, and posterior midgut, but these were found with very low frequency.

The maximum levels of polyteny found in these cell types were estimated from band width measurements in intact nuclei and a comparison to data relating band width to DNA content (Laird et al., 1980): prothoracic gland (256C to 512C, where 1C is the haploid euchromatic DNA content); hindgut (between 256C and 512C); and midgut (512C to 1024C) (Hochstrasser and Sedat, submitted). Salivary gland nuclei, by comparison, were estimated to be in the 1024C and 2048C size classes. Fig. 1 demonstrates the high level of polyteny reached by prothoracic gland chromosomes by a comparison to mitotic chromosomes and a (presumably) diploid nucleus. One difficulty with these tissues is that relative to salivary glands with some 250 cells, they consist of comparatively few cells. This necessitates a greater number of squashes to get analyzable spreads. In addition, squashing conditions must sometimes be modified to achieve optimal chromosome spreading (Materials and Methods).

1. Comparison of chromosome banding

The banding patterns in the three new tissues, in their general features, are very similar to the standard maps of salivary gland

chromosomes (Bridges, 1935; Lefevre, 1976). To illustrate this, typical quality squashes showing the distal part of 2R are compared in detail in Fig. 2. This similarity of banding is consistent with previous studies on different polytene tissues (Holden and Ashburner, 1978; Richards, 1980). In very good preparations, the degree of banding detail revealed is at least as good as the best salivary gland squashes (see Fig. 5, for example); in these cases, it is often easier to align the banding with the revised maps of Bridges (in Lindsley and Grell, 1968). Even at this level of resolution, the banding is very similar, if not identical, between tissues.

Subtle differences in banding between tissues that have been reported by others (Beermann, 1952; Zhimulev et al., 1981) can also be found in the tissues studied in the present work. These include differences in relative staining intensity, in the spacing between certain bands, and in singlet vs. doublet appearance. An example of the latter is found at 22A. In salivary glands, 22A1-3 generally appears as 2 heavy bands or at most a triplet. In prothoracic glands, on the other hand, 4 heavy bands are often distinguished in this position. Another example is 84AB. In fat body cells, 4 and sometimes 5 heavy bands are counted (Richards, 1980), whereas in all the tissues studied here, including the salivary gland, only 3 heavy bands are found.

A primary diagnostic feature of intercalary heterochromatin in salivary glands is the presence of a constriction or weak point in chromosome squashes. Such constrictions are observed in the 3 other tissues as well and occur in the same places previously mapped in salivary gland chromosomes (Kaufmann and Iddles, 1963; Zhimulev et al., 1982). While not investigated in detail, exceptions to this similarity

appear to be rare. An example of a midgut chromosomal weak point that is apparently not present in salivary glands is 94A. In Fig. 5c this region appears as a conspicuous narrowing of the chromosome. In midgut chromosomes, constrictions sometimes occur as long fibers; an example at the 89E weakpoint on 3R can be seen in Fig 6a. Long constrictions have also been observed in intact, unfixed midgut nuclei at this and several other intercalary heterochromatin loci (Hochstrasser and Sedat, submitted). Zhimulev et al. (1982) have previously noted the similar positions of weak points in the salivary gland and hindgut.

2. Band substructure in intact nuclei

In prothoracic and hindgut nuclei, an unusual type of band substructure is occasionally seen. The optical section in Fig. 3a from an unfixed, unembedded hindgut nucleus shows a large band with obliquely arranged band elements. This type of organization has not been directly observed in unfixed DAPI-stained salivary gland chromosome bands, perhaps because of their large size. Electron microscopic examination of chromosomes from different tissues also shows evidence of obliquely arrayed subchromosomal structures (Fig. 3b). Although more difficult to discern in salivary gland chromosomes, suggestions of an oblique substructure may also be seen (Fig. 3c; also see Mortin and Sedat, 1982).

Such a substructural organization, while not often apparent, may be characteristic of polytene chromosomes. Labeling of interbands or puffs with anti-RNP monoclonal antibodies (Saumweber et al., 1980) frequently gives a zig-zag staining across the chromosome, suggesting that the antibodies are decorating substructural elements arranged at a tilt from

the chromosome axis (Hochstrasser et al., 1987). High resolution in situ mapping of biotinylated DNA with salivary gland chromosome squashes also sometimes shows a cross-hatched hybridization signal (Simon et al., 1985a). Obliquely arranged substructures can sometimes be discerned in acid-fixed Chironomus chromosomes as well (Beermann, 1952). The present data suggest that these are not fixation or squashing artifacts.

3. Puffing differences between tissues

Based on a careful comparison of puffing in chromosome arm 3L and a less detailed survey of puffs on the other arms, it was found that puffing patterns show a considerable number of differences between tissues. Roughly 50 nuclei were analyzed from both prothoracic glands and middle midguts, while about 10 hindgut nuclei were studied. No attempt was made to define the developmental sequence of puffing changes in each tissue, yet even within the limited survey that has been done, many puffs that are not observed in the third-instar salivary gland (Ashburner, 1972) were found. Fig. 4 gives examples of tissue-specific puffs from each cell type.

Chromosome arm 3L was chosen to illustrate the extent of tissue-specific puffing differences as both Holden and Ashburner (1978) and Richards (1982) focused their detailed comparisons between tissues on this arm. Each tissue bears puffs that are either unique to it or to a subset of tissues (Table 1). For example, there are at least 8 3L puffs found in prothoracic glands that are not observed in salivary glands at any stage studied; a minimum of 8 puffs seen in 3L in midguts are never observed in salivary glands either. Also, while 9 of the 14 prothoracic 3L puffs reported by Holden and Ashburner (1978) in the

DTS-3 mutant appear to be held in common with the wild-type chromosomes studied here, at least 12 loci found to puff in the wild-type were not reported to do so in the mutant. Though a few of the disparities may perhaps be attributable to differences in the interpretation of band locations, it is likely that there are quite a number of real puffing differences between the mutant and wild-type tissues. This was found to be true for salivary glands (Holden and Ashburner, 1978). Nevertheless, the finding of considerable tissue heterogeneity in puffing made by these authors is corroborated by the wild-type data reported here.

4. Heat shock puffing pattern in the midgut

As a way of exploiting the non-salivary gland tissues for comparative puffing studies, the heat shock puffing response was investigated. While the response appears to be similar in different cell types, some tissue differences in the set of proteins induced have been noted (see Ashburner and Bonner, 1979). During heat shock or a variety of other stresses, D. melanogaster salivary gland chromosomes form visible puffs at 9 specific loci (Ashburner, 1970). The 6 most prominent puffs, at 63BC, 67B, 87A, 87C, 93D, and 95D, have all been shown to encode major heat inducible RNAs. All but 93D also code for known heat shock proteins (reviewed by Craig, 1984).

The puffing response has been analyzed in greatest detail in the middle midgut. Figs. 5 and 6 display examples from midgut squashes of the 6 major loci known to be induced in salivary glands. Cytologically detectable puffs are found at all of these loci in the middle midgut as well. These loci are unpuffed in the absence of the 37°C temperature treatment except occasionally at 93D and 95D (Figs. 3b, 6a). To verify

that what was regarded as a transcriptional puff was indeed such, midguts from heat shocked larvae were briefly labeled with 5-^{3}H-uridine and studied by autoradiography. Labeling is observed over all 6 loci (Fig. 5d; Fig. 7). 95D shows less consistent labeling than the other sites, paralleling the relatively small puff usually observed here. The same was found to be true of salivary glands (Fig. 7). Of the three minor salivary gland heat shock puff loci, 33B and 70A were puffed only weakly or not at all in virtually all the midgut squashes examined. Grain counts above background were also not detected in pulse-labeled midguts. The 64F locus occasionally showed a small puff and was labeled, albeit infrequently, with radioactive uridine. Exactly analogous results were obtained under the conditions used here in parallel experiments with salivary glands (data not shown; also see Bonner and Pardue, 1976).

Although the general pattern of heat induced puffing is similar or identical between the midgut and salivary gland, an unanticipated variation in the response at the two hsp70 loci was discovered. In salivary glands, 87A and 87C puff to roughly equal extent, in agreement with previous studies. In marked contrast, the 87C locus in the midgut from larvae raised at 16°C is much more strongly induced than 87A (Fig. 6). The ratio of 87C/87A puff widths is about 1.4 (±0.2, n=29) [variable stretching of puffed regions means this value should be regarded only as a rough estimate of the relative puff sizes]. The 87A locus puffs only weakly, in some cases being almost completely unpuffed (e.g., Fig. 6e). In highly stretched chromosomes, two thin bands just distal to the 87A7 puff can be observed (data not shown); these are presumably 87A8,9. These two bands decondense simultaneously with 87A7

in the salivary gland upon heat shock (Semeshin et al., 1982), suggesting that the domain of decondensation may differ in the two tissues.

This differential puffing is not due to a simple kinetic effect since larvae heated shocked for 10, 20, 30, or 60 min all have the same bias in relative puff dimensions (Fig. 6). At the 60 min timepoint in the salivary gland, the 87A puff often appears to have regressed further than 87C, so that it is somewhat smaller than the latter puff. These kinetics appear to be slightly different from those published by Ashburner (1970), perhaps because of the different growth conditions used.

To show that the unequal puffing is not a cytological artifact of the squashing and staining technique, midguts were pulse-labeled with tritiated uridine and analyzed autoradiographically. As shown in Fig. 7, there are far more grains over 87C than 87A, the excess being approximately five-fold (Materials and Methods). Labeling at these two loci in heat shocked salivary glands, on the other hand, is roughly the same (Fig. 7c). The 93D puff is heavily labeled in both tissues. When heat shock puffing in other tissues was examined, both hsp70 loci were found to puff strongly (Fig. 8). Hence, the unequal activity of the two sites appears to be tissue-specific and not a function of polyteny.

Remarkably, a very different situation obtains if larvae are raised at 25° C rather than 16°C. Here again, 87A and 87C in salivary glands puff to roughly equal extend, as found in previous studies. However, in the midgut, 87A is now far more active than 87C (Fig. 9). There is usually no detectable decondensation of the 87C1 band at all, although a small puff developing from the proximal edge of 87C1,2-3 is sometimes

observed. This is precisely the opposite of the relative activities of these loci in midguts from larvae raised at 16°C. In 25°C reared animals, the ratio of 87A to 87C puff sizes is about 1.7 (±0.1, n=24). Thus, there is a ~2.5-fold difference in the relative puff widths of the hsp70 loci between the two growth temperatures tested. The size of the 87A puff increases by ~25% (relative to the unpuffed 86F1 reference band) when the growth temperature is augmented; the 87C puff is ~100% larger at the lower growth temperature.

Several different wild-type stocks were examined and showed the same differential puffing under both growth conditions (Fig. 9), so the differential puffing is unlikely to be due to a peculiarity of a particular set of second site modifiers. Finally, in some of the experiments, egg laying at 25°C for 1-2 d was allowed before transferring the bottles to 16° C. The larvae showed the high 87C/low 87A activities seen with animals grown entirely at the low temperature. Thus, the potential of each locus to be activated does not appear to be irreversibly established very early in development.

DISCUSSION

Levels of polyteny sufficient for detailed cytogenetic analysis are clearly present with reasonable frequency in a number of D. melanogaster tissues. Methods for obtaining well spread squashes are also less laborious than the technique found by Richards (1980) to be necessary for squashing fat body chromosomes. Previously, prothoracic gland chromosomes had been studied in larvae carrying a dominant, conditionally lethal mutation, DTS-3, but were found to be too small for cytological analysis in wild-type glands (Holden and Ashburner, 1978).

However, it was found here, particularly in the OR-isoX stock, that chromosomes suitable for detailed study can be prepared with the squashing conditions described in Materials and Methods. There is one published report on wild-type hindgut chromosomes, in which the location of weak points is described, but the micrograph shown suggests a lower level of polyteny than found here (Zhimulev et al., 1982). No data on the chromosomes in the middle midgut "large cells" are published. Of the three tissues, the midgut proved the most amenable to routine analysis. This tissue may have been overlooked previously because screening was always done in squash preparations. Without knowing precisely where the small group of high polyteny cells are, it is difficult to find them in squashes of whole guts.

The banding patterns in the three non-salivary gland somatic tissues studied are readily aligned both with each other and with the salivary gland pattern. Hence, the conclusion that the banding pattern in different cell types is constant is generally upheld (Beermann, 1952). Nevertheless, subtle differences in band spacing, relative intensity, and/or local band number are observed in a few regions (see Results). This is also true of fat body chromosomes (Richards, 1980). Zhimulev and his colleagues (1981) have proposed that the majority of interbands represent "housekeeping genes" that are active in all cell types, thus accounting for the overall similarity of banding patterns between tissues. The small differences in banding would, in their view, reflect tissue-specific gene activities. More specifically, they propose that many bands are multifunctional and that such bands may be split in some tissues because of the decondensation of regions within the bands that bear tissue-specific gene functions. This will lead to either an

altered spacing or number of bands in the region. Considerable evidence for multifunctional bands has since been accumulated by this group (Semeshin et al., 1986 and references therein).

Ultimately, proof of this functional view of polytene banding will require a combination of high resolution in situ localization (Simon et al., 1985a; Kress et al., 1985) of both genes with housekeeping or with tissue-specific functions and detailed mapping of the banding pattern in the regions of interest by electron microscopy in several tissues. The tissues described in this report should prove ideal for such an analysis. The wealth of genetic and molecular information available in D. melanogaster also makes it the organism of choice in the proposed experiments. Another type of analysis for which the lower polyteny chromosomes in these tissues should be helpful is in the elucidation of the native structure of bands. The obliquely arranged band elements seen here (Fig. 3) provide a clue as to how the chromatin within a band is folded. One possible interpretation, for example, is that the chromatids are helically wrapped about the chromosome axis. This might be superimposed on other folding motifs within each band. This type of substructure is more difficult to discern in the very large, electron dense bands of native salivary gland chromosomes. It also appears that the smaller, less electron-dense bands in these tissues will greatly simplify three-dimensional tomographic analysis of band structure (D. Agard, personal communication).

Previous comparisons of puffing in different polytene tissues have shown that the patterns of puffing overlap between cell types but are not identical (Berendes, 1965; 1966; Holden and Ashburner, 1978; Richards, 1982). The proportion of tissue-specific puffs found in the

present study is significantly higher than found in Berendes's work on Malpighian tubules, salivary glands and anterior midguts in D. hydei. Much of this difference may be due to the lower resolution in the localization of D. hydei puffs, resulting in the assignment of different puffs to the same band. The banding maps of D. hydei are far less detailed than those in D. melanogaster, thereby limiting the ability to resolve puffs over short chromosome stretches. On the other hand, the proportion of tissue-specific puffs found in the hypertrophied prothoracic glands from DTS-3 larvae (Holden and Ashburner, 1978) is comparable to what was found here in wild-type glands. However, the fact that wild-type prothoracic gland chromosomes bear a considerable number of puffs not observed in the mutant suggests that the significance of the mutant puffs should be interpreted with caution. Finally, Richards (1982) emphasized the puffing disparities between fat body and salivary gland chromosomes, a view consistent with the picture obtained from the four tissues examined here.

Two comments must be made about the puffing comparisons made in this study. First, as emphasized by Holden and Ashburner (1978), it is not possible to establish unequivocally from cytological data alone that puffs in a similar chromosome region in fact involve the same gene(s) in each case. Moreover, for Table 1, only puffs in different letter subdivisions are regarded as distinct. This will almost certainly lead to an underestimate of the number of puffing differences between tissues. For example, 68C bears a puff in both salivary and prothoracic glands; Holden and Ashburner (1978) find in the DTS-3 mutant that the 68C puffs actually involve different bands in each tissue. Second, because the sample sizes are relatively small and specific developmental

times have not been selected, the absence of a puff at a particular locus does not necessarily mean that no puff ever occurs there. This will be especially true in the very limited hindgut data. On the other hand, the observation of a puff at a locus that does not puff in the salivary gland, which has been meticulously analyzed (Ashburner, 1972), can be regarded with high confidence as an indication of tissue-specific activity.

The comparison of heat shock puffing in non-salivary gland tissues has demonstrated the overall similarity of the puff response to the salivary gland response (Figs. 5,6). Ritossa (1964) reported a similar finding in several tissues of D. busckii. Quite unexpectedly, however, the response at either of the two hsp70 loci was found to vary in an unusual but specific fashion in the middle midgut. When larvae are raised at 16°C, the 87C hsp70 locus is about 5 times more active than 87A. Conversely, when they are raised at 25°C, 87C is inactive or only slightly active and the 87A puff is considerably larger. In the salivary gland, these loci are expressed to a similar extent under both growth conditions. The autoradiographic analysis of transcriptional activity -the first comparative study of puffing in different tissues to include such an analysis- shows that these cell type-specific differences are not simply a cytological artifact.

Differential regulation of the two hsp70 loci has actually been documented in salivary glands under certain extreme growth conditions and in vitro treatments, but the characteristics are quite different from what has been reported here. In larvae reared at extremely low temperature (10°C), the 87A puff was reduced, having ~40% fewer silver grains than 87C after ^{3}H-uridine labeling (Lakhotia and Singh, 1985).

The 93D puff was also not induced. If glands (from larvae raised at 24°C) are heat shocked and then treated with benzamide, the 87A puff is again reduced to a similar extent as after 10°C growth, but 87C is now almost completed uninduced; 93D is also less active than with heat shock alone (Lakhotia and Mukherjee, 1980). From these data, Lakhotia and his colleagues argued that 93D activity regulates the relative expression of 87A and 87C since its repression correlated with the differential activity at these loci.

The variable puffing at the midgut 87A/87C loci can be contrasted with these results. First, no in vitro treatments were employed. Second, the reduction in puffing and transcriptional activity at 87A in midguts is more drastic than in salivary glands from cold-reared larvae. Third, 93D is strongly induced in the midgut under both growth conditions while 87A and 87C are differentially expressed. This argues against the idea that reduced 93D activity is responsible for unequal expression of the two hsp70 loci. On the other hand, it is consistent with the fact that flies carrying overlapping deletions of the 93D locus show no change in the characteristics of the heat shock response except for the absence of the 93D puff itself (Mohler and Pardue, 1984). Finally and perhaps most importantly, the relative expression of 87A and 87C in midguts is strictly anticorrelated: when 87C is strongly expressed, 87A is only weakly induced and vice versa. In contrast, 87A expression in salivary glands was similarly reduced when 87C was either fully active or almost completely inactive under the conditions used by Lakhotia and Mukherjee (1980) and Lakhotia and Singh (1985). In conclusion, while the results from the above two reports demonstrate the possibility of differential activity at the two hsp70 loci, their

relevance to the midgut data presented here and to commonly encountered environmental conditions is unclear.

Evolutionarily, the hsp70 protein is one of the most highly conserved proteins known, a fact thought to reflect some essential function of the polypeptide to all cells (Craig, 1984). D. melanogaster and D. pseudoobscura diverged some 35 million years ago, yet both species maintain two separate sites containing hsp70 genes that are essentially identical between loci; this is true of a wide range of other Drosophila species as well (Brown and Ish-Horowicz, 1981). The fact that under different growth temperatures, expression from the hsp70 loci is inversely regulated in the midgut (and perhaps other tissues as well) suggests an explanation for the conservation of two separate coding sites: expression from either locus may simply not be sufficient under certain conditions for survival of a stress. Both 16°C and 25°C are temperatures the larva may be expected to encounter in the wild; various environmental stresses may provide the selective pressure required to maintain distinct coding loci.

Previously, Gausz et al. (1981) attempted to identify visible or lethal mutations in hsp70 in flies bearing a single hsp70 gene, at 87A, but were unsuccessful; however, their screen for temperature sensitivity involved only a 29°C treatment for 4 d. The data presented here suggest that a 37°C shock of larvae raised at low temperature might allow such temperature-sensitive mutations to be isolated in this deletion strain.

How might the unusual modulation of the 87A/87C loci be achieved? The sequences 5' to the hsp70 genes, which include the elements required for heat inducible expression (Dudler and Travers, 1984; Simon et al., 1985b), are 85% homologous between the two loci (Craig, 1984). Thus,

the differential expression of these loci was unexpected. A variety of hypotheses based, for example, on multiple tissue-specific transcription factors with different affinities for each locus and temperature-dependent steady state concentrations could account for the unequal expression of these sites. Alternatively, the magnitude of the transcriptional response may be mediated by varying local chromatin structures at the two loci. Without further characterization of the phenomenon, such as temperature shift experiments or study of P-element mediated hsp70 transformants using sequences from either locus, it would not be fruitful to discuss such models in any detail at the present time.

Regardless of the actual mechanism, the finding of a tissue and condition-specific modulation of puffing provides a model system for analyzing band organization and its unfolding during transcription. Several new questions could be addressed. For example: is band substructure of the uninduced 87C1 different under conditions where it can or cannot be efficiently activated? Are there fine scale differences in the local banding in the two temperature conditions such as might be expected in the theory of Zhimulev et al. (1981)? Does a small puff unfold by a different mechanism than a large puff at the same locus, e.g., are there different "origins of unfolding" that are used under different conditions at each locus? Consistent with this suggestion is the observation in the midgut that when 87A7 in the 16°C condition puffs, the neighboring 87A8,9 bands appear to remain condensed, while in salivary glands these bands decondense simultaneously with 87A7. It is interesting in this regard that specialized chromatin structures have been found to flank the 87A7 hsp70

genes in diploid cells (Udvardy et al., 1985). By combining high resolution in situ mapping of DNA sequences with electron microscopic analysis of the local band sequence and structure (see above), a link may be forged with the extensive body of data from nuclease digestion experiments on the chromatin structure of the hsp70 loci (e.g., Wu, 1980; Udvardy et al., 1985).

Table 1. Puffs observed in chromosome arm 3L. SG=salivary glands; MG=midgut; HG=hindgut; PG=prothoracic gland. *From Ashburner (1972) and Holden and Ashburner (1978). Puffs listed in the former reference but not the latter are only included here if a puff in the same subdivision was observed in another tissue as well. "(+)" refers to cases where the apparent puff is very small.

Locus	SG*	MG	HG	PG	PG(DTS-3)*
61AB	-	-	+	-	-
61C	+	+	-	+	-
61E	-	-	-	+	-
62A	+	+	-	-	+
62E	+	+	(+)	+	+
63A	-	-	-	-	+
63B	-	-	+	(+)	-
63D	-	-	-	+	-
63E	+	-	(+)	+	+
63F	+	-	-	-	-
64A	+	-	-	+	-
64B	+	+	+	-	-
64D	-	+	-	-	-
64E	-	-	+	+	-
65A	-	+	-	-	-
65C	-	-	-	+	-
65D	-	-	-	+	+
66A	-	+	-	-	-
66B	+	-	+	-	-

66CD	-	-	-	+	-
66E	+	(+)	-	-	+
67A	+	-	-	-	+
67B	-	-	-	-	-
67C	-	+	-	-	-
67F	+	-	(+)	+	+
68C	+	-	-	+	+
69A	+	-	-	-	-
69C	-	-	-	-	+
69DE	-	+	-	-	-
70E	+	+	-	+	-
71B	+	-	-	-	-
71DE	+	-	+	-	-
72B	-	+	-	-	-
72D	+	+	-	+	-
73EF	-	+	+	-	-
74A	-	-	-	+	+
74C	+	-	-	+	-
74EF	+	+	(+)	+	+
75B	+	+	-	+	+
75CD	+	-	-	+	+
76D	+	+	+	-	-
77D	-	+	-	-	-
78D	+	-	(+)	+	-
79B	-	-	-	+	-

Fig. 1. Polytene chromosome from prothoracic gland compared to mitotic chromosomes and a (presumably) diploid nucleus. The octaploid mitotic figure is from a brain ganglion cell. Bar, 5 µm.

Fig. 2a-c. Detailed comparison of banding patterns of distal 2R in a salivary gland, b prothoracic gland, and c middle midgut. Bars, 5 µm (magnification is the same in b,c).

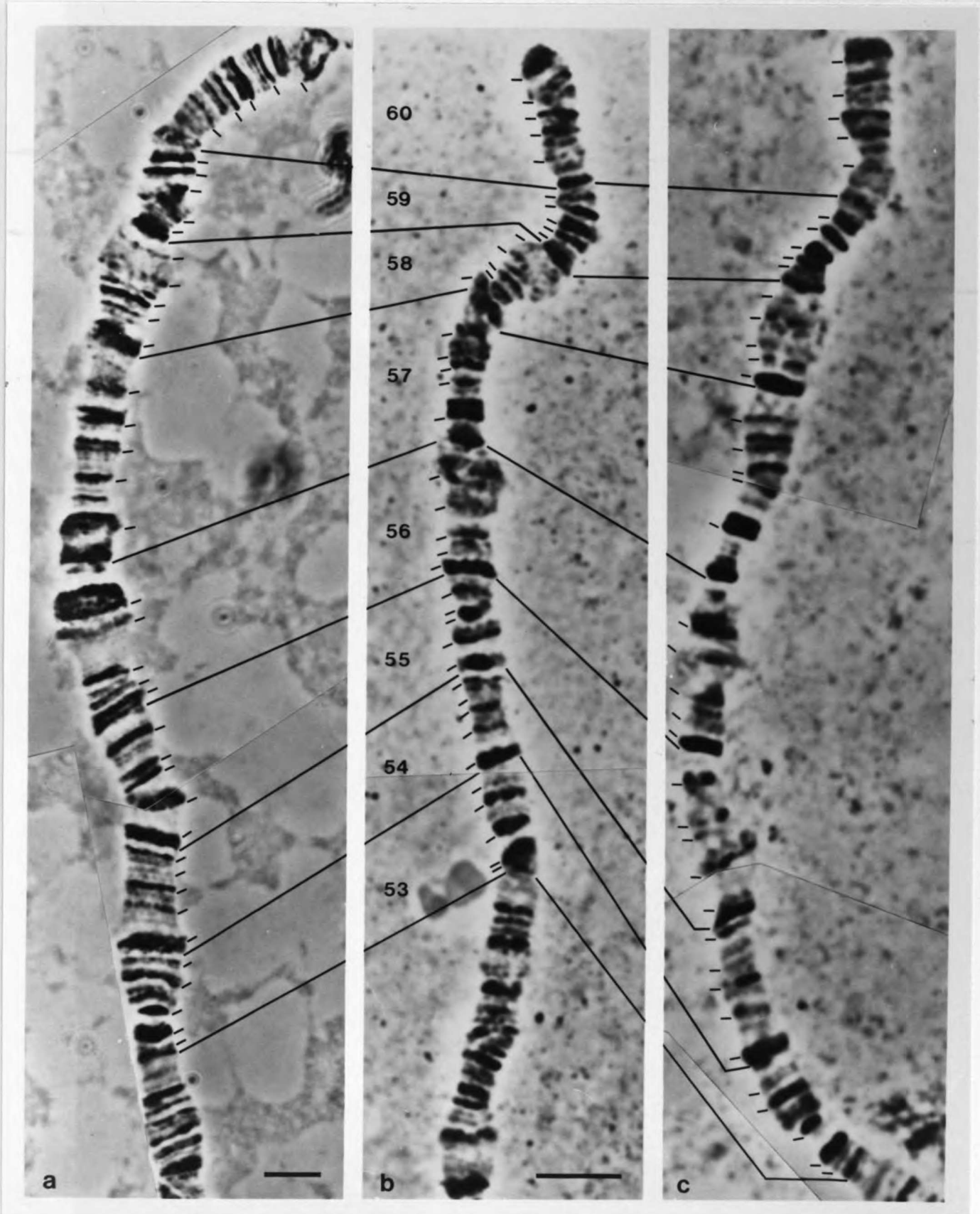
60
59
58
57
56
55
54
53
a
b
c

Fig. 3a-c. Band substructure in different polytene tissues. a Optical section from an unfixed hindgut stained with DAPI. Arrow points to 19F1-2 on X; obliquely arranged substructural elements are evident. Bar, 2 µm. b Electron micrograph of a chromosome in a formaldehyde/glutaraldehyde-fixed prothoracic gland. Arrowhead highlights the substructural band order. c Electron micrograph of a chromosome in a glutaraldehyde/osmium tetraoxide-fixed salivary gland. Most bands are very dense. Bar (for b,c), 1 µm.

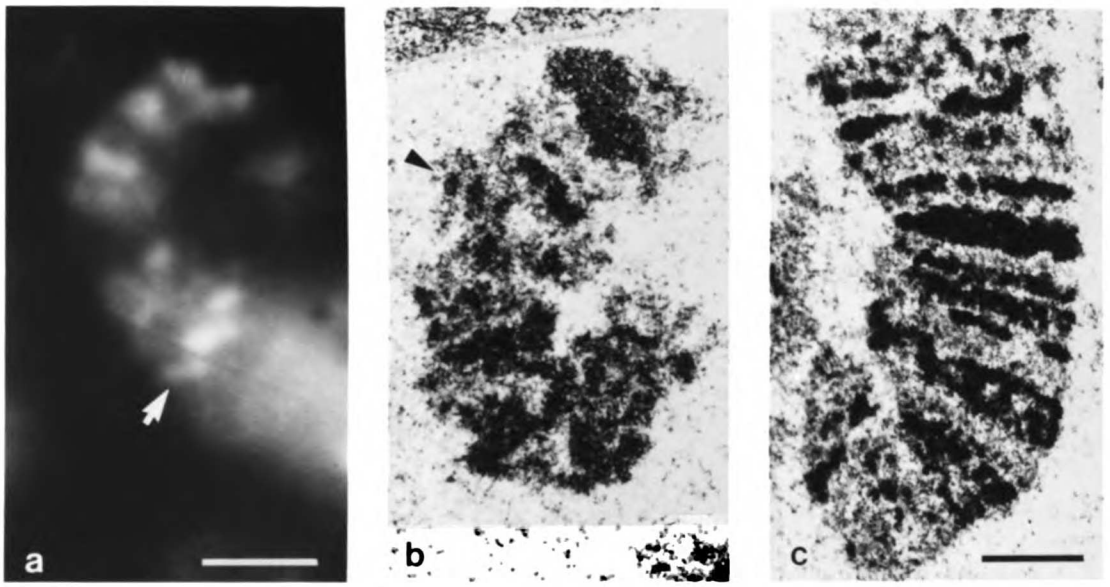
a
b
c

Fig. 4a-c. Examples of puffs found in three other larval tissues that are not found at any stage in the third-instar salivary gland (Ashburner, 1972). a Hindgut, 3R; b middle midgut, 3L; and c prothoracic gland, 2L. Bars, 5 μm.

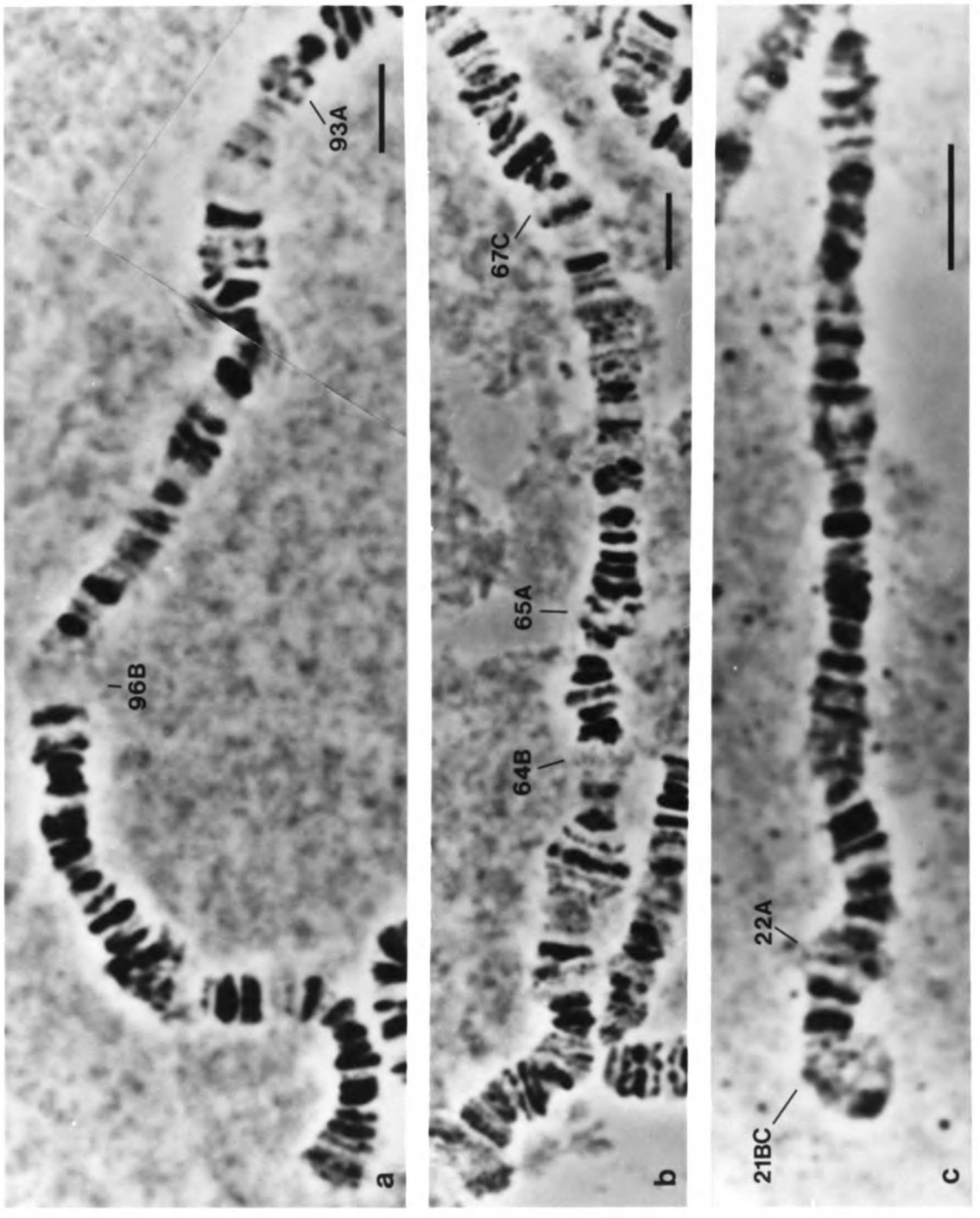
96B
93A
a
64B
65A
67C
b
22A
21BC
c

Fig. 5a-d. Puffs at the major heat shock loci in middle midgut chromosomes from heat-shocked larvae. 37°C treatments lasted a 10 min, b 60 min, c 10 min, and d 30 min. d is an autoradiograph from a 5 min pulse labeling with 5-^{3}H-uridine. Bar, 10 µm.

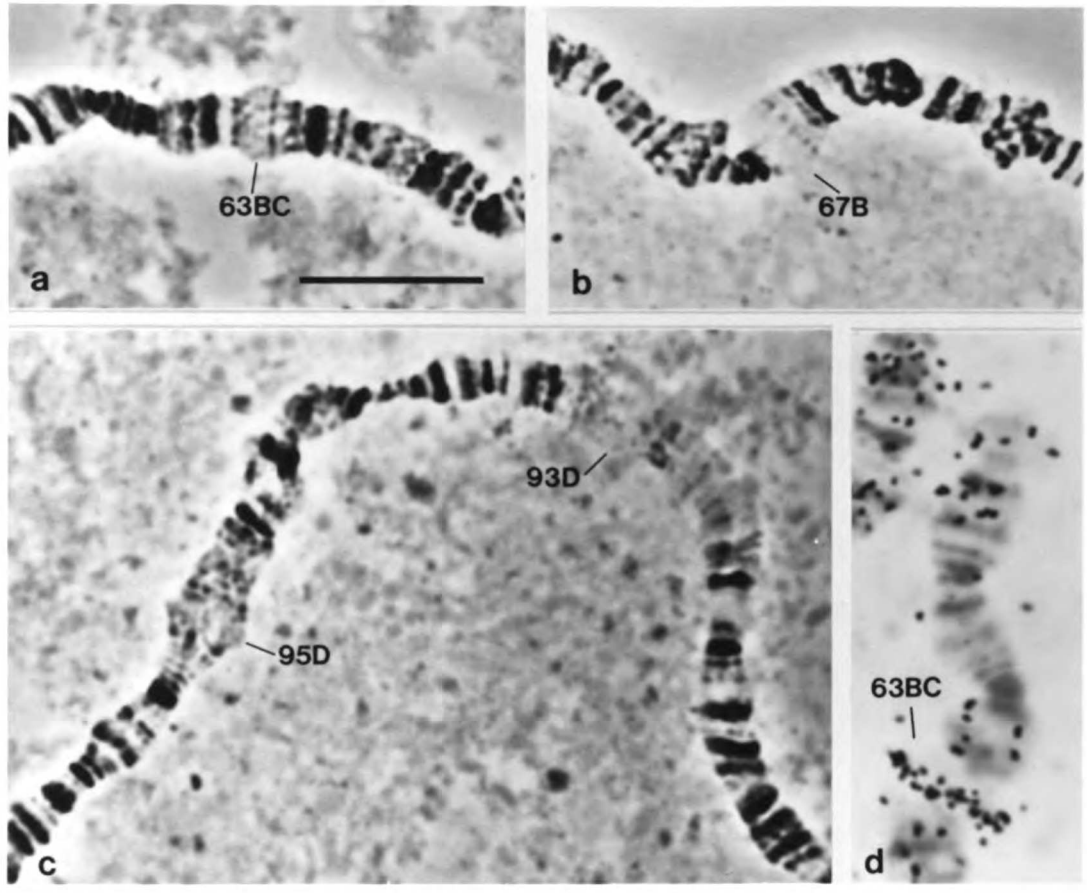
63BC
a
67B
b
93D
95D
c
63BC
d

Fig. 6a-f. Differential puffing at the two hsp70 loci, 87A1 and 87C1. a Control, no heat shock; b 60 min; c 10 min; and d-f 30 min heat shocks at 37° C. Larvae were raised at 16°C. The much larger response at the 87C locus is seen at all time points. The small arrowhead in 6a marks a long constriction at 89E. Bar, 10 μm.

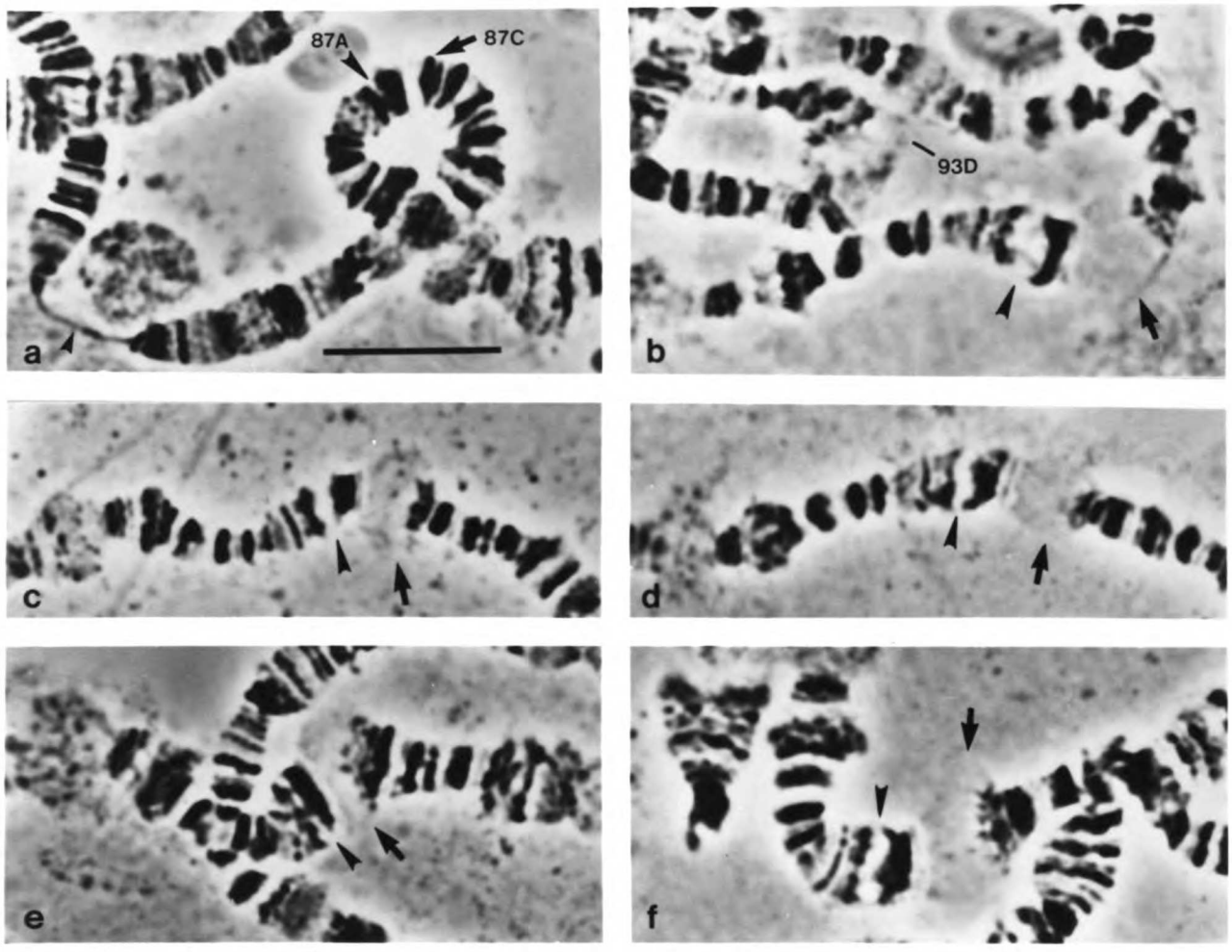
87A
87C
a
93D
b
c
d
e
f

Fig. 7a-c. Pulse-labeling of midgut (a and b) and salivary gland (c) nuclei for 5 min with 5-^{3}H-uridine after a 37°C heat shock for 30 min. Larvae were raised at 16°C. 87C has roughly 5 times the number of grains as 87A in midgut nuclei. The arrowhead in b points to 87B, between the two heat shock loci. The 93D locus is highly active in both tissues. Bars (a,b), 5 um; (c), 10 µm.

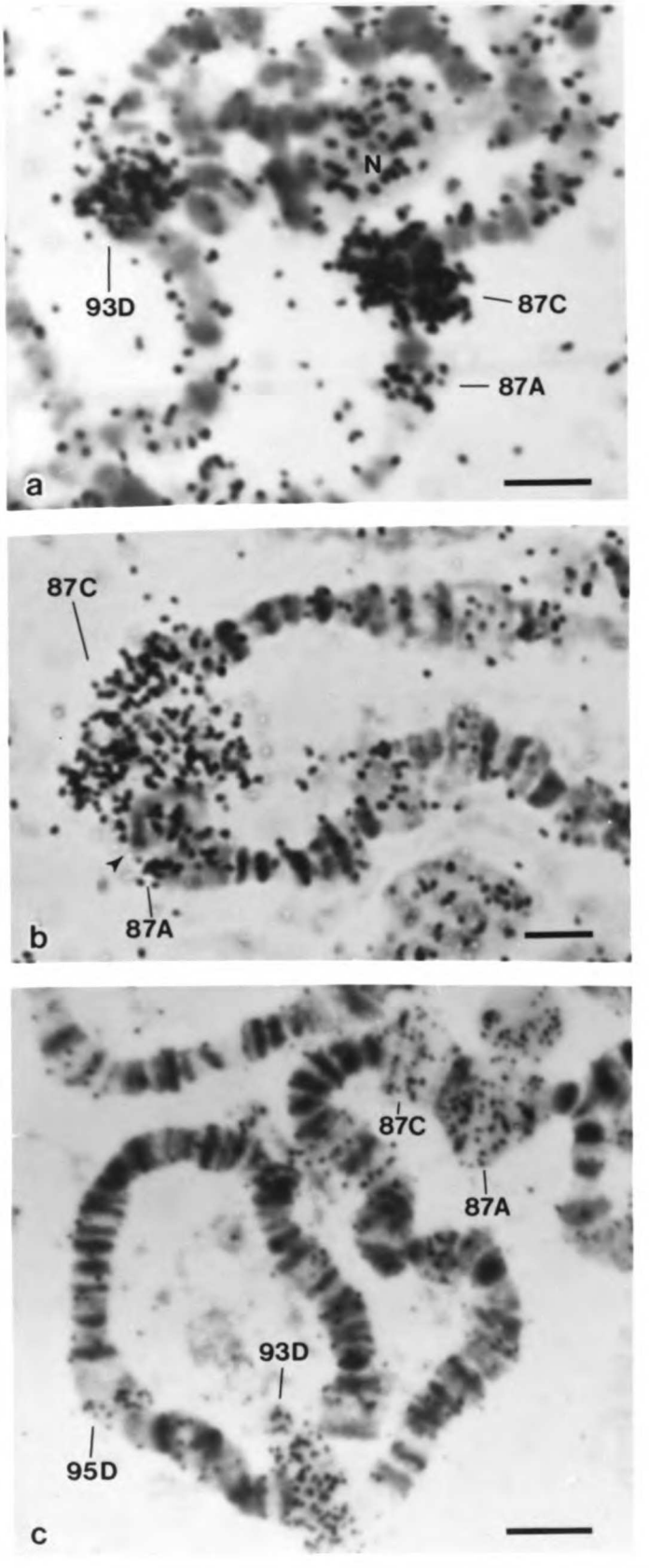
N
93D
87C
87A
a
87C
87A
b
87C
87A
93D
95D
c

Fig. 8a-c. Puffing at the hsp70 loci in a salivary gland, b hindgut, and c prothoracic gland. Larvae were raised at 16°C. A 10 min, 37°C heat shock was used in a, 30 min in b and c. Bars (a), 11 um; (b,c), 5 μm.

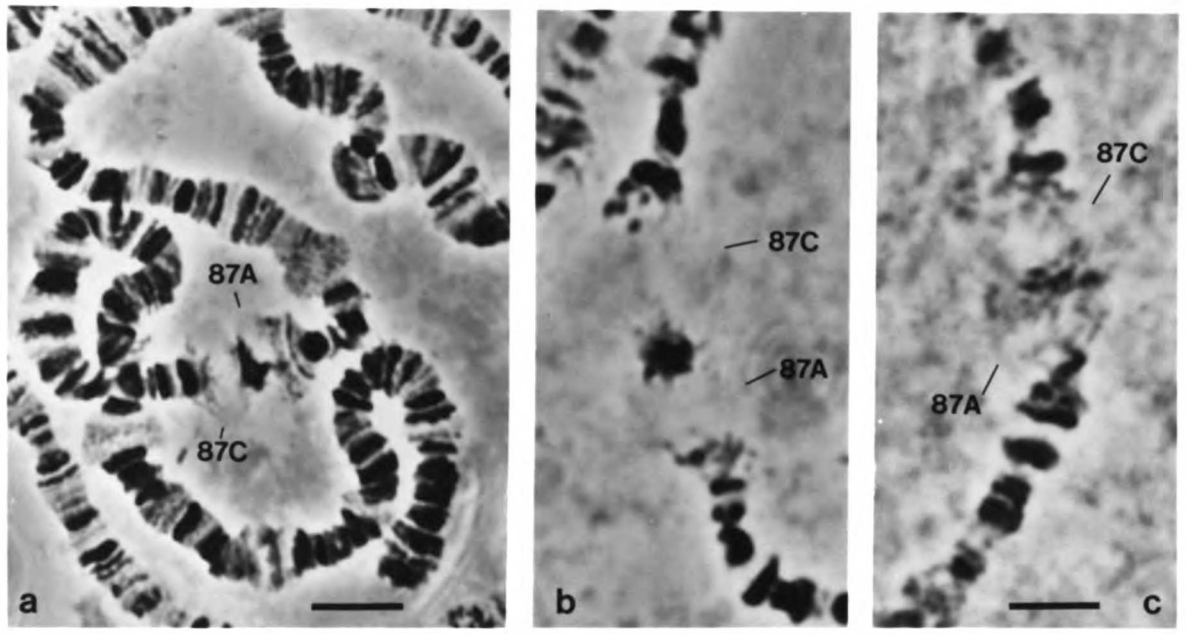
87A
87C
a
87C
87A
b
87C
87A
c

Fig. 9a-b. Puffing at the midgut hsp70 loci from larvae raised at 25°C. a is from an Oregon-R larva, b from Canton-S. The heat shock in both cases was for 30 min at 37°C. Bar, 5 μm.

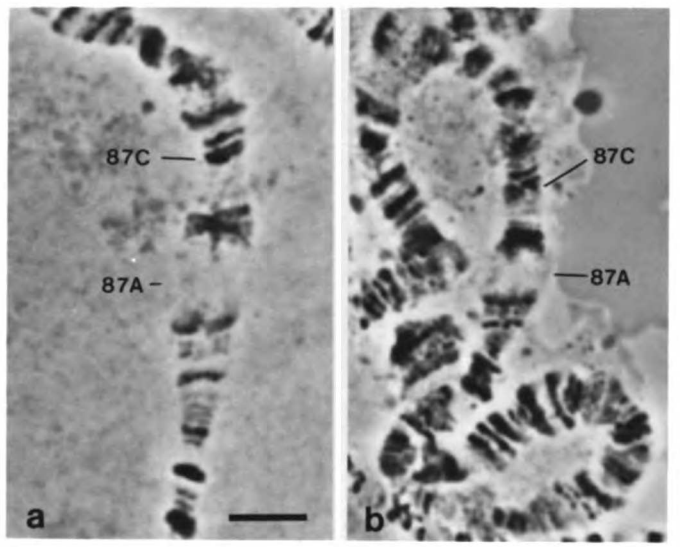
87C
87A
a
87C
87A
b

LITERATURE CITED

Agard D.A. and J.W. Sedat. 1983 Three-dimensional architecture of a polytene nucleus. Nature 302:676-681.

Aggarwal, S.K., and R.C. King. 1969. A comparative study of the ring glands from wild type and 1(2)gl mutant Drosophila melanogaster. J. Morph. 129:171-200.

Alberts B., Worcel, A., and Weintraub, H. 1977 On the biological implications of chromatin structure. In The Organization of the Eukaryotic Genome. E.M. Bradbury and K. Javakenier, editors. Academic Press. 165-192.

Ananiev, E.V., V.E. Barsky, Y.V. Ilyin, and N.A. Churikov. 1981. Localization of nucleoli in Drosophila melanogaster polytene chromosomes. Chromosoma 81:619-628.

Ananiev, E.V., and V.E. Barsky. 1985. Elementary structures in polytene chromosomes of Drosophila melanogaster. Chromosoma 93:104-112.

Appels, R., D.M. Steffensen, and S. Craig. 1979. A new method for mapping the three-dimensional distribution of DNA sequences in nuclei. Exp. Cell Res. 124:436-441.

Ashburner, M. 1970. Patterns of puffing activity in the salivary gland chromosomes of Drosophila. V. Responses to environmental treatments. Chromosoma 31:356-376.

Ashburner, M. 1972a. Patterns of puffing activity in the salivary gland chromosomes of Drosophila. VI. Induction by ecdysone in salivary glands of D. melanogaster cultured in vitro. Chromosoma 38:255-281.

Ashburner, M. 1972b. Puffing patterns in Drosophila melanogaster and related species. In Developmental Studies on Giant Chromosomes. Results and Problems in Differentiation. Vol. 4. W. Beermann, editor. Springer Verlag, Berlin. 101-151.

Ashburner, M. 1976. Aspects of polytene chromosome structure and function. In Organization and expression of chromosomes. V.G. Allfrey, E.K.F. Bautz, B.J. McCarthy, R.T. Schimke, and A. Tissieres, editors. Abakon Verlagsgesellschaft. 81-95.

Ashburner, M., and H.D. Berendes. 1978. Puffing of polytene chromosomes. In The Genetics and Biology of Drosophila. Volume 2B. M. Ashburner and T.R.F. Wright, editors. Academic Press, Inc., New York. 316-395.

Ashburner, M., and J.J. Bonner. 1979. The induction of gene activity in Drosophila by heat shock. Cell 17:241-254.

Ashley, T. 1979. Specific end to end attachment of chromosomes of Ornithogalum virens. J. Cell Sci. 38:357-367.

Avivi, L. and M. Feldman. 1980 Arrangement of chromosomes in the interphase nucleus of plants. Hum. Genet. 55:281-295.

Baker, W.K. 1968 Position-effect variegation. Adv. Genet. 14:133-169.

Barr, H.J. and J.R. Ellison. 1972. Ectopic pairing of chromosome regions containing chemically similar DNA. Chromosoma 39:53-61.

Becker, H.J. 1969 The influence of heterochromatin, inversion-heterozygosity and somatic pairing on x-ray induced mitotic recombination in Drosophila melanogaster. Molec. Gen. Genet. 105:203-218.

Beermann, W. 1952. Chromosomenstruktur und spezifische Modifikation der Chromosomenstruktur in der Entwicklung und Organdifferenzierung von Chrironomus tentans. Chromosoma 5:139-198.

Beermann, W. 1962. Riesenchromosomen. Protoplasmatologia. VI/C:1-161.

Belmont, A.S., F. Bignone, and P.O.P. Ts'o. 1986. The relative intranuclear positions of barr bodies in XXX non-transformed human fibroblasts. Exp. Cell Res. 165:165-179.

Bennett, M.D. 1982. Nucleotypic basis of the spatial ordering of chromosomes in eukaryotes and the implications of the order for genome evolution and phenotypic variation. In Genome Evolution.. G.A. Dover and R.B. Flavell, editors. Academic Press, Inc. New York. 239-261.

Berendes, H.D. 1963. The salivary gland chromosomes of Drosophila hydei sturtevant. Chromosoma 14:195-206.

Berendes, H.D. 1965. The induction of changes in chromosomal activity in different polytene types of cell in Drosophila hydei. Devel. Biol. 11:371-384.

Berendes, H.D. 1966. Gene activities in the malphigian tubules of Drosophila hydei at different developmental stages. J. Exp. Zool. 162:209-218.

Berendes, H.D., and M. Ashburner. 1978. The salivary glands. In The Genetics and Biology of Drosophila. M. Ashburner and T.R.F. Wright, editors. Academic Press, Inc. New York. 453-498.

Berg, O.G., and P.H. von Hippel. 1985. Diffusion-controlled macromolecular interactions. Ann. Rev. Biophys. and Biophys. Chem. 14:131-160

Berrios, M., N. Osherhoff, and P.A. Fisher. 1985. In situ localization of DNA topoisomerase II, a major polypeptide component of the Drosophila nuclear matrix fraction. Proc. Natl. Acad. Sci. U.S.A. 82:4142-4156.

Biessman, H., F.G. Falkner, H. Saumweber, and M.F. Walter. 1982. Disruption of the vimentin cytoskeleton may play a role in heat shock response. In Heat Shock. From Bacteria to Man. M.J. Schlesinger, M.

Ashburner, and A. Tissieres, editors. Cold Spring Harbor Laboratory, Cold Spring Harbor, N.Y. 275-281.

Bingham, P.M., and Z. Zachar. 1985. Evidence that two mutations, w(DZL) and z(1), affecting synapsis-dependent genetic behavior of white are transcriptional regulatory mutations. Cell. 40:819-825.

Blobel, G. 1985. Gene gating: A hypothesis. Proc. Natl. Acad. Sci. U.S.A. 82:8527-8529.

Bonner, J.J. and M.L. Pardue. 1976. The effect of heat shock on RNA synthesis in Drosophila tissues. Cell 8:43-50.

Bostock, C.J., and A.T. Sumners, 1978. The Eukaryotic Chromosome. Elsevier/North-Holland Biomedical Press, Amsterdam.

Boveri, T. 1888. In Zellen-Studien H.2, pp. 1-189. Fischer, Jena.

Brash, K. and G. Setterfield. 1974. Structural organization of chromosomes in interphase nuclei. Expl. Cell Res. 83:175-185.

Braun, W. 1983. Representation of short and long-range handedness in protein structures by signed distance maps. J. Mol. Biol. 163:613-621.

Bridges, C.B. 1935. Salivary chromosome maps. J. Hered. 26:60-64.

Bridges, P.N. 1942. A new map of the salivary gland 2L-chromosome of Drosophila melanogaster. J. Hered. 33:403-408.

Brown, J.J.L. and D. Ish-Horowicz. 1981. Evolution of the 87A and 87C heat-shock loci in Drosophila. Nature 290:677-682.

Burgoyne, L.A., M.A. Wagar, and M.R. Atkinson. 1971. Calcium dependent priming of DNA synthesis in isolated rat liver nuclei. Biochem. Biophysis. Res. Commun. 39:254-259.

Callow, R.S. 1985. 1985. Comments on Bennett's model of somatic chromosome disposition. Heredity. 54:171-177.

Coates, D.J. and D. Smith. 1984. The spatial distribution of chromosomes in metaphase neuroblast cells from subspecific F1 hybrids of the grasshopper Caledia captiva. Chromosoma 90:338-348.

Cohen, M.M. and M.W. Shaw. 1964. Effects of mitomycin C on human chromosomes. J. Cell Biol. 23:386-395.

Coll, M.D., Cuadras, C.M. and J. Egozcue. 1980. Distribution of human chromosomes on the metaphase plate. Symmetrical arrangement in human male cells. Genet. Res. 36:219-234.

Comings, D.E. 1968. The rational for an ordered arrangement of chromatin in the interphase nucleus. Am. J. Hum. Genet. 20:440-460.

Comings, D.E. 1980. Arrangement of chromatin in the nucleus. Human Genetics 53:131-143.

Cooper, K.W. 1948. The evidence for long range specific attractive forces during the somatic pairing of Dipteran chromosmes. J. Exp. Zool. 108:327-332.

Cozzarelli, N.R., M.A. Krasnow, S.P. Gerrard, and J.H. White. 1984. A topological treatment of recombination and topoisomerases. Cold Spring Harbor Symp. Quant. Biol. 49:383-400.

Craig, E.A. 1984. The heat shock response. CRC Crit. Rev. Biochem. 18:239-280.

Cremer, T., C. Cremer, H. Baumann, E.- K. Luedke, K. Sperling, V. Teuber, and C. Zorn. 1982. Rabl's model of the interphase chromosome arrangement tested in chinese hamster cells by premature chromosome condensation and laser-UV-microbeam experiments. Hum. Genet. 60:46-56.

D'Angelo, E.G. 1950. Salivary gland chromosomes. Annals N.Y. Acad. Sci. 50:910-919.

Dangli, A., P. Kloetzel, and E.K.F. Bautz. Heat-shcok puff 93D from Drosophila melanogaster: Accumulation of a RNP-specific antigen associated with giant particles of possible storage function. EMBO J. 2:1747-1751.

Darlington, C.D. 1965. Recent Advances in Cytology. J. & A. Churchill Ltd., London.

DeSalle, R., and A.R. Templeton. 1986. The molecular through ecological genetics of abnormal abdomen. II. Tissue-specific differential replication of ribosomal genes modulates the abnormal abdomen phenotype in Drosophila mercatorum. Genetics 112:877-886.

Dudler, R. and Travers, A.A. 1984. Upstream elements necessary for optimal function of the hsp70 promoter in transformed flies. Cell 38:391-398.

Dupraw, E.J. 1965. The organization of nuclei and chromosomes in honey bee embryonic cells. Proc. Natl. Acad. Sci. U.S.A. 53:161-168.

Echalier, G. and Ohanessian, A. 1970. In vitro culture of Drosophila melanogaster embryonic cells. In Vitro 6:162-172.

Ede, D.A., and S.J. Counce. 1956. A cinematographic study of the embryology of Drosophila melanogaster. Wilhelm Roux Arch. Entwicklungmech. Org. 148:402-415.

Ellison, J.R. and G.C. Howard. 1981. Non-random position of the A-T rich DNA sequences in early embryos of Drosophila virilis. Chromosoma 83:555-561.

Endow. S.A. 1983. Nucleolar dominance in polytene cells of Drosophila. Proc. Natl. Acad. Sci. U.S.A. 80:4427-4431.

Fakan, S., E. Puvion, and Spohr. G. 1976. Localization and characterization of newly synthesized nuclear RNA in isolated rat hepatocytes. Exp. Cell Res. 99:155-164.

Feldman, M., and L. Avivi. 1984. Ordered arrangement of chromosomes in wheat. In Chromosomes Today. Volume 8. M.D. Bennett, A. Gropp, and U. Wolf, editors. Elsevier North-Holland Biomedical Press, Amsterdam. 181-189.

Felsenfeld, G., and J.D. McGhee. 1986. Structure of the 30 nm chromatin fiber. Cell 44:375-377.

Filshie, B.K., D.F. Poulson, and D.F. Waterhouse. 1971. Ultrastructure of the copper-accumulating region of the Drosophila larval midgut. Tissue and Cell 3:77-102.

Finch, R.A., J.B. Smith, M.D. Bennett. 1981. Hordeum and Secale mitotic chromosomes lie apart in a hybrid. J. Cell Sci. 52:391-403.

Foe, V.E. and B.M. Alberts. 1985. Reversible chromosome condensation induced in Drosophila embryos by anoxia: visualization of interphase nuclear organization. J. Cell Biol. 100:1623-1636.

Fox, D.P. 1966. The effects of X-rays on the chromosomes of locust embryos. II Chromatid interchanges and the organization of the interphase nucleus. Chromosoma 20:173-194.

Franke, W.W., U. Scheer, F.F. Krohne, and E.D. Jarasch. 1981. The nuclear envelope and the architecture of the nuclear periphery. J. Cell Biol. 91:39s-50s.

Fried, M.G., and D.M. Crothers. 1984. Kinetics and mechanism in the reaction of gene regulatory proteins with DNA. J. Mol. Biol. 172:263-282.

Fussell, C.P. 1975. The position of interphase chromosomes and late replicating DNA in centromere adn telomere regions of Allium cepa L. Chromosoma 50:201-210.

Gausz, J., H. Gyurkovics, G. Bencze, A.A.M. Awad, J.J. Holden, and D. Ish-Horowicz. 1981. Genetic characterization of the region between 86F1, 2 and 87B15 on chromosome 3 of Drosophila melanogaster. Genetics 98:775-789.

Gay, H. 1955. Chromosome-nuclear membrane-cytoplasmic interrelations in Drosophila. J. Biophysic. and Biochem. Cytol. 2 (Suppl.):407-414.

Gay, H. 1956. Nucleocytoplasmic relations in Drosophila. Cold Spring Harbor Symp. Quant. Biol. 21:257-269.

Gelbart, W.M. 1982. Interactions of zeste mutations with loci exhibiting transvection effects in Drosophila melanogaster. Proc. Natl. Acad. Sci. U.S.A. 79:2636-2640.

Giloh, H., and J.W. Sedat. 1982. Fluorescence microscopy: reduced photobleaching of rhodamine and fluorescein protein conjugates by n-propyl gallate. Science 217:1252-1255.

Gruenbaum, Y., M. Hochstrasser, D. Mathog, H. Saumweber, D.A. Agard, and J.W. Sedat. 1984. Spatial organization of the Drosophila nucleus: A three-dimensional cytogenetic study. J. Cell Sci. (Suppl.) 1:223-234.

Halfer, C. and C. Barigozzi. 1973. Prophase synapsis in somatic cells of Drosophila melanogaster. In Chromosomes Today. Vol. 4. A. de la Chapelle and M. Sorsa, editors. Elsevier North-Holland Biomedical Press, Amsterdam. 181-186.

Hammond, M.P. and C.D. Laird. 1985. Control of DNA replication and spatial distribution of defined DNA sequences in salivary gland cells of Drosophila melanogaster. Chromosoma 91:279-286.

Hancock, R. and T. Boulikas. 1982. Functional organization in the nucleus. Inter. Rev. Cyt. 79:165-214.

Hartmann-Goldstein, I., and D.J. Goldstein. 1979. Effect of temperature on morphology and DNA-content of polytene chromosomes in Drosophila. Chromosoma 71:333-346.

Herreros, B. and F. Giannelli. 1967. Spatial distribution of old and new chromatid sub-units and frequency of chromatid exchanges in induced human lymphocyte endoreduplications. Nature 216:286-288.

Heslop-Harrison J.S. and M.D. Bennett, 1984. Chromosome order-possible implications for development. J. Embryol. Exp. Morph. 83(Suppl.):51-73.

Hewish, D.R. and L.A. Burgoyne. 1973. Chromatin sub-structure. The digestion of chromatin DNA at regularly spaced sites by a nuclear deoxyribonuclease. Biochem. Biophys. Res. Commun. 52:504-510.

Hill, R.J., M.R. Mott, E.J. Burnett, S.M. Abmayr, K. Lowenhaupt, S.C.R. Elgin. 1982. Nucleosome repeat structure is present in native salivary gland chromosomes of Drosophila melanogaster. J. Cell Biol. 95:262-266.

Hilliker, A.J. 1986. Assaying chromosome arrangement in embryonic interphase nuclei of Drosophila melanogaster by radiation induced interchanges. Genet. Res. 47:13-18.

Hochstrasser, M., D. Mathog, Y. Gruenbaum, H. Saumweber, and J.W. Sedat. 1986. Spatial organization of chromosomes in the salivary gland nuclei of Drosophila melanogaster. J. Cell Biol. 102:112-123.

Hochstrasser, M., D. Mathog, Y. Gruenbaum, H. Saumweber, H. and J.W. Sedat. 1987. Three-dimensional organization of interphase chromosmes in polytene nuclei of Drosphila melanogaster. In: Kahl G (ed) Architecture of eukaryotic genes. Verlag Chemie, Weinheim. In press.

Holden, J.J., and M. Ashburner. 1978. Patterns of puffing activity in the salivary gland chromosomes of Drosophila. IX. The salivary and prothoracic gland chromosomes of a dominant temperature sensitive lethal of D. melanogaster. Chromosoma 68:205-227.

Holliday, R. 1964. The induction of mitotic recombination by mitomycin C in Ustilago and Saccharomyces. Genetics 50:323-335.

Hutchison, N., and H. Weintraub. 1985. Localization of DNAaseI-hypersenstive sequences to specific regions of interphase nuclei. Cell 43:471-482.

Hsu, T.C., J.E.K. Cooper, M.L. Mace, and B.R. Brinkley. 1971. Arrangement of centromeres in mouse cells. Chromosoma 34:73-87.

Ivarie, R.D., B.S. Schacter, and P.H. O'Farrell. 1983. The level of expression of rat growth hormone gene in liver tumor cells is at least eight orders of magnitude less than that in anterior pituitary cells. Molec. Cell. Biol. 3:1460-1467.

Jack, J.W., and B.H. Judd. 1979. Allelic pairing and gene regualtion: a model for the zeste-white interaction in Drosophila melanogaster. Proc. Natl. Acad. Sci. 76:1368-1372.

Jackson, D.A. 1986. Organization beyond the gene. Trends Biochem. Sci. 11:249-252.

James, T.C., and S.C.R. Elgin. 1986. Identification of a nonhistone chromosomal protein associated with heterochromatin in Drosophila melanogaster and its gene. Molec. Cell. Biol. (In press).

Kaufmann, B.P., and H. Gay. 1958. The nuclear membrane as an intermediary in gene-controlled reactions. Nucleus 1:57-74.

Kauffman, B.P. and M.K. Iddles. 1963. Distributional pairing in salivary gland chromosomes of Drosophila melanogaster (I. Distributional patterns in relation to puffing). Port. Acta. Biol. A7:225-248.

Kaufmann, S.H., A.P. Fields, and J.H. Shaper. 1986. The nuclear matrix: current concepts and unanswered questions. Meth. Achiev. Exp. Pathol. 12:141-171.

Khoury, G. and Gruss, P. 1983. Enhancer elements. Cell 33:313-314.

Kmiec, E.B., F. Razvi, and A. Worcel. 1986. The role of DNA-mediated transfer of TFIIIA in the concerted gyration and differential activation of the Xenopus 5S RNA genes. Cell. 45:209-218.

Koller, P.C. 1935. The internal mechanics of the chromosomes. IV. Pairing and coiling in salivary gland nuclei of Drosophila. Proc. R. Soc. Lond. B Biol. Sci. 118:371-396.

Kornher, J.S., and D. Brutlag. 1986. Proximity-dependent enhancement of Sgs-4 gene expression in D. melanogaster. Cell 44:879-883.

Kress, H., Meyerowitz, E.M. Davidson, N. 1985. High resolution mapping of in situ hybridized biotinylated DNA to surface-spread Drosophila polytene chromosomes. Chromosoma 93:113-122.

Laird, C. 1973. DNA of Drosophila chromosomes. Ann. Rev. Genet. 7:177-204.

Laird, C.D., Ashburner, M., and L. Wilkinson. 1980. Relationship between relative dry mass and average band width in regions of polytene chromosomes of Drosophila. Chromosoma 76:175-189.

Lakhotia, S.C., and J. Jacob. 1974. EM autoradiographic studies of polytene nuclei of Drosophila melanogaster. Exp. Cell Res. 86:253-263.

Lakhotia, S.C., and T. Mukherjee. 1980. Specific activation of puff 93D of Drosophila melanogaster by benzamide and the effect of benazmide treatment on the heat shock induced puffing activity. Chromosoma 81:125-136.

Lakhotia, S.C., and P. Sinha. 1983. Replication in Drosophila chromosomes. X. Two kinds of active replicons in salivary gland polytene nuclei and their relation to chromosomal replication patterns. Chromosoma 88:265-276.

Lakhotia, S.C. and A.K. Singh. 1985. Non-inducibility of the 93D heat-shock puff in cold-reared larvae of Drosophila melanogaster. Chromosoma 92:48-54.

Lawrence, J.B. and R.H. Singer. 1986. Intracellular localization of messenger RNAs for cytoskeletal proteins. Cell 45:407-415.

Lefevre, G. 1976. A photographic representation and interpretation of the polytene chromosomes of Drosophila melanogaster salivary glands. The Genetics and Biology of Drosophila, Vol. 1A. M. Ashburner and E. Novitski, editors. Academic Press, New York, 31-66.

Lewin, R. 1981. Do chromosomes cross talk? Science. 214:1334-1335.

Lewis, E.B. 1954. The theory and application of a new method of detecting chromosomal rearrangements in Drosophila melanogaster. Am. Nat. 88:73-89.

Lifschytz, E. and D. Haravan. 1982. Heterochromatin markers: Arrangement of obligatory heterochromatin, histone genes, and multisite gene families in the interphase nucleus of D. melanogaster. Chromosoma 86:443-455.

Lindsley, D.L., and E.H. Grell. 1968. Genetic variations of Drosophila melanogaster. Carnegie Inst. Wash. Publ. 627.

Lindsley, D.L. and K. Tokayasu. 1980. Spermatogenesis. In The Genetics and Biology of Drosphila, Vol. 3d. M. Ashburner and T.R.F. Wright, editors. Academic Press, New York, 223-294.

McGinnis, W., A.W. Shermoen, J. Heemskerk, and S.K. Beckendorf. 1983. DNA sequence changes in an upstream DNase I-hpersensitive region are correlated with reduced gene expression. Proc. Natl. Acad. Sci. U.S.A. 80:1063-1067.

Manton, I., and J. Smiles. 1943. Observations on the spiral structure of somatic chromosomes in Osmunda with the aid of ultraviolet light. Ann. Bot. 7:195-212.

Manton, I. 1950. The spiral structure of chromosomes. Biol. Rev. 1:486-508.

Mathog, D., M. Hochstrasser, Y. Gruenbaum, H. Saumweber, and J. Sedat. 1984. Characteristic folding pattern of the polytene chromosomes in Drosophila salivary gland nuclei. Nature 308:414-421.

Mathog, D. 1985. Light microscope based analysis of three-dimensional structure: applications to the study of Drosophila salivary gland nuclei. II. Algorithms for model analysis. J. Microsc. 137:254-275.

Mathog, D., M. Hochstrasser, and J.W. Sedat. 1985. Light microscope based analysis of three-dimensional structure: Applications to the study of Drosophila salivary gland nuclei. I. Data collection and analysis. J. Microsc. 137:241-253.

Moens, P.B., and K. Church. (1977). Centromere sizes, positions, and movements in the interphase nucleus. Chromosoma 61:41-48.

Mohler, J., M.L. Pardue. 1984. Mutational analysis of the region surrounding the 93D heat shock locus of Drosophila melanogaster. Genetics 106:249-265.

Mortin, L.I., and J.W. Sedat. 1982. Structure of Drosophila polytene chromosomes. Evidence of a toroidal organization of the bands. J. Cell Sci. 57:73-113.

Nelson, W.G., L.F. Liu, and D.S. Coffey. 1986. Newly replicated DNA is associated with DNA topoisomerase II in cultured rat prostatic adenocarcinoma cells. Nature. 322:187-189.

Ohnuki, Y. 1968. Structure of chromosomes. I. Morphological studies of the spiral structure of human somatic chromosomes. Chromosoma 25:402-428.

Osheim, Y.N., and O.L. Miller Jr. 1983. Novel amplification and transcriptional activity of chorion genes in Drosophila melanogaster follicle cells. Cell. 33:543-553.

Painter, T.S. 1933. A new method for the study of chromosome rearrangements and plotting of chromosome maps. Science 78:585-586.

Pardue, M.L., S.A. Gerbi, R.A. Eckhardt, and J.G. Gall. 1970. Cytological localization of DNA complementary to ribosomal RNA in polytene chromosomes of Diptera. Chromosoma 29:268-290.

Pardue, M.L., D.D. Brown, and M.L. Birnstiel. 1973. Location of the genes for 5S ribosomal RNA in Xenopus laevis. Chromosoma 42:191-203.

Pavan, C., M.E. Breuer. 1952. Polytene chromosomes in different tissues of Rhynchosciara. J. Hered. 43:152-157.

Pearson, M.J. 1974. Polyteny and the functional significance of the polytene cell cycle. J. Cell Sci. 15:457-479.

Pelham, H.R.B. 1984. Hsp70 accelerates the recovery of nucleolar morphology after heat shock. EMBO J. 3:3095-3100.

Pera, F., and H.G. Schwarzacher. 1970. Lokalisation der heterochromatischen chromosomen von Microtus agrestis in interphase und mitose. Cytobiologie 2:188-199.

Poulson, D.F., and D.F. Waterhouse. 1960. Experimental studies on pole cells and midgut differentiation in Diptera. Aust. J. Biol. Sci. 13:541-567.

Probeck, H., and L. Rensing. 1974. Cellular patterns of differing circadian rhythms and levels of RNA synthesis in Drosophila salivary glands. Cell Differ. 2:337-345.

Quick, P. 1980. Junctions of polytene chromosomes and the inner nuclear membrane. Experientia 36:457-458.

Rabl, C. 1885. Uber Zelltheilung. Morph. Jb. 10:214-330.

Rasch, E.M., H.J. Barr, and R.W. Rasch. 1971. The DNA content of sperm of Drosophila melanogaster. Chromosoma 33:1-18.

Richards, G. 1980. The polytene chromosomes in the fat body nuclei of Drosophila melanogaster. Chromosoma 79:241-250.

Richards, G. 1982. Sequential gene activation by ecdysteroids in polytene chromosomes of Drosophila melanogaster. VII. Tissue specific puffing. Wilhelm Roux Archiv. 191:103-111.

Risau, W., P. Symmons, H. Saumweber, and M. Frasch. 1983. Nonpackaging and packaging proteins of hnRNA in Drosophila melanogaster. Cell 33:529-541.

Ritossa, F. 1962. A new puffing pattern induced by heat shock and DNP in Drosophila. Experientia 18:571-573.

Ritossa, F.M. 1964. Experimental activation of specific loci in polytene chromosomes of Drosophila. Exp. Cell Res. 35:601-607.

Robertson, C.W. 1936. The metamorphosis of Drosophila melanogaster, including an accurately timed account of the principal morphological changes. J. Morph. 59:351-399.

Rossman, M.G. and Liljas, A. 1974. Recognition of structural domains in globular proteins. J. Molec. Biol. 85:177-181.

Rudkin, G.T. 1972. Replication in polytene chromosomes. In Developmental Studies on Giant Chromosomes. Results and Problems in Cell Differentiation. Vol. 4. W. Beermann, editor. Springer Verlag, Berlin. 59-85.

Sachs, L. 1983. Applied Statistics. Spring Verlag, New York.

Saumweber, H., P. Symmons, R. Kabisch, H. Will, and F. Bonhoeffer. 1980. Monoclonal antibodies against chromosomal proteins of Drosophila melanogaster. Chromosoma 80:253-275.

Sedat, J.W., and L. Manuelidis. 1978. A direct approach to the structure of eukaryotic chromosomes. Cold Spring Harbor Symp. Quant. Biol. 42:331-350.

Semeshin, V.F., E. Baricheva, E.S. Belyaeva and I.F. Zhimulev. 1982. Electron microscopical analysis of Drosophila polytene chromosomes. I. Mapping of the 87A and 87C heat shock puffs in development. Chromosoma 87:229-237.

Semeshin, V.F., E.S. Belyaeva, I.F. Zhimulev, J.T. Lis, G. Richards and M. Bourouis. 1986. Electron microscopical analysis of Drosphila polytene chromosomes. IV. Mapping of morphological structures appearing as a

result of transformation of DNA sequences into chromosomes. Chromosoma 93:461-468.

Semionov, E.P. and N. Kh. Kirov. 1986. Increased number of nucleoli in the salivary gland cells of Drosophila melanogaster under conditions of rDNA dose compensation. Chromosoma 93:477-482.

Shield, G., and J.H. Sang. 1970. Characteristics of five cell types appearing during in vitro culture of embryonic material from Drosophila melanogaster. J. Embryol. Exp. Morph. 23:53-69.

Simon, J.A., C.A. Sutton and J.T. Lis. 1985. Localization and expression of transformed DNA sequences within heat shock puffs of Drosophila melanogaster. Chromosoma 93:26-30.

Simon, J.A., C.A. Sutton, R.B. Lobell, R.L. Glaser, and J.T. Lis. 1985. Determinants of heat shock-induced chromosome puffing. Cell 40:805-817.

Skaer, R.J. and S. Whytock. 1975. Interpretation of the three-dimensional structure of living nuclei by specimen tilt. J. Cell Sci. 19:1-10.

Skaer, R.J. and S. Whytock, 1976. The fixation of nuclei and chromosomes. J. Cell Sci. 20:221-231.

Skaer, R.J., Whytock, S. and Emmines, J.P. 1976. Intranuclear electrophoresis of the chromatin of living cells. J. Cell. Sci. 21:479-496.

Sonnenblick, B.P. 1950. The early embryology of Droopshila melanogaster. In Biology of Drosophila. M. Demerec, editor. J. Wiley & Sons, New York. 62-167.

Spear, B.B. 1977. Differential replication of DNA sequences in Drosophila chromosomes. Amer. Zool. 17:695-706.

Sperling, K. and E.- K. Luedtke. 1981. Arrangement of prematurely condensed chromosomes on cultured cells and lymphocytes of the Indian muntjac. Chromosoma 83:541-553.

Spofford, J.B. 1976. Position effect variegation in Drosophila. In The Genetics and Biology of Drosophila. Volume 1C. M. Ashburner and E. Novitski, editors. Academic Press, Inc., New York. 955-1018.

Spradling, A.C., and G.M. Rubin. 1983. The effect of chromosomal position on the expression of the Drosophila xanthine dehydrogenase gene. Cell 34:47-57.

Strasburger, M. 1932. Bau, Funktion und Variabilitat des Darmtractus von Drosophila melanogaster. Meigen. Z. Wiss. Zool. 140:539-659.

Steffenson, D.M. 1977. Chromosome architecture and the interphase nucleus: data and theory on the mechanisms of differentiation and determination. In Chromosomes Today. Volume 6. A. de la Chapelle and M. Sorsa, editors. Elsevier North-Holland Biomedical Press, Amsterdam. 247-253.

Steier, H. 1975. Heated microscope stage: A temperature control for live-cell microscope. Lab Pract. 24:417.

Strasburger, M. 1932. Bau, Funktion und Variabilitat des Darmtractus von Drosophila melanogaster Meigen. Z. Wiss. Zool. 140:539-649.

Sundin, O., and A. Varshavsky. 1981. Arrest of segregation leads to accumulation of highly intertwined catenated dimers: dissection of the final stages of SV40 DNA replication. Cell 25:659-669.

Sutton, W.S. 1903. The chromosomes in heredity. Biol. Bull. 4:231-251.

Sved, J.A. 1976. Hybrid dysgenesis in Drosophila melanogaster: A possible explanation in terms of spatial organization of chromosomes. Aust. J. Biol. Sci. 29:375-388.

Udvardy, A., E. Maine, and P. Schedl. 1985. The 87A7 chromomere. Identification of novel chromatin structures flanking the heat shock locus that may define the boundaries of higher order domains. J. Mol. Biol. 185:341-358.

Vogel, F.and T.M. Shroeder. 1974. The internal order of the interphase nucleus. Humangenetik 25:265-297.

Wainwright, S.A., W.D. Biggs, J.D. Currey, and J.M. Gosline. 1982. Mechanical Design in Organisms. John Wiley & Sons, New York.

Weintraub, H. 1985. Assembly and propagation of repressed and derepressed chromosomal states. Cell. 42:705-711.

Welch, R.M. 1957. A developmental analysis of the lethal mutant l(2)gl of Drosophila melanogaster based on cytophotometric determination of nuclear desoxyribonucleic acic (DNA) content. Genetics 42:544-559.

Werry, P.A. Th. J., K. Stoffelsen, F.M. Engels, F. vander Laaen and A.W. Spanjers. 1977. The relative arrangement of chromosomes in mitotic interphase and metaphase in Haplopappus gracilis. Chromosoma 62:93-101.

Williams, S.P., B.D., Athey, L.J. Muglia, R.S. Schappe, A.H. Gough, and J.P. Langmore. 1986. Chromatin fibers are left-handed double helices with diameter and mass per unit length that depend on linker length. Biophys. J. 49:233-248.

Wilson, E.B. 1925. The Cell in Development and Heredity (3rd edition). Macmillan, New York.

Wu, C. 1980. The 5' ends of Drosophila heat shock genes in chromatin are hypersensitive to DNase I. Nature 286:854-860.

Zelechowska, M.G., and E.F. Potworoski. 1985. Improved adhesion of ultrathin sections to filmless grids. J. Electron Microsc. Technique. 2:389-390.

Zhimulev, I.F., E.S. Balyaeva and V.F. Semeshin. 1981. Informational content of polytene chromosome bands and puffs. CRC Crit. Rev. Biochem. 11:303-340.

Zhimulev, I.F., V.F. Semeshin, V.A. Kulchicov, and E.S. Belyaeva. 1982. Intercalary heterochromatin in Drosophila. I. Localization and general characteristics. Chromosoma (Berl.) 87:197-228.

Zorn, C., C. Cremer, T. Cremer, and J. Zimmer. 1979. Unscheduled DNA synthesis after partial U.V.-irradiation of the cell nucleus. Distribution in interphase and metaphase. Exp. Cell Res. 124:111-119.

Zuchowski, C.I., and A.G. Harford. 1977. Chromosomal rearrangements which affect the chromosomal integration of the ribosomal genes in Drosophila melanogaster. Cell 11:383-388.

Appendix

Antibody Staining of Tissue Whole Mounts and Isolated Nuclei for Fluorescence Optical Section Microscopy

One of the initial motivations of the present study was to examine the three-dimensional distribution of active genes. In particular, the aim was to determine whether there is any functional compartmentalization or segregation of chromosomal loci within the interphase nucleus. A direct way to assay this is by immunofluorescently labeling active loci in intact tissues with antibodies directed against nuclear ribonucleoproteins (RNPs). Monoclonal antibodies which bind specifically to particular RNPs have been shown to concentrate in chromosome puffs and specific subsets of active interbands (Saumweber et al., 1981; Risau et al., 1983). I have worked out methods to stain whole tissues (some of the early work was done in collaboration with Harald Saumweber) so that fluorescently tagged antibodies can be visualized in intact cells by optical sectioning microscopy.

All steps are done at room temperature on glass depression slides; for the longer incubations, slides are put in moist chambers. Salivary glands dissected from third instar larvae in Buffer A (see Sedat and Manuelidis, 1978) are fixed for 10-15 minutes in freshly prepared 3.7% formaldehyde (paraformaldehyde from Polysciences) in Buffer A containing 0.1% Triton X-100. After rinsing with buffer, glands are permeabilized by incubating in Buffer A containing 1.0% Triton X-100 and 1% sodium deoxycholate for 20 minutes. All subsequent incubations and rinses use Buffer A sans 2-mercaptoethanol and containing 0.1% Triton X-100. After preincubating the glands for 30-60 minutes in 10% normal goat serum (NGS) in this buffer, they are incubated for 4-14 hours at room temperature in a solution containing 0.1-1.0 ug/ml of monoclonal antibody (Saumweber et al., 1981); undiluted hybridoma supernatants can

also be used (Triton X-100 added to 0.1%). After washing in buffer, goat anti-mouse IgG, conjugated to tetramethyl-rhodamine isothiocyanate (Cappel), is added at a 1:40 dilution, and the glands are incubated for 4-6 hours. After washing, glands are stained with 1 ug/ml DAPI for °10 minutes, rinsed, and then stepped into 100% glycerol containing 1% n-propyl gallate (Sigma) to limit fluorescence fading (Giloh and Sedat, 1982). Glands are mounted under a bridged coverslip on a slide and are examined on a Zeiss Universal microscope fitted with epifluorescence optics.

A major difficulty with optical sectioning of fixed salivary glands is the greatly increased light scattering caused by the fixation. By selecting glands from late third instar glands at a stage when they are swollen and almost translucent, optical clarity after fixation is maximized. It was also found that for whole gland staining, changing from a PIPES or HEPES base to a Tris buffer generally gave clearer glands with well preserved nuclear structure and strong antibody labeling. Tris is apparently modified by the formaldehyde since the pH of the fixing solution drops markedly after a short time; this may contribute directly or indirectly (by reducing fixation efficiency) to the reduction in scattering. Not all antigens may be preserved under these conditions. Stronger fixation regimes that lead to a large increase in light scattering can be used if glands are embedded in Spurr's resin after antibody staining (and secondary fixation) and studied in physical sections.

Isolation of salivary gland nuclei is done according to the method of Sedat and Manuelidis (1978). Nuclei are fixed and stained in a manner similar to that outlined above, but with shorter incubation times

for all steps (each roughly half as long); the Triton/deoxycholate permeabilization step is also omitted. Embedding of glands is performed as described previously (Hochstrasser et al., 1986).

Fig. 1 provides examples of optical sections from both antibody stained whole salivary glands and isolated nuclei. The monoclonal antibodies used in Figs. 1A and 1C are against different RNPs, that in Fig. 1E against a microtubule associated protein, MAP1. Several interesting observations have been made with the anti-RNP antibodies. First, active regions sometimes are closely associated so that the antibody forms a "bridge" of stain between the different loci. This could represent either a kind of channeling of transcript processing components between heterologous sites or simply the fortuitous juxtaposition of such sites. From our analysis of chromosome folding, we know that the particular pair of loci so linked cannot be the same in each nucleus (Hochstrasser et al., 1986). For a comparison of such bridges to the distribution of silver grains in [3H]-uridine labeled glands, see Gruenbaum et al. (1984).

A second observation from these experiments is that the antibody within a labeled site frequently has a distinctive distribution. This involves a zig-zag pattern of label across the interband or puff; some examples are highlighted by arrows in Fig. 1. The antibody thus appears to decorate chromosomal substructural elements that are arranged obliquely within the interband/puff. An analogous substructural organization has now been seen in the bands of lower polyteny tissues both in optical sections of unfixed nuclei and in the electron microscope (see Appendix 2). Finally, the anti-MAP1 antibody, which was raised against purified bovine brain MAP1 (T. Karr, personal

communication), shows a surprising specificity in salivary glands, weakly labeling chromosomes and concentrating in large puffs, and to a lesser extent, in a subset of interbands. This antibody stains the cytoskeleton, nuclei and centrosomes in Drosophila embryos, while in mammalian cells, it stains actin stress fibers and centrosomes (T. Karr, personal communication).

The anti-MAP1 labeling demonstrates the general utility of the procedures described here. Harsh acid treatments and severe stretching and distortion of chromosomes are avoided, allowing chromosomal and nuclear structures to be viewed in their unperturbed three-dimensional milieu. We hope, for example, to study chromosome-nuclear envelope attachments in this fashion. Monoclonal antibodies specific to Drosophila centric and intercalary heterochromatin (James and Elgin, 1986) -portions of the genome known to bind to the envelope (Hochstrasser et al., 1986)- can be used for this analysis. This approach offers the possibility of directly comparing envelope attachments in diploid and polytene cells. Several of the predictions made from the study of polytene chromosome spatial organization (Chapters 3-5) can thus be tested.

Figure 1. Antibody staining of whole salivary glands and isolated nuclei. The first column (A,C,E) shows the rhodamine fluorescence of labeled antibodies; the second column (B,D,F) displays the corresponding DNA distribution as visualized by DAPI staining. A. An isolated salivary gland nucleus stained with the anti-RNP monoclonal X4 (Saumweber et al., 1981). C. A nucleus in a whole, unembedded salivary gland stained with the anti-RNP monoclonal S5. E. A nucleus in a whole gland stained with an anti-MAP1 monoclonal antibody (provided by T. Karr). Arrows in A and C highlight labeled regions with a distinctive zig-zag substructure.

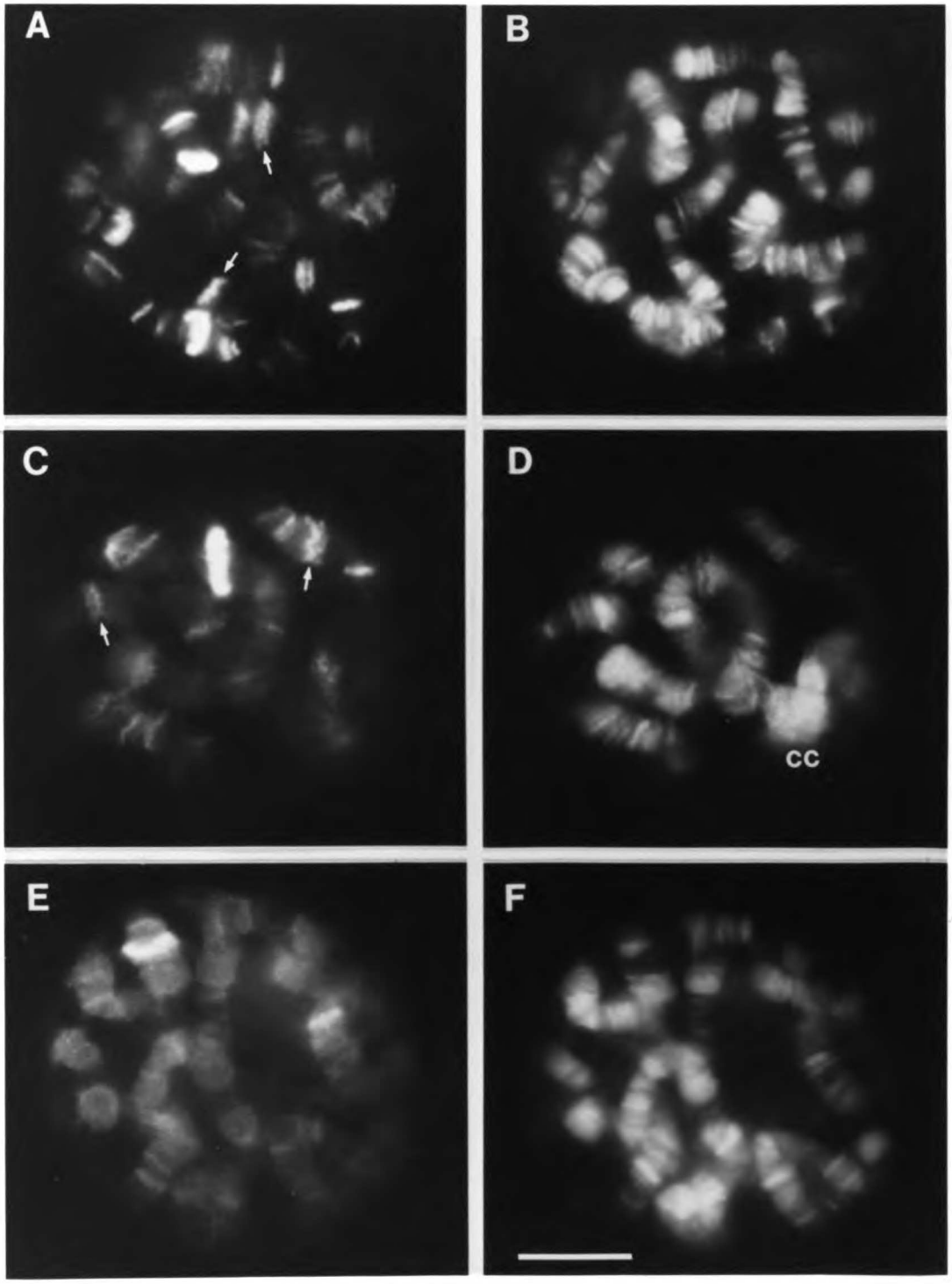
A
B
C
D
CC
E
F

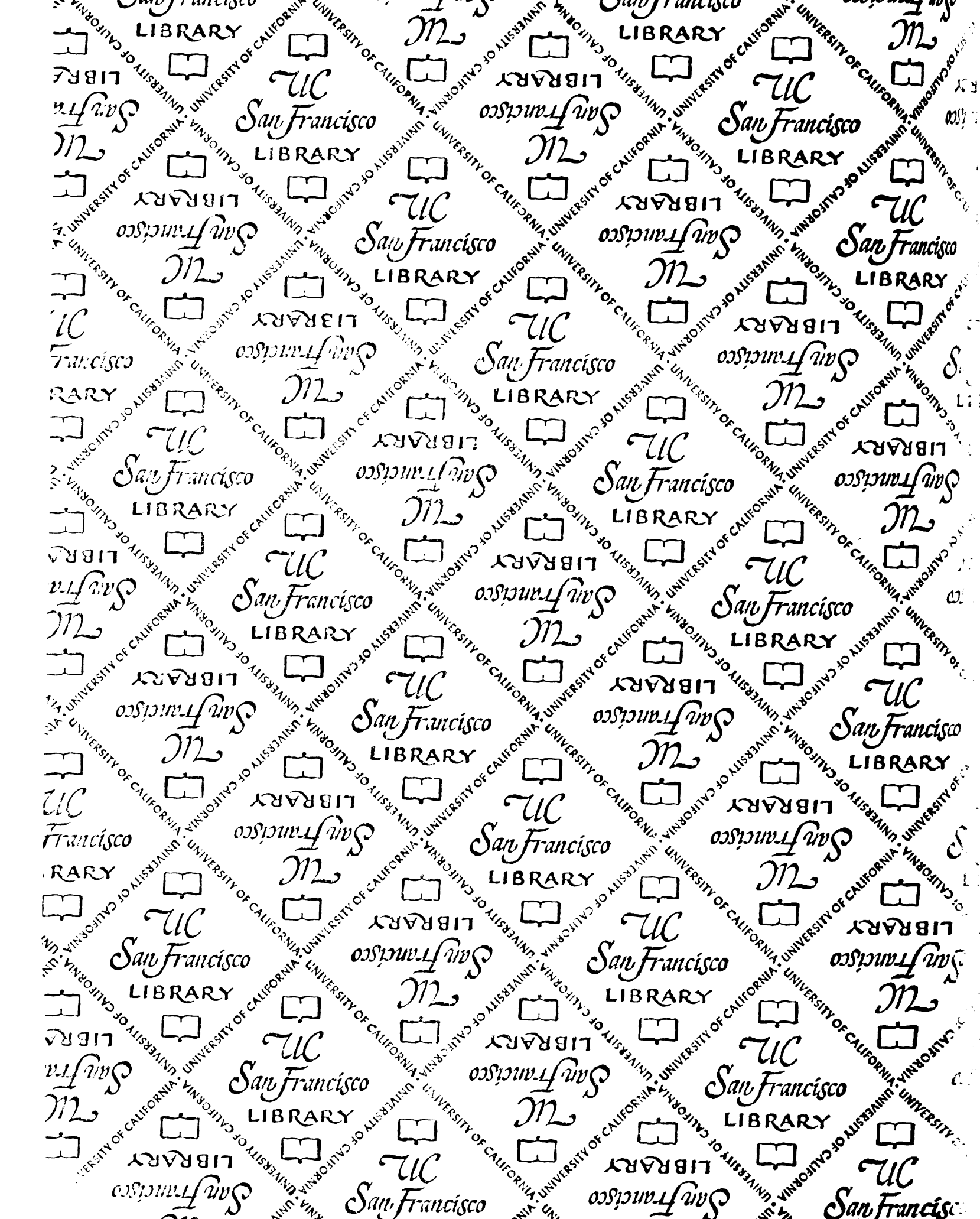
UNIVERSITY OF CALIFORNIA
UC
San Francisco
LIBRARY